

Copyright  
by  
Fei Yan  
2018

The Dissertation Committee for Fei Yan  
certifies that this is the approved version of the following dissertation:

## **Aspects of Class- $\mathcal{S}$ Theories**

Committee:

---

Jacques Distler, Supervisor

---

Andrew Neitzke, Co-Supervisor

---

Willy Fischler

---

Vadim Kaplunovsky

---

Sonia Paban

**Aspects of Class- $\mathcal{S}$  Theories**

by

**Fei Yan**

**DISSERTATION**

Presented to the Faculty of the Graduate School of  
The University of Texas at Austin  
in Partial Fulfillment  
of the Requirements  
for the Degree of

**DOCTOR OF PHILOSOPHY**

THE UNIVERSITY OF TEXAS AT AUSTIN

August 2018

*Dedicated to my parents.*

## Acknowledgments

The six years that I spent at UT Austin have been a wonderful experience and it would not have been so without the support from many people. I wish to acknowledge them here.

First of all, I would like to thank my supervisors Jacques Distler and Andrew Neitzke for their tremendous help and support in pursuing my research career. It is definitely a great pleasure to be their student and to work with them on various projects. I would also like to thank Willy Fischler for guidance and collaboration at an earlier stage of graduate school. Though I didn't have the opportunity to collaborate with other faculty of the Theory Group and the Geometry Group, I have certainly benefited a lot from interactions with David Ben-Zvi, Elena Caceres, Dan Freed, Vadim Kaplunovsky, Can Kilic, Sonia Paban and Steven Weinberg. I wish to express my gratitude here.

I would like to thank former Theory Group postdoc Bei Jia and current Theory Group postdoc Mario Martone for interesting discussions and collaborations. I would like to thank former and current fellow graduate students for their companionship. On the physics side I especially thank Behzat Ergun, Qianyu Hao, Ali Shehper and Anderson Trimm for collaborations and helpful discussions. On the mathematics side, I have benefited a lot from discussions with Arun Debray, Richard Hughes, Sebastian Schulz and Ivan

Tulli and I thank them for their help. I would also like to thank Aswin Balasubramanian, Anindya Dey and Tom Mainiero for helpful discussions and for being an inspiration. The list of (former) fellow students to thank should also include Vikas Anagam, Aditya Aravind, Dan Carney, Jacob Claussen, Lee Cohn, Josiah Couch, Brandon DiNunno, Stefan Eccles, Laura Fredrickson, Tyler Gugliemo, Matt Klimek, Dustin Lorshbough, Ravi Mohan, Phuc Nguyen, Robert Rosati, Maria Rosell, Siva Swaminathan, Walter Tangarife, Cynthia Trendafilova, Minglei Xiao, Yuan-Pao Yang and Yinan Zhu. I would also like to thank Jan Duffy, AJ Bunyard and Josh Perlman for help with administration and IT issues.

Finally I would like to thank my parents and Dustin for their endless encouragement and support, without which this dissertation would not exist.

This material is based upon work supported by the National Science Foundation under Grant Number PHY-1620610.

# Aspects of Class- $\mathcal{S}$ Theories

Fei Yan, Ph.D.

The University of Texas at Austin, 2018

Supervisors: Jacques Distler  
Andrew Neitzke

This dissertation discusses certain aspects of class- $\mathcal{S}$  theories [1,2]. First we give an overview of class- $\mathcal{S}$  theories. Then we report on the study of product SCFTs in class- $\mathcal{S}$  theories. We first describe an algorithm to determine whether an isolated 4d  $\mathcal{N} = 2$  SCFT is a product of two (or more) theories and apply this algorithm to a large subset of class- $\mathcal{S}$  theories that have been catalogued. This part is based on joint work with Jacques Distler and Behzat Ergun [3]. Afterwards we report on some preliminary studies of the supersymmetric vacuum moduli space of product SCFTs. Finally we turn our attention to supersymmetric (half) line defects in 4d  $\mathcal{N} = 2$  theories. In particular we describe a close relation between the Schur index in the presence of a supersymmetric (half) line defect and the vacuum expectation value of such line defect in  $U(1)_r$ -invariant vacua of the theory compactified on a circle. We explicitly check such relation in some special class- $\mathcal{S}$  theories: the Argyres-Douglas theories of type  $(A_1, A_2)$ ,  $(A_1, A_4)$ ,  $(A_1, A_6)$ ,  $(A_1, D_3)$  and  $(A_1, D_5)$ . This part is based on joint work with Andrew Neitzke [4].

# Table of Contents

<b>Acknowledgments</b>	v
<b>Abstract</b>	vii
<b>List of Figures</b>	x
<b>Chapter 1. Introduction</b>	1
1.1 A brief overview of theories of class- $\mathcal{S}$	2
1.2 Compactifying the 6d $(2,0)$ theory	4
1.3 Relation to Hitchin systems	7
<b>Chapter 2. Product SCFTs in class <math>\mathcal{S}</math></b>	10
2.1 Introduction	10
2.2 Counting stress tensors	13
2.3 Superconformal Index for Class- $\mathcal{S}$ Theories	16
2.4 Examples	19
2.5 Gauge theory fixtures	24
2.6 The new product SCFT	28
2.7 Moduli space of product SCFTs: a case study	28
<b>Chapter 3. Line defect Schur indices, Verlinde algebras and <math>U(1)_r</math> fixed points</b>	35
3.1 Introduction	35
3.1.1 Schur indices and chiral algebras	35
3.1.2 Schur indices with half line defects and Verlinde algebra	36
3.1.3 A simple example	38
3.1.4 Diagonalizing the Verlinde algebra	40
3.1.5 Verlinde algebra and $U(1)_r$ -fixed points in three dimensions	41
3.1.6 Fixed points and vevs	42



3.1.7	The commutative diagram	43
3.1.8	Flavor symmetries	45
3.1.9	Interpretations and comments	47
3.2	Schur indices and their IR formulas	51
3.2.1	The Schur index	51
3.2.2	The IR formula for the Schur index	52
3.2.3	The Schur index with half line defects	55
3.2.4	The IR formula for the line defect Schur index	57
3.3	Fixed points of the $U(1)_r$ action	60
3.3.1	The $U(1)_r$ action	60
3.3.2	Line defect vevs in $U(1)_r$ -invariant vacua	61
3.3.3	Classical monodromy action in Argyres-Douglas theories	65
3.4	Line defects and their framed BPS states in class $\mathcal{S}[A_1]$	68
3.4.1	Line defect generators in $\mathcal{N} = 2$ theories of quiver type	69
3.4.2	Framed BPS states from framed quivers	73
3.4.3	Line defects in class $\mathcal{S}[A_1]$ theories	74
3.4.4	Framed BPS indices in class $\mathcal{S}[A_1]$ theories, without spin	75
3.4.5	Framed BPS indices in class $\mathcal{S}[A_1]$ theories, with spin	77
3.5	$(A_1, A_{2N})$ Argyres-Douglas theories	81
3.5.1	$(A_1, A_2)$ Argyres-Douglas theory	81
3.5.2	An intermission on the homomorphism property	86
3.5.3	$(A_1, A_4)$ Argyres-Douglas theory	89
3.5.4	$(A_1, A_6)$ Argyres-Douglas theory	96
3.6	$(A_1, D_{2N+1})$ Argyres-Douglas theories	104
3.6.1	$(A_1, D_3)$ Argyres-Douglas theory	104
3.6.2	$(A_1, D_5)$ Argyres-Douglas theory	113
3.7	Verlinde algebra from Fixed Points Analysis	125

**Bibliography**

**131**

## List of Figures

2.1	An interacting fixture in the $D_4$ theory . . . . .	19
2.2	Resolving the atypical puncture in the gauge theory fixture $1_{\text{gauge}}$ . . . . .	25
2.3	Degeneration A of the 4-punctured sphere relevant to $1_{\text{gauge}}$ . . . . .	25
2.4	Degeneration B of the 4-punctured sphere relevant to $1_{\text{gauge}}$ . . . . .	26
2.5	Resolving the atypical puncture in the gauge theory fixture $2_{\text{gauge}}$ . . . . .	26
2.6	Degeneration A of the 4-punctured sphere relevant to $2_{\text{gauge}}$ . . . . .	27
2.7	Degeneration B of the 4-punctured sphere relevant to $2_{\text{gauge}}$ . . . . .	27
2.8	Choice of branch cuts for $\overline{\Sigma'}$ and cycles in homology classes $\gamma_1$ (blue) and $\gamma_2$ (green) in $H_1(\overline{\Sigma'}, \mathbb{Z})$ . The four branch points are at $z_1 = 0$ , $z_2 = z_p$ , $z_3 = 1$ and $z_4 = \infty$ . The four branch cuts are represented by wavy lines and they meet at some point on $\mathbb{CP}^1$ . Each branch cut is labeled with the corresponding sheet permutation and the direction to do the gluing. . . . .	32
3.1	The quadrilateral $Q_E$ associated to edge $E$ . . . . .	66
3.2	Action of a flip on the quadrilateral $Q_E$ . . . . .	67
3.3	An example of a WKB triangulation of the once-punctured triangle and a lamination, corresponding to the line defect $B_2$ in the $(A_1, D_3)$ Argyres-Douglas theory. . . . .	76
3.4	Left: a triangle with branch point and branch cuts marked. Middle: lifted left-turn paths. Right: lifted right-turn paths. . . . .	80
3.5	One of the lifted paths contributing to the term (3.72). . . . .	80
3.6	Rules for assigning powers of $q$ to self-crossings of the lifted path. . . . .	80
3.7	A BPS quiver for $(A_1, A_2)$ Argyres-Douglas theory. . . . .	81
3.8	The classical monodromy action in the $(A_1, A_2)$ theory, which rotates the triangulation of the pentagon clockwise by 2 units, is equivalent to a single flip which replaces the 35 edge by a 14 edge. . . . .	84
3.9	A BPS quiver for $(A_1, A_4)$ Argyres-Douglas theory. . . . .	89

3.10	The classical monodromy action in the $(A_1, A_4)$ theory is realized by a sequence of flips of triangulations of the 7-gon. The initial triangulation differs from the final one by a clockwise rotation by 2 units.	93
3.11	A BPS quiver for $(A_1, A_6)$ Argyres-Douglas theory.	97
3.12	Monodromy action via a sequence of flips of triangulations of the 9-gon.	101
3.13	A BPS quiver for the $(A_1, D_3)$ Argyres-Douglas theory.	104
3.14	(a): $\mathbb{CP}^1 \setminus D_\infty$ where $D_\infty$ is a disk around $z = \infty$ bounded by $S^1$ with three marked points colored in blue. The regular singularity at $z = 0$ is colored in black. (b): A triangulation in the $(A_1, D_3)$ Argyres-Douglas theory. There are three boundary edges. The blue marks correspond to the positions of three Stokes rays.	106
3.15	Three types of laminations in $(A_1, D_3)$ Argyres-Douglas theory.	107
3.16	Classical monodromy action via two flips in $(A_1, D_3)$ Argyres-Douglas theory.	111
3.17	A BPS quiver for the $(A_1, D_5)$ Argyres-Douglas theory.	113
3.18	$\mathbb{CP}^1 \setminus D_\infty$ where $D_\infty$ is a disk around $z = \infty$ bounded by $S^1$ with five marked points colored in blue. The regular singularity at $z = 0$ is colored in black.	114
3.19	A triangulation in the $(A_1, D_5)$ Argyres-Douglas theory. There are five boundary edges. The blue marks correspond to positions of five Stokes rays.	114
3.20	Five types of laminations in $(A_1, D_5)$ Argyres-Douglas theory.	116
3.21	Monodromy action as a sequence of flips in the $(A_1, D_5)$ Argyres-Douglas theory.	124

# Chapter 1

## Introduction

Supersymmetric quantum field theories have been playing an important role in theoretical physics. The existence of supersymmetry keeps quantum corrections under control and makes many physical quantities exactly calculable. A particularly nice class of supersymmetric quantum field theories are those with  $\mathcal{N} = 2$  supersymmetry in four dimensions. In general there are mainly three ways to construct large classes of 4d  $\mathcal{N} = 2$  theories. The first way is to use a Lagrangian description, though there are a lot of 4d  $\mathcal{N} = 2$  theories that don't admit any Lagrangian description. The second way is the so-called “geometric engineering” [5,6], where 4d  $\mathcal{N} = 2$  theories are realized as the field theory limit of string compactifications on Calabi-Yau singularities. The third way is the class- $\mathcal{S}$  construction [1,2], where 4d  $\mathcal{N} = 2$  theories are obtained by twisted compactifications of 6d  $(2,0)$  SCFTs on a Riemann surface. This thesis studies 4d  $\mathcal{N} = 2$  theories arising from the third construction. These theories are often also called theories of class- $\mathcal{S}$ .

This dissertation is organized as follows. In sections [1.1] - [1.3] we give a brief review of class- $\mathcal{S}$  theories. In chapter [2] we first talk about an algorithm to determine whether an isolated 4d  $\mathcal{N} = 2$  SCFT is a product of two (or more)

theories and apply this algorithm to a large subset of class- $\mathcal{S}$  theories that have been catalogued so-far. This is based on joint work with Jacques Distler and Behzat Ergun [3]. Then we talk about some preliminary studies of the supersymmetric vacuum moduli space of product SCFTs, based on some past work with Anderson Trimm and ongoing work with Jacques Distler, Behzat Ergun, Qianyu Hao and Andrew Neitzke. In chapter 3 we turn our attention to supersymmetric (half) line defects in 4d  $\mathcal{N} = 2$  theories. In particular, we describe a close relation between the Schur index in the presence of a supersymmetric (half) line defect and the vacuum expectation value of such line defect in  $U(1)_r$ -invariant vacua of the theory compactified on a circle. We explicitly check such relation in some special class- $\mathcal{S}$  theories: the Argyres-Douglas theories of type  $(A_1, A_2)$ ,  $(A_1, A_4)$ ,  $(A_1, A_6)$ ,  $(A_1, D_3)$  and  $(A_1, D_5)$ . Chapter 3 is joint work with Andrew Neitzke [4].

## 1.1 A brief overview of theories of class- $\mathcal{S}$

In this section we give a brief overview of class- $\mathcal{S}$  theories. This part is mainly based on [1, 2, 7].

A 4d  $\mathcal{N} = 2$  theory of class- $\mathcal{S}$ , originating from compactification of a 6d  $(2, 0)$  theory on a Riemann surface with a partial twist, is specified by the following data:

- A choice of a 6d  $(2, 0)$  theory of type  $\mathfrak{g}$ , where  $\mathfrak{g} \in \{A_n, D_n, E_6, E_7, E_8\}$ .
- A choice of a genus- $g$   $n$ -punctured Riemann surface  $C_{g,n}$ .

- A decoration of the punctures of  $C_{g,n}$  by codimension-two defect operators of the 6d  $(2,0)$  theory.

Properties of class- $\mathcal{S}$  theories are closely tied to the internal Riemann surface  $C_{g,n}$ :

- In absence of twisted punctures (as introduced in e.g. [8,9]), the moduli space of exactly-marginal deformations of the SCFT is identified with the complex structure moduli space of  $C_{g,n}$  [2]. Different pairs-of-pants decompositions of  $C_{g,n}$  (in the degeneration limit) correspond to different weakly coupled descriptions of the same SCFT which are related to each other by the generalized S-duality. With twisted punctures the conformal manifold is modified to be a branched cover of the complex structure moduli space [10-12].
- Putting a class- $\mathcal{S}$  theory on  $S^4$ , the partition function corresponds to the  $n$ -point correlation function in Liouville/Toda theory on the corresponding Riemann surface [13-17].
- The superconformal index of a class- $\mathcal{S}$  theory is interpreted as the  $n$ -point correlation function of a 2d topological quantum field theory living on the corresponding Riemann surface [18]. This interpretation is very powerful such that it allows one to bootstrap the superconformal index of class- $\mathcal{S}$  theories given some input from class- $\mathcal{S}$  theories that do have a Lagrangian description [19,20].

- Class- $\mathcal{S}$  theories are closely related to Hitchin systems. Compactifying to three dimensions on a circle, at low energies the effective three-dimensional theory is a  $\mathcal{N} = 4$  sigma model with a hyperkähler target space  $\mathcal{M}$ , which is identified to be the moduli space of solutions to Hitchin's equations [21] with prescribed boundary conditions on punctures of  $C_{g,n}$  [1]. In this picture new algorithms have been developed to compute the spectrum of BPS states of class- $\mathcal{S}$  theories [1, 22–25].

## 1.2 Compactifying the 6d (2, 0) theory

In this section we review general aspects of the compactification of 6d (2, 0) theory on a Riemann surface  $C$  with a partial topological twist. This part is following [1].

The (2, 0) superconformal theories in six dimensions have  $\mathfrak{osp}(6, 2|4)$  as their superconformal algebra. They could be constructed by taking a low-energy decoupling limit of type IIB string theory on  $\mathbb{R}^{1,5} \times \mathbb{C}^2/\Gamma$ , where  $\Gamma$  is a discrete subgroup of  $SU(2)$  of the type  $A$ ,  $D$  or  $E$ . There exists a basis operators labeled by Casimir operators of  $\mathfrak{j} = A, D$  or  $E$  and transforming in short representations of  $\mathfrak{osp}(6, 2|4)$ . Within the  $k$ -th short multiplet the subspace of operators  $V_k$  with lowest conformal weight is an irreducible representation of the  $\mathfrak{so}(5)$   $R$ -symmetry. The conformal weight is twice the exponent  $d_k$  of  $\mathfrak{j}$ . The vacuum expectation values of these chiral operators parametrize the Coulomb branch of the six-dimensional theory, which is isomorphic to  $(\mathbb{R}^5)^{\text{rank}(\mathfrak{j})}/\mathcal{W}_{\mathfrak{j}}$ , where  $\mathcal{W}_{\mathfrak{j}}$  is the Weyl group of  $\mathfrak{j}$ .

To compactify a 6d  $(2, 0)$  theory on a Riemann surface  $C$  while preserving 4d  $\mathcal{N} = 2$  supersymmetry, a partial twisting must be performed. The super Poincaré subalgebra of  $\mathfrak{osp}(6, 2|4)$  has bosonic part  $\mathfrak{so}(5, 1) \oplus \mathfrak{so}(5)$ . The Poincaré supercharges transform in the  $(\mathbb{C}^4 \otimes \mathbb{C}^4)_+$  of  $\mathfrak{so}(5, 1) \oplus \mathfrak{so}(5)$ , where  $+$  indicates a symplectic Majorana reality constraint. Compactifying on  $C$  breaks  $\mathfrak{so}(5, 1) \oplus \mathfrak{so}(5)$  to  $\mathfrak{so}(3, 1) \oplus \mathfrak{so}(2)_C \oplus \mathfrak{so}(3) \oplus \mathfrak{so}(2)_R$  under which the supercharges transform as

$$\left( \left( (2, 1)_{1/2} \oplus (1, 2)_{-1/2} \right) \otimes \left( 2_{1/2} \oplus 2_{-1/2} \right) \right)_+. \quad (1.1)$$

The twisting identifies the diagonal  $\mathfrak{so}(2)$  of  $\mathfrak{so}(2)_C \oplus \mathfrak{so}(2)_R$  with the holonomy algebra of  $C$ . After the twisting the supercharges transform under  $\mathfrak{so}(3, 1) \oplus \mathfrak{so}(3) \oplus \mathfrak{so}(2)'_C$  as

$$(2, 1; 2)_1 \oplus (2, 1; 2)_0 \oplus (1, 2; 2)_0 \oplus (1, 2; 2)_{-1}. \quad (1.2)$$

The middle two summands are uncharged under  $\mathfrak{so}(2)'_C$  and become well-defined  $\mathcal{N} = 2$  supercharges in four dimensions. We denote them as  $Q^{\alpha A}$  and  $\bar{Q}^{\dot{\alpha} A}$ .

The moduli space of the 4d theory could be obtained via dimensional reduction from the Coulomb branch of the 6d  $(2, 0)$  theory. Concretely choose a Cartan subalgebra  $\mathfrak{so}(2)_R \oplus \mathfrak{so}(2) \subset \mathfrak{so}(5)$  and denote the operator in  $V_k$  with weight  $(d_k, 0)$  as  $\mathcal{O}_k$ . In the  $k$ -th short multiplet  $\mathcal{O}_k$  has the largest  $\mathfrak{so}(2)_R$  charge, therefore  $\mathcal{O}_k$  is annihilated by supercharges with positive  $\mathfrak{so}(2)_R$  charges such as  $\bar{Q}^{\dot{\alpha} A}$ . The vacuum expectation values of this type of chiral operators parametrize the Coulomb branch  $\mathcal{B}$  of the four-dimensional theory.



Note that after the partial twist  $\mathcal{O}_k$  becomes a section of  $K^{\otimes d_k}$  over  $C$ , moreover its vacuum expectation value  $\langle \mathcal{O}_k \rangle$  is annihilated by  $\bar{\partial}$ . Therefore the 4d Coulomb branch is given by

$$\mathcal{B} = \bigoplus_{k=1}^{\text{rank}(j)} H^0(C, K^{\otimes d_k}). \quad (1.3)$$

The 6d (2, 0) theory of type  $A_{N-1}$  could be realized as the low-energy worldvolume theory of  $N$  coincident  $M5$ -branes. In this picture  $\mathcal{B}$  has a nice geometric interpretation. The four-dimensional theory is obtained by wrapping the  $N$   $M5$ -branes on a holomorphic cycle  $C$  inside a hyperkähler four-manifold  $Q$ . Going to the Coulomb branch corresponds to separating the  $M5$ -branes such that they wrap some other cycle  $\Sigma \subset Q$ , where  $\Sigma$  is a connected divisor. One could identify a neighborhood of  $C$  with  $T^*C$  by viewing  $Q$  as a holomorphic symplectic manifold and choosing holomorphic Darboux coordinates  $(x, z)$ . A point in  $\mathcal{B}$  corresponds to a set of coefficients  $u_k \in H^0(C, K^{\otimes k})$  for the following equation:

$$x^N + \sum_{k=2}^N u_k(z) x^{N-k} = 0. \quad (1.4)$$

This equation defines  $\Sigma \subset T^*C$ .  $\Sigma$  is identified with the Seiberg-Witten curve of the low energy four-dimensional theory. And the canonical one-form

$$\lambda = x dz \quad (1.5)$$

restricted to  $\Sigma$  is identified with the Seiberg-Witten differential.

For 6d (2, 0) theories of type  $D$  or  $E$  the story is very similar. However, the coefficients in the defining equation for  $\Sigma$  are in general, polynomial

expressions when expressed in terms of the natural linear coordinates at the origin of the Coulomb branch. Concretely there are polynomial constraints on the coefficients of the  $k$ -differentials which need to be solved before one sees the natural linear structure. Moreover the Coulomb branch could have graded components of degrees other than the exponents  $d_k$ . In general the Coulomb branch takes the form [26]:

$$\mathcal{B} \subset V = \bigoplus_k H^0(C, K^{\otimes d_k}) \oplus \bigoplus_k W_k, \quad (1.6)$$

where  $W_k$  are vector spaces of degree  $k$  and  $\mathcal{B}$  is the subvariety satisfying the collection of polynomial constraints, which are linear in at least one variable and of homogeneous degree.

### 1.3 Relation to Hitchin systems

In this section we briefly review the relation of class- $\mathcal{S}$  theories to Hitchin systems following [1].

To do so we consider the theory obtained by further dimensional reduction from 4d to 3d on  $S^1$ . At low energies the 3d effective theory is an  $\mathcal{N} = 4$  sigma model into a hyperkähler target space  $\mathcal{M}$  fibered over the 4d Coulomb branch  $\mathcal{B}$  with generic fiber being a compact torus [27, 28].

To study  $\mathcal{M}$  the logic is to reverse the order of compactifications. Due to the partial topological twist, the BPS-protected quantities are insensitive to the conformal scale of the metric on  $C$ , therefore no phase transition in the low energy physics is expected when one exchanges the relative length scales

of  $C$  and  $S^1$ . By first compactifying the  $(2, 0)$  theory on  $S^1$  with radius  $R$ , one obtains at low energies five-dimensional  $\mathcal{N} = 2$  supersymmetric Yang-Mills theory. The next step is to compactify this five-dimensional theory further on the Riemann surface  $C$  with an appropriate topological twist. The moduli space of the resulting 3d theory is then the space of 5d BPS configurations that are Poincaré invariant in  $\mathbb{R}^3$ . Denote the five adjoint scalars of the 5d  $\mathcal{N} = 2$  super Yang-Mills theory by  $\Phi_I$ ,  $I = 1, \dots, 5$  such that

$$\phi := \frac{1}{2}(\Phi_1 + i\Phi_2) \quad (1.7)$$

has  $\mathfrak{so}(2)_R$  charge  $+1$ . ( $\Phi_{3,4,5}$  have charge zero.) In the twisted theory  $\phi$  becomes a  $(1, 0)$  form on  $C$ . The BPS equations are the Hitchin equations for the gauge field  $A = A_z dz + A_{\bar{z}} d\bar{z}$  cotangent to  $C$  and the adjoint scalar  $\phi$ :

$$\begin{aligned} F_A + R^2[\phi, \bar{\phi}] &= 0, \\ \bar{\partial}_A \phi &:= d\bar{z}(\partial_{\bar{z}} \phi + [A_{\bar{z}}, \phi]) = 0, \\ \partial_A \bar{\phi} &:= dz(\partial_z \bar{\phi} + [A_z, \bar{\phi}]) = 0. \end{aligned} \quad (1.8)$$

$\mathcal{M}$  is therefore identified with the moduli space of solutions to Hitchin's equations on  $C$ .  $\mathcal{M}$  is hyperkähler and in one distinguished complex structure  $\mathcal{M}$  is a fibration over the 4d Coulomb branch  $\mathcal{B}$ . The projection from  $\mathcal{M}$  to  $\mathcal{B}$  is given by:

$$(A, \phi) \rightarrow \{\text{Casimirs of } \phi\}. \quad (1.9)$$

This map is the well-known Hitchin fibration [21] with generic fiber being an abelian variety. The Seiberg-Witten curve  $\Sigma \subset T^*C$  is identified with the spectral curve determined by  $\phi$ :

$$\det(\lambda - \phi) = 0, \quad (1.10)$$

where  $\lambda = xdz$ . Namely the positions  $x_i$  of various sheets of  $\Sigma$  in the cotangent directions are interpreted as the eigenvalues of the matrix-valued 1-form field  $\phi$ .

For most of the class- $\mathcal{S}$  theories that we study, the Riemann surface  $C$  has finitely many marked points with half-BPS codimension-2 defects of the 6d (2,0) theories living at those points. The presence of such defects give rise to various boundary conditions for  $(A, \phi)$ . A systematic study of such codimension-2 defects has been carried out in [\[9\]](#).

## Chapter 2

### Product SCFTs in class S<sup>1</sup>

#### 2.1 Introduction

The class-S construction [1,2] has yielded a wealth of information about 4D  $\mathcal{N} = 2$  supersymmetric field theories and their superconformal fixed points. Generically,  $\mathcal{N} = 2$  SCFTs come in families, where the exactly-marginal deformation corresponds to varying a complex gauge coupling (whose  $\beta$ -function vanishes). If we turn off the gauge coupling(s), these theories decompose into a product of free vector multiplets with an isolated SCFT, a subgroup of whose global symmetry we had previously gauged.

So, to classify such theories, it suffices to classify the isolated theories and their possible gauging. In class-S, the isolated theories further decompose into products of SCFTs associated to 3-punctured spheres (“fixtures”), on which one performs a partially-twisted compactification of a 6d  $(2,0)$  theory. The fixtures fall<sup>2</sup> into three broad types: free hypermultiplets, an isolated

---

<sup>1</sup>[2.1-2.6] has appeared as J. Distler, B. Ergun, and F. Yan, “Product SCFTs in Class-S”, arXiv: 1711.04727[hep-th] [3]. In collaboration with Jacques Distler and Behzat Ergun, I contributed to formulating the algorithm to identify product SCFTs, applying the algorithm to some examples, and writing part of the preprint.

<sup>2</sup>This is not quite true in the twisted compactifications of the  $(2,0)$  theories with outer-automorphisms. There [10-12,29], one encounters a fourth type of fixture, with a hidden marginal deformation, which we called a “gauge theory fixture.” Some of these also turn

*interacting* SCFT, or a mixture of both.

For any *given*  $(2, 0)$  theory, the list of fixtures is finite, permitting a complete classification of the resulting 4D SCFTs [9–12, 26, 29–35]. It turns out that the *same* isolated 4D SCFT can have many different realizations as fixtures in (different)  $(2, 0)$  theories. That redundancy is not too difficult to keep track of. More serious is the possibility that some (many? most?) fixtures could *themselves* correspond to product SCFTs, introducing a further (unexpected) level of redundancy.

This has already been noted, in examples, in [10, 12, 26, 32, 35], where the fact that one has a product SCFT can be seen by doing some gauging and then using S-duality (see, e.g., the discussion in §7 of [12]). But how prevalent the phenomenon – of a fixture corresponding to a product SCFT – is, was unknown.

Our purpose here is to develop a technique for deciding the issue, and applying it to a large (but far from exhaustive) subset of the class-S theories which have been catalogued so-far. The technique will involve using (certain limits of) the superconformal index to compute the number of  $\mathcal{N} = 2$  stress tensor multiplets (after suitably removing the contribution to the index from any free hypermultiplets that might be present).

For the  $A_{N-1}$  and  $D_N$   $(2, 0)$  theories (at least for low  $N$ ), the number of known product theories is very small. We verify that these are indeed product

---

out to be product theories, as we shall see below.

theories and that there are no additional ones.

We then turn our attention to the  $E_6(2,0)$  theory. In the untwisted theory [32], there were 10 fixtures which were known to be products. We checked all 881 fixtures and found no additional product theories. In the twisted sector of the  $E_6(2,0)$  theory [12], the fixtures were known to include 12 corresponding to product SCFTs. We checked that these were, indeed, product theories and found that there is only one additional previously unknown product theory among the 2078 fixtures in the twisted sector of  $E_6$ .

From this large, but admittedly still limited sample, we seem to be led to two conclusions.

- Fixtures that are product SCFTs are relatively rare (at most, a few percent of the total).
- In all of the examples we have found, whenever you *do* find a product SCFT, one of the factors in the product is always a (rank- $k$ ) Minahan-Nemeschansky theory [36,37] (the SCFT whose Higgs branch is the  $k$ -instanton moduli space of  $E_{6,7,8}$ ). This phenomenon becomes understandable using the unitarity bound criterion, which is an alternative way to identify product theories [38,39].

## 2.2 Counting stress tensors

The unrefined superconformal index of a 4d  $\mathcal{N} = 2$  SCFT is defined as [19, 40]:

$$I(p, q, t) = \text{Tr}_{\mathcal{H}} (-1)^F p^{\frac{1}{2}(\Delta+2j_1-2R-r)} q^{\frac{1}{2}(\Delta-2j_1-2R-r)} t^{R+r}. \quad (2.1)$$

Here  $p, q, t$  are the three superconformal fugacities,  $\Delta$  is the dilatation generator (conformal Hamiltonian),  $j_1$  and  $j_2$  are the Cartan generators of the  $SU(2)_1 \times SU(2)_2$ ,  $R$  and  $r$  are the Cartan generators of the  $SU(2)_R \times U(1)_r$  R-symmetry. The trace is taken over the Hilbert space  $\mathcal{H}$  on  $\mathbb{S}^3$  in radial quantization. We will be interested in two specializations of the superconformal index: the Schur index, defined as

$$I_{\text{Schur}} = \text{Tr}_{\mathcal{H}} p^{\Delta-R} (-1)^F \quad (2.2)$$

and the Hall-Littlewood index,

$$I_{\text{HL}} = \text{Tr}_{\mathcal{H}_{\text{HL}}} \tau^{2(\Delta-R)} (-1)^F \quad (2.3)$$

where  $\mathcal{H}_{\text{HL}}$  is the subspace of  $\mathcal{H}$  defined by  $\Delta - 2R - r = j_1 = 0$ . The superconformal index does not receive contributions from generic long multiplets of the 4d  $\mathcal{N} = 2$  superconformal algebra (or from combinations of short multiplets that can recombine into long multiplets).

In the notation of [41], the Hall-Littlewood index receives contributions from the short multiplets  $\hat{B}_R$  (whose superconformal primary contributes  $\tau^{2R}$ ) and  $D_{R(0, j_2)}$  (whose first superconformal descendent contributes  $\tau^{2(R+j_2+1)} (-1)^{1+2j_2}$ ).



The Schur index receives contributions from  $\hat{C}_{R(j_1, j_2)}$ ,  $\hat{B}_R$ ,  $D_{R,(0, j_2)}$  and  $\bar{D}_{R(j_1, 0)}$ . The contribution from each of these short multiplets is listed in the table below.

Short Multiplet	$I_{\text{Schur}}(p)$	$I_{\text{HL}}(\tau)$
$\hat{C}_{R(j_1, j_2)}$	$(-1)^{2(j_1 + j_2)} \frac{p^{R+j_1+j_2+2}}{1-p}$	0
$\hat{B}_R$	$\frac{p^R}{1-p}$	$\tau^{2R}$
$D_{R,(0, j_2)}$	$(-1)^{2j_2+1} \frac{p^{R+j_2+1}}{1-p}$	$(-1)^{2j_2+1} \tau^{2(R+j_2+1)}$
$\bar{D}_{R(j_1, 0)}$	$(-1)^{2j_1+1} \frac{p^{R+j_1+1}}{1-p}$	0

The representation  $\hat{B}_{1/2}$  is the free half-hypermultiplet.  $D_{0(0,0)} + \bar{D}_{0(0,0)}$  is the free vector multiplet. We assume that there are no free vector multiplets. If there are free hypermultiplets present, we want to remove their contribution by hand.  $n$  free half-hypermultiplets contribute a factor of

$$\begin{aligned}
 I_{\text{Schur}} &= \left( \text{PE} \left[ \frac{p^{1/2}}{1-p} \right] \right)^n = \prod_{k=0}^{\infty} \left( \frac{1}{1-p^{k+1/2}} \right)^n \\
 I_{\text{HL}} &= (\text{PE}[\tau])^n = \frac{1}{(1-\tau)^n}
 \end{aligned} \tag{2.4}$$

to the index.

After removing the free hypers, we have an isolated interacting SCFT. As such, there should be no higher-spin conserved currents in the spectrum. Various  $D_{R,(0, j_2)}$  and  $\bar{D}_{R(j_1, 0)}$  multiplets contain such higher spin currents and hence must be absent from the spectrum. In particular,

$$\begin{aligned}
 \#D_{1/2(0,1/2)} &= \#\bar{D}_{1/2(1/2,0)} = \#D_{0(0,1)} = \#\bar{D}_{0(1,0)} = \#D_{1/2(0,0)} \\
 &= \#\bar{D}_{1/2(0,0)} = \#D_{0(0,1/2)} = \#\bar{D}_{0(1/2,0)} = 0
 \end{aligned}$$

The remaining contributions to the Schur and Hall-Littlewood indices can be

written as follows

$$\begin{aligned} I_{\text{Schur}} &= 1 + s_1 p + s_{3/2} p^{3/2} + s_2 p^2 + \dots \\ I_{\text{HL}} &= 1 + h_1 \tau^2 + h_{3/2} \tau^3 + h_2 \tau^4 + \dots \end{aligned} \tag{2.5}$$

where

$$\begin{aligned} h_1 &= s_1 = \#\hat{B}_1 \\ h_{3/2} &= s_{3/2} = \#\hat{B}_{3/2} \\ h_2 &= \#\hat{B}_2 - \#D_{1(0,0)} \\ s_2 &= \#\hat{B}_1 + \#\hat{B}_2 - \#D_{1(0,0)} - \#\bar{D}_{1(0,0)} + \#\hat{C}_{0(0,0)} \end{aligned} \tag{2.6}$$

Rearranging these, we obtain

$$\#\hat{C}_{0(0,0)} = s_2 - h_1 - h_2 + \#\bar{D}_{1(0,0)} \tag{2.7}$$

In general, this gives us only a lower bound

$$\#\hat{C}_{0(0,0)} \geq s_2 - h_1 - h_2 \tag{2.8}$$

Because of the recombination formula,

$$\hat{C}_{0(0,0)} + D_{1(0,0)} + \bar{D}_{1(0,0)} + \hat{B}_2 = \text{long multiplet}$$

the superconformal index cannot do better than this lower bound. We need some dynamical information. The key point is that  $D_{1(0,0)} + \bar{D}_{1(0,0)}$  is the multiplet containing an  $(\mathcal{N} = 1)$ -preserving (but  $(\mathcal{N} = 2)$ -breaking) marginal perturbation (exactly-marginal, if it's a flavour singlet [\[42\]](#)). If such an operator *is* present in our product theory, then one of the factors in the product is actually a special point of enhanced  $\mathcal{N} = 2$  superconformal symmetry in a *family* of  $\mathcal{N} = 1$  superconformal theories. While this is certainly possible, it seems

unlikely in the cases at hand. So we will simply assume that  $\#\overline{D}_{1(0,0)} = 0$  and (2.8) is an *equality*.  $\hat{C}_{0(0,0)}$  is the  $\mathcal{N} = 2$  stress tensor multiplet and computing the RHS of (2.8) allows us to count them.

### 2.3 Superconformal Index for Class-S Theories

In this section, we'll recall some facts about class-S theories and their superconformal indices. A class-S theory of type  $\mathfrak{j}$  is obtained by a partially-twisted compactification of a 6d (2, 0) theory of type  $\mathfrak{j}$ , where  $\mathfrak{j}$  is a simply-laced Lie algebra, on a genus- $g$ ,  $n$ -punctured Riemann surface  $\mathcal{C}_{g,n}$ . The punctures are the locations of codimension-two defects in the 6d (2, 0) theory. In the untwisted sector, the punctures are labelled by nilpotent orbits in  $\mathfrak{j}$  or, equivalently, embeddings  $\rho : \mathfrak{su}(2) \rightarrow \mathfrak{j}$  up to conjugation. The global symmetry associated to a puncture is then the centralizer  $\mathfrak{f}$  of  $\rho(\mathfrak{su}(2)) \subseteq \mathfrak{j}$  [9].

For a fixture, i.e. a 3-punctured sphere, the Schur and Hall-Littlewood limits of the unrefined superconformal indices have the following form [19, 20]

$$I_{Schur}(p) = \sum_{\Lambda} \frac{\prod_{i=1}^3 \mathcal{K}_S(\mathbf{a}_i) \chi_{\Lambda}(\mathbf{a}_i)}{\mathcal{K}_S(\{p\}) \chi_{\Lambda}(\{p\})} \Bigg|_{\mathbf{a}_i \rightarrow 1} \quad (2.9)$$

$$I_{HL}(\tau) = \sum_{\Lambda} \frac{\prod_{i=1}^3 \mathcal{K}_{HL}(\mathbf{a}_i) P_{\Lambda}(\mathbf{a}_i)}{\mathcal{K}_{HL}(\{\tau\}) P_{\Lambda}(\{\tau\})} \Bigg|_{\mathbf{a}_i \rightarrow 1} \quad (2.10)$$

where

1. The sum is over highest weights  $\Lambda$  labeling the finite dimensional irreducible representations of  $\mathfrak{j}$ .

2. Flavor fugacities  $\mathbf{a}_i$  associated to the  $i^{\text{th}}$  puncture are determined by decomposition of the fundamental representation of  $\mathfrak{j}$  under  $\rho_i(\mathfrak{su}(2)) \times \mathfrak{f}_i$ .  $\{p\}$  and  $\{\tau\}$  are the fugacities for the trivial puncture.
3. The  $\mathcal{K}$ -factor associated to the  $i^{\text{th}}$  puncture is determined by the decomposition of the adjoint representation  $\text{ad}_{\mathfrak{j}}$  of  $\mathfrak{j}$  under  $\rho_i(\mathfrak{su}(2)) \times \mathfrak{f}_i$ :

$$\text{ad}_{\mathfrak{j}} = \bigoplus_n V_n \otimes R_{n,i} \quad (2.11)$$

where  $V_n$  is the  $n$ -dimensional irreducible representation of  $\mathfrak{su}(2)$  and  $R_{n,i}$  is the corresponding representation of  $\mathfrak{f}_i$ , possibly reducible. Upon this decomposition, the  $\mathcal{K}$ -factors are

$$\mathcal{K}_S(\mathbf{a}_i) = \text{PE} \left[ \sum_n \frac{p^{\frac{n+1}{2}}}{1-p} \chi_{R_{n,i}}^{\mathfrak{f}_i}(\mathbf{a}_i) \right] \quad (2.12)$$

$$\mathcal{K}_{HL}(\mathbf{a}_i) = (1-\tau^2)^{\frac{\text{rank}(\mathfrak{j})}{2}} \text{PE} \left[ \sum_n \tau^{n+1} \chi_{R_{n,i}}^{\mathfrak{f}_i}(\mathbf{a}_i) \right] \quad (2.13)$$

4. The polynomials appearing in the index  $\chi_{\Lambda}$  and  $P_{\Lambda}$  are characters and Hall-Littlewood polynomials for the corresponding representation labeled by  $\Lambda$ . The HL polynomial is defined as:

$$P_{\Lambda}(\mathbf{a}_i) = \frac{1}{W_{\Lambda}(\tau)} \sum_{w \in W} e^{w(\Lambda)} \prod_{\alpha \in \Phi_+} \frac{1 - \tau^2 e^{-w(\alpha)}}{1 - e^{-w(\alpha)}} \quad (2.14)$$

$$W_{\Lambda}(\tau) = \sqrt{\sum_{w \in \text{Stab}_W(\Lambda)} \tau^{2l(w)}} \quad (2.15)$$

where  $\Phi_+$  are the positive roots of  $\mathfrak{j}$  and flavor fugacities  $\{\mathbf{a}_i\}$  are assigned once we choose a basis for the weight lattice of  $\mathfrak{j}$ .

In the twisted sector, some of the defects are associated with a twist by an outer automorphism  $o \in \text{Out}(\mathfrak{j})$ . Let  $\mathfrak{g} \subset \mathfrak{j}$  be the invariant subalgebra. Twisted defects are labeled by, up to conjugation, homomorphisms  $\rho : \mathfrak{su}(2) \rightarrow \mathfrak{g}^\vee$  where  $\mathfrak{g}^\vee$  is Langlands dual of  $\mathfrak{g}$ . As in the untwisted case, the flavor symmetry is the centralizer of the image of  $\rho$  [9]. Twisted-sector fixtures have 2 twisted punctures and 1 untwisted puncture. Unrefined superconformal indices for such fixtures have almost the same form as before but are slightly modified as [11, 12, 20]

$$I_{Schur}(p) = \sum_{\Lambda'} \frac{\mathcal{K}_S(\mathbf{b}) \chi_\Lambda^{\mathfrak{j}}(\mathbf{b}) \prod_{i=2}^3 \bar{\mathcal{K}}_S(\mathbf{a}_i) \chi_{\Lambda'}^{\mathfrak{g}^\vee}(\mathbf{a}_i)}{\mathcal{K}_S(\{p\}) \chi_\Lambda^{\mathfrak{j}}(\{p\})} \Big|_{\mathbf{a}_i, \mathbf{b} \rightarrow 1} \quad (2.16)$$

$$I_{HL}(\tau) = \sum_{\Lambda'} \frac{\mathcal{K}_{HL}(\mathbf{b}) P_\Lambda^{\mathfrak{j}}(\mathbf{b}) \prod_{i=2}^3 \bar{\mathcal{K}}_{HL}(\mathbf{a}_i) P_{\Lambda'}^{\mathfrak{g}^\vee}(\mathbf{a}_i)}{\mathcal{K}_{HL}(\{\tau\}) P_\Lambda^{\mathfrak{j}}(\{\tau\})} \Big|_{\mathbf{a}_i, \mathbf{b} \rightarrow 1} \quad (2.17)$$

where the sum is now over the weights  $\Lambda'$  of  $\mathfrak{g}^\vee$ , extended<sup>3</sup> (in the case of the untwisted puncture) to weights of  $\mathfrak{j}$  (denoted as  $\Lambda$  in the formulas). The  $\bar{\mathcal{K}}$  and flavor fugacities  $\mathbf{a}_i$  for twisted punctures are determined as in the untwisted case but with  $\mathfrak{j}$  replaced by  $\mathfrak{g}^\vee$ .

The main computational bottleneck is computing and evaluating the Hall-Littlewood polynomials, which requires a sum over the elements of the Weyl group. For low rank classical algebras  $A_N$  and  $D_N$ , the Weyl groups are rather small and the HL polynomials can be evaluated with ease. However,  $|W_{E_6}| = 51840$ , which makes the evaluation of HL polynomials very tedious.

---

<sup>3</sup>For the main case of interest here, namely  $\mathfrak{g}^\vee = \mathfrak{f}_4$  and  $\mathfrak{j} = \mathfrak{e}_6$ , the precise extension can be found in §4.1 of [12].

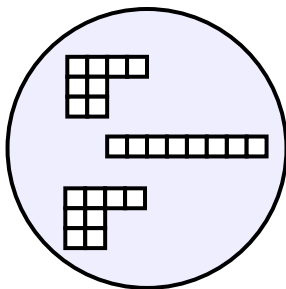


Figure 2.1: An interacting fixture in the  $D_4$  theory

And we need to compute them for every representation that contributes to a given order in  $\tau$ . Fortunately, one can exploit the freedom in the choice of flavor fugacity assignments to deduce whether or not a given representation will contribute to a desired order.

For the untwisted  $E_6$  theory, it turns out there are 71 representations that contribute to the order  $p^2$  and  $\tau^4$ . The highest dimensional representation that occur has Dynkin labels  $[0, 0, 1, 0, 0, 2]_{\mathfrak{e}_6}$  and dimension = 1911195. In the twisted  $E_6$  case, there are 30 representations that contribute, 15 of which already appeared in the untwisted case. The largest  $\mathfrak{f}_4$  and  $\mathfrak{e}_6$  representations that contribute to order  $p^2$  and  $\tau^4$  have  $\dim[1, 1, 0, 1]_{\mathfrak{f}_4} = 379848$  and  $\dim[2, 1, 0, 1, 2, 0]_{\mathfrak{e}_6} = 688740975$ .

## 2.4 Examples

As a simple example, consider an interacting fixture in the  $D_4$  theory as given in Figure 2.1. The corresponding 4d  $\mathcal{N} = 2$  SCFT was identified as the product of two copies of rank-1 Minahan-Nemeschansky  $E_6$  SCFT in [26].

The unrefined Schur and Hall-Littlewood indices for this fixture to the order of  $p^2$  ( $\tau^4$ ) are

$$\begin{aligned} I_{\text{Schur}} &= 1 + 156p + 11102p^2 + \dots \\ I_{\text{HL}} &= 1 + 156\tau^2 + 10944\tau^4 + \dots \end{aligned} \tag{2.18}$$

We read off  $h_1 = s_1 = 156$ , which equals the dimension of  $\mathfrak{e}_6 \oplus \mathfrak{e}_6$ . The lower bound on  $\#\hat{C}_{0(0,0)}$  is

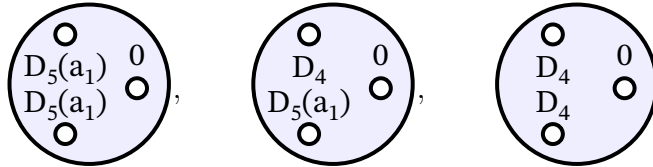
$$s_2 - h_1 - h_2 = 11102 - 156 - 10944 = 2.$$

The lower bound is clearly saturated in this example.

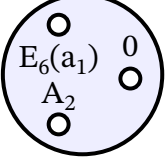
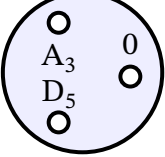
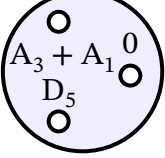
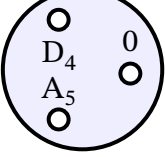
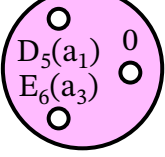
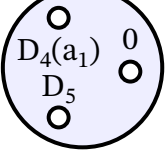
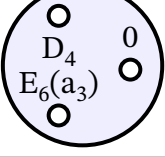
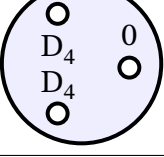
At least for low  $N$ , there are not too many further examples of product SCFTs among the (twisted or untwisted) fixtures of the  $A_N$  or  $D_N$  theories. For most of the interacting fixtures the lower bound on  $\#\hat{C}_{0(0,0)}$  is equal to 1. However, there are more interesting product SCFTs in theories of type  $E_6$ .

In the untwisted  $E_6$  case, our results can be summarized in the table below. We find 10 product theories among the 881 good fixtures (the numbering is the one used in [32]) with regular punctures. The first 7 were known to be product theories in [32]. The last 3 were not.

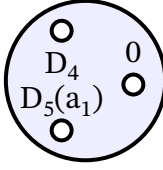
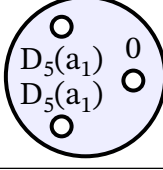
Those three fixtures,



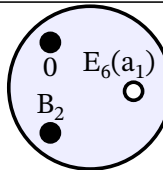
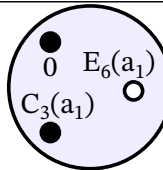
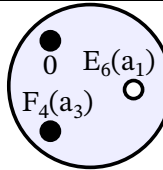
(respectively, #59, #61 and #99 in the table of interacting fixtures in [32]) were later identified as product theories in [12] by gauging a subgroup of the flavour symmetry and using S-duality.

$\#_{type}$	Fixture	$I_{Schur}(p)$	$I_{HL}(\tau)$	$\#\hat{C}_{0(0,0)}$	Theory
$1_{int}$		$1 + 496p + 116002p^2 + \dots$	$1 + 496\tau^2 + 115504\tau^4 + \dots$	2	$[(E_8)_{12} \text{ SCFT}]^2$
$8_{int}$		$1 + 222p + 216p^{\frac{3}{2}} + 23880p^2 + \dots$	$1 + 222\tau^2 + 216\tau^3 + 23656\tau^4 + \dots$	2	$[(E_7)_8 \text{ SCFT}] \times [(E_6)_{16} \times Sp(2)_{10} \times U(1) \text{ SCFT}]$
$6_{int}$		$1 + 269p + 266p^{\frac{3}{2}} + 35045p^2 + \dots$	$1 + 269\tau^2 + 266\tau^3 + 34774\tau^4 + \dots$	2	$[(E_7)_8 \text{ SCFT}] \times [(E_7)_{16} \times SU(2)_9 \text{ SCFT}]$
$39_{int}$		$1 + 329p + 156p^{\frac{3}{2}} + 50739p^2 + \dots$	$1 + 329\tau^2 + 156\tau^3 + 50408\tau^4 + \dots$	2	$[(E_8)_{12} \text{ SCFT}] \times [(E_6)_{12} \times SU(2)_7 \text{ SCFT}]$
$11_{mix}$		$1 + 54p^{\frac{1}{2}} + 1641p + 36198p^{\frac{3}{2}} + 640688p^2 + \dots$	$1 + 54\tau + 1641\tau^2 + 36144\tau^3 + 637614\tau^4 + \dots$	2	$[(E_6)_6 \text{ SCFT}]^2 + 1(27)$
$5_{int}$		$1 + 399p + 75582p^2 + \dots$	$1 + 399\tau^2 + 75180\tau^4 + \dots$	3	$[(E_7)_8 \text{ SCFT}]^3$
$18_{int}$		$1 + 404p + 77039p^2 + \dots$	$1 + 404\tau^2 + 76632\tau^4 + \dots$	3	$[(E_8)_{12} \text{ SCFT}] \times [(E_6)_6 \text{ SCFT}]^2$
$99_{int}$		$1 + 172p + 14886p^2 + \dots$	$1 + 172\tau^2 + 14712\tau^4 + \dots$	2	$[(E_6)_6 \text{ SCFT}] \times [(E_6)_{18} \times SU(3)_{12}^2 \text{ SCFT}]$



$\#_{type}$	Fixture	$I_{\text{Schur}}(p)$	$I_{\text{HL}}(\tau)$	$\#\hat{C}_{0(0,0)}$	Theory
$61_{\text{int}}$		$1 + 165p + 164p^{\frac{3}{2}} + 13451p^2 + \dots$	$1 + 165\tau^2 + 164\tau^3 + 13284\tau^4 + \dots$	2	$[(E_6)_6 \text{ SCFT}]$ $\times$ $[(E_6)_{18} \times SU(3)_{12} \times U(1) \text{ SCFT}]$
$59_{\text{int}}$		$1 + 212p + 112p^{\frac{3}{2}} + 22273p^2 + \dots$	$1 + 212\tau^2 + 112\tau^3 + 22059\tau^4 + \dots$	2	$[(E_6)_6 \text{ SCFT}]$ $\times$ $[(E_7)_{18} \times U(1) \text{ SCFT}]$

In the twisted  $E_6$  case, we identify 13 product theories among 2078 good fixtures with regular punctures. Only one interacting fixture, namely fixture #91, was not previously listed in [12] as a product theory. We also find that three gauge theory fixtures are product theories. One was explicitly noted as such in §3.6 of [12]. We discuss the other two below. Our results can be summarized in the following table.

$\#_{type}$	Fixture	$I_{\text{Schur}}(p)$	$I_{\text{HL}}(\tau)$	$\#\hat{C}_{0(0,0)}$	Theory
$111_{\text{int}}$		$1 + 136p + 104p^{\frac{3}{2}} + 9036p^2 + \dots$	$1 + 136\tau^2 + 104\tau^3 + 8898\tau^4 + \dots$	2	$[(E_6)_6 \text{ SCFT}]$ $\times$ $[(F_4)_{12} \times SU(2)_7^2 \text{ SCFT}]$
$103_{\text{int}}$		$1 + 159p + 156p^{\frac{3}{2}} + 12229p^2 + \dots$	$1 + 159\tau^2 + 156\tau^3 + 12068\tau^4 + \dots$	2	$[(E_6)_6 \text{ SCFT}]$ $\times$ $[(E_6)_{12} \times SU(2)_7 \text{ SCFT}]$
$99_{\text{int}}$		$1 + 234p + 25779p^2 + \dots$	$1 + 234\tau^2 + 25542\tau^4 + \dots$	3	$[(E_6)_6 \text{ SCFT}]^3$

$\#_{type}$	Fixture	$I_{\text{Schur}}(p)$	$I_{\text{HL}}(\tau)$	$\#\hat{\mathcal{C}}_{0(0,0)}$	Theory
$91_{\text{int}}$		$1 + 186p + 16142p^2 + \dots$	$1 + 186\tau^2 + 15954\tau^4 + \dots$	2	$[(E_7)_8 \text{ SCFT}] \times [(F_4)_{10} \times U(1) \text{ SCFT}]$
$14_{\text{int}}$		$1 + 326p + 49102p^2 + \dots$	$1 + 326\tau^2 + 48774\tau^4 + \dots$	2	$[(E_8)_{12} \text{ SCFT}] \times [(E_6)_6 \text{ SCFT}]$
$5_{\text{int}}$		$1 + 170p + 14601p^2 + \dots$	$1 + 170\tau^2 + 14429\tau^4 + \dots$	2	$[(E_6)_6 \text{ SCFT}] \times [(E_6)_{18} \times (G_2)_{10} \text{ SCFT}]$
$4_{\text{int}}$		$1 + 162p + 312p^{\frac{3}{2}} + 13365p^2 + \dots$	$1 + 162\tau^2 + 312\tau^3 + 13201\tau^4 + \dots$	2	$[(E_6)_{12} \times SU(2)_7 \text{ SCFT}]^2$
$3_{\text{int}}$		$1 + 159p + 160p^{\frac{3}{2}} + 12464p^2 + \dots$	$1 + 159\tau^2 + 160\tau^3 + 12303\tau^4 + \dots$	2	$[(E_6)_6 \text{ SCFT}] \times [(E_6)_{18} \times SU(2)_{20} \text{ SCFT}]$
$2_{\text{int}}$		$1 + 237p + 156p^{\frac{3}{2}} + 27140p^2 + \dots$	$1 + 237\tau^2 + 156\tau^3 + 26900\tau^4 + \dots$	3	$[(E_6)_6 \text{ SCFT}]^2 \times [(E_6)_{12} \times SU(2)_7 \text{ SCFT}]$
$1_{\text{int}}$		$1 + 312p + 46540p^2 + \dots$	$1 + 312\tau^2 + 46224\tau^4 + \dots$	4	$[(E_6)_6 \text{ SCFT}]^4$

$\#_{type}$	Fixture	$I_{\text{Schur}}(p)$	$I_{\text{HL}}(\tau)$	$\#\hat{\mathcal{C}}_{0(0,0)}$	Theory
$1_{\text{gauge}}$		$1 + 133p + 52p^{\frac{3}{2}} + 8446p^2 + \dots$	$1 + 133\tau^2 + 52\tau^3 + 8311\tau^4 + \dots$	2	
$2_{\text{gauge}}$		$1 + 156p + 11830p^2 + \dots$	$1 + 156\tau^2 + 11672\tau^4 + \dots$	2	
$3_{\text{gauge}}$		$1 + 326p + 12558p^2 + \dots$	$1 + 326\tau^2 + 12400\tau^4 + \dots$	2	

## 2.5 Gauge theory fixtures

The  $\underline{F}_4(a_1)$  puncture, in the twisted sector of the  $E_6$  theory, is “atypical” (in the nomenclature of [10]). That is, it carries a “hidden” marginal deformation. To access the full space of marginal couplings, we should resolve it to a pair of punctures:  $\underline{F}_4$  (the simple puncture from the twisted sector) and  $E_6(a_1)$  (the simple puncture from the untwisted sector). The coincident limit of those two punctures does not imply any gauge coupling becoming weak, instead we simply obtain  $\underline{F}_4(a_1)$ .

A fixture with an  $\underline{F}_4(a_1)$  puncture is thus a 4-punctured sphere in disguise, where the gauge theory is at a strong coupling point in the interior of the conformal manifold. (See Figure 2.2 for the gauge theory fixture  $1_{\text{gauge}}$  in our table.)

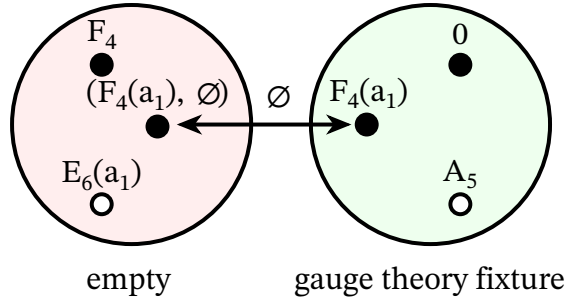


Figure 2.2: Resolving the atypical puncture in the gauge theory fixture  $1_{\text{gauge}}$

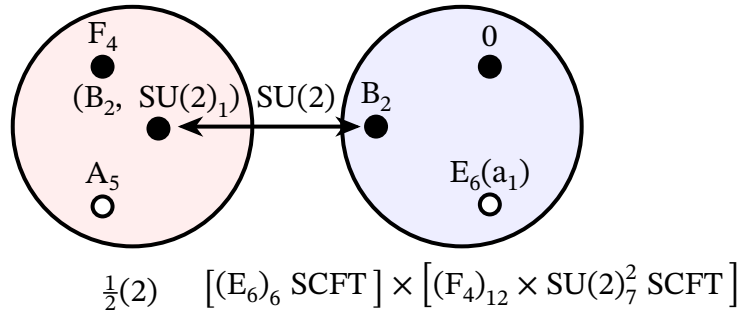


Figure 2.3: Degeneration A of the 4-punctured sphere relevant to  $1_{\text{gauge}}$

We computed that the theory has two stress tensors, and is thus a product SCFT. That is indeed the case, as we can see by examining the other degenerations of the 4-punctured sphere. Degeneration A is given in Figure 2.3, where one of the  $SU(2)$ s of the  $(F_4)_{12} \times SU(2)_7^2$  SCFT is gauged. Degeneration B is given in Figure 2.4, where a  $G_2$  subgroup of the  $E_8$  is gauged. In each case, there is a decoupled Minahan-Nemeschansky  $(E_6)_6$  SCFT, as anticipated.

The same remarks apply, *mutatis mutandis*, to the gauge theory fixture  $2_{\text{gauge}}$ . (Gauge theory fixtures  $2_{\text{gauge}}$  and  $3_{\text{gauge}}$  were also discussed in detail in §8.1 of [12].) In particular, Figures 2.6 and 2.7 show the two degenerations

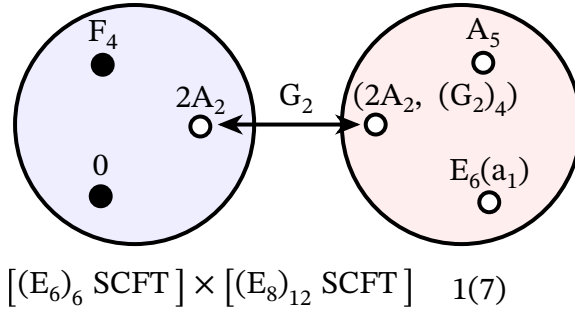


Figure 2.4: Degeneration B of the 4-punctured sphere relevant to  $1_{\text{gauge}}$

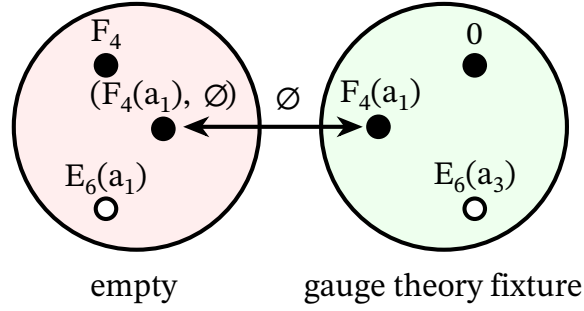


Figure 2.5: Resolving the atypical puncture in the gauge theory fixture  $2_{\text{gauge}}$  where there is a decoupled  $(E_6)_6$  SCFT.

This is a nice check that our formalism works, even when the SCFTs are not isolated.

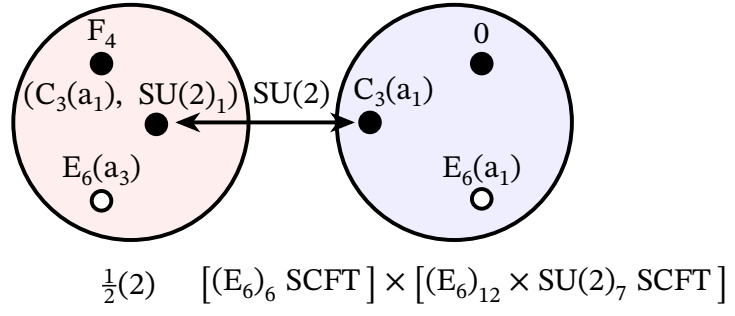


Figure 2.6: Degeneration A of the 4-punctured sphere relevant to  $2_{\text{gauge}}$

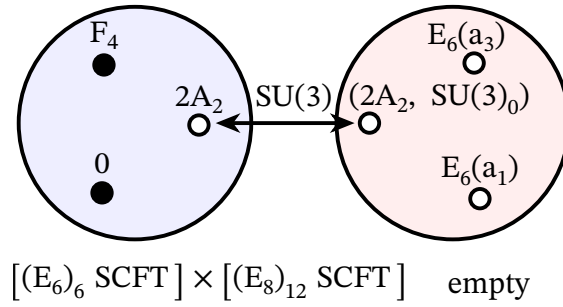
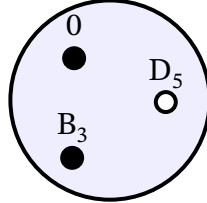


Figure 2.7: Degeneration B of the 4-punctured sphere relevant to  $2_{\text{gauge}}$

## 2.6 The new product SCFT

The following fixture



$$[(E_7)_8 \text{ SCFT}] \times [(F_4)_{10} \times U(1) \text{ SCFT}]$$

is a product SCFT that hasn't been identified previously<sup>4</sup>. Since it has rank-3, it must be a product of a rank-1 and a rank-2 theory. The possibilities for rank-1  $\mathcal{N} = 2$  SCFTs are very limited [43–46]. The only one consistent with the global symmetries and R-charges of the Coulomb branch parameters is the Minahan-Nemeschansky  $(E_7)_8$  SCFT. The other factor in the product is, then, a new rank-2 SCFT, with global symmetry  $(F_4)_{10} \times U(1)$ ,  $n_4 = n_5 = 1$  and  $(n_h, n_v) = (32, 16)$ . So far, we are not aware of an alternative class-S construction of this theory.

## 2.7 Moduli space of product SCFTs: a case study

We have identified a list of product SCFTs by counting the  $\mathcal{N} = 2$  stress tensor multiplet  $\hat{C}_{0(0,0)}$ . However, a product SCFT has more interesting properties than having more than one stress tensor. In particular, the

---

<sup>4</sup>Only an  $(F_4)_{18} \times SU(2)_{24} \times U(1)$  subgroup of the global symmetry is manifest. Of this, only (a subgroup of the)  $(F_4)_{18} \subset (E_7)_8 \times (F_4)_{10}$  is gaugeable, which makes the usual S-duality tricks useless for discerning that this is a product SCFT.

supersymmetric vacuum moduli space of a product SCFT should better be factorized into a product of moduli spaces of simple SCFTs. In this subsection we will explore the moduli space of the simplest product SCFT, namely the interacting fixture in the  $D_4$  theory as shown in Figure 2.1. In the following we will denote this theory as  $\mathcal{T}_{D_4}$ .

The Higgs branch of the rank-1 Minahan-Nemeschansky  $E_6$  SCFT is given by the centered moduli space of the one  $E_6$ -instanton on  $\mathbb{R}^4$ , or equivalently the minimal nilpotent orbit in  $\mathfrak{e}_6$  [47]. Its refined Hilbert series is given by [48]:

$$\mathcal{I}_{M(E_6,1)}(z) = \sum_{k=0}^{\infty} [0, k, 0, 0, 0, 0]_z \tau^{2k}. \quad (2.19)$$

Here  $z$  is the  $\mathfrak{e}_6$  fugacity and  $[0, k, 0, 0, 0, 0]_z$  is the character of the irreducible representation with Dynkin label  $[0, k, 0, 0, 0, 0]$ , where  $[0, 1, 0, 0, 0, 0]$  corresponds to the 78-dimensional adjoint representation of  $\mathfrak{e}_6$ .

It was argued in [19] that, for class- $\mathcal{S}$  theories whose corresponding Riemann surfaces have the topology of a sphere, the Higgs branch Hilbert series coincides with the Hall-Littlewood index. Concretely in those theories, the contribution from short multiplets of the type  $D_{R(0,j_2)}$  to the Hall-Littlewood index is the same as imposing constraints between Higgs branch operators in the Hilbert series calculation. From this perspective the factorization of the Higgs branch would be reflected through the refined Hall-Littlewood index for the theory  $\mathcal{T}_{D_4}$  being a “square” of (2.19). We have computed the refined



Hall-Littlewood index for  $\mathcal{T}_{D_4}$  up to  $\tau^6$  order<sup>5</sup>:

$$\begin{aligned} \mathcal{I}_{HL, \mathcal{T}_{D_4}}(z_1, z_2) = & 1 + [(78, 1) + (1, 78)]_{z_1, z_2} \tau^2 \\ & + [(2430, 1) + (1, 2430) + (78, 78)]_{z_1, z_2} \tau^4 \\ & + [(43758, 1) + (1, 43758) + (78, 2430) + (2430, 78)]_{z_1, z_2} \tau^6 + \dots \end{aligned} \tag{2.20}$$

In the above expression for simplicity we have denoted the irreducible representations using their dimensions.

We remark here that computing the refined Hall-Littlewood index to higher order in  $\tau$  is very challenging and thus refrains us from making further checks. Moreover, studying the Higgs branch at the level of Hilbert series does not involve its structure as a hyperkähler manifold. For other product SCFTs in our list, if all simple SCFTs that appear in the factorization have an alternative class- $\mathcal{S}$  realization, we could then compute the Hall-Littlewood indices to certain order in  $\tau$  and confirm the factorization of the index to that order.

Now we turn to study the Coulomb branch of the theory  $\mathcal{T}_{D_4}$ <sup>6</sup>. For this purpose we would need the Coulomb branch analysis for the rank-1 Minahan-Nemeschansky  $E_6$  SCFT. A realization of this theory in class- $\mathcal{S}$  is given by a fixture in the  $A_2$  theory with three full punctures, which is often called the  $T_3$  theory.  $T_3$  has a one-dimensional Coulomb branch, parametrized by  $u \in \mathbb{C}$ . The Seiberg-Witten geometry of  $T_3$  was analyzed in [49]. In particular, the

---

<sup>5</sup>This was part of results from a project with Anderson Trimm.

<sup>6</sup>The study of Coulomb branch of product SCFTs is ongoing work with Jacques Distler, Behzat Ergun, Qianyu Hao and Andy Neitzke.

period integrals are proportional to  $u^{1/3}$ , which is consistent with the fact that  $u$  has scaling dimension 3. Below we will analyze the Seiberg-Witten geometry of  $\mathcal{T}_{D_4}$  and we will see some first evidence that the Coulomb branch of  $\mathcal{T}_{D_4}$  is factorized into a product of two copies of the Coulomb branch of the  $T_3$  theory (the rank-1 Minahan-Nemeschansky  $E_6$  SCFT).

We use the  $PSL(2, \mathbb{C})$  symmetry of  $\mathbb{CP}^1$  to fix the three punctures to be located at  $(z_1, z_2, z_3) = (0, 1, \infty)$ , where punctures 1 and 2 are the ones labeled by the  $D$ -partition  $[3, 3, 1, 1]$  and puncture 3 is the full puncture in the  $D_4$  theory. The UV curve is  $C = \mathbb{CP}^1 \setminus \{0, 1, \infty\}$ . The  $k$ -differentials in the  $D_4$  theory are  $\phi^{(2)}, \phi^{(4)}, \phi^{(6)}$  and the Pfaffian  $\tilde{\phi}$ . The pole structures and constraints (as worked out in [26]) at the three punctures yield that the only non-vanishing  $k$ -differential is  $\phi^{(6)}$ , which has at most fourth-order poles at  $z_{1,2} = 0, 1$ , and at most a fifth-order pole at  $z_3 = \infty$ . Moreover, the leading pole coefficients of  $\phi^{(6)}$  at  $z_{1,2} = 0, 1$  satisfy constraints of the form  $c_{1,2} = (a_{1,2})^2$ , where  $a_{1,2}$  parametrizes the Coulomb branch [9, 26]. The Seiberg-Witten curve  $\Sigma \subset T^*C$  is then given by:

$$\lambda^2(\lambda^6 - \phi^{(6)}) = 0, \tag{2.21}$$

where

$$\phi^{(6)} = \frac{a_1^2 + (a_2^2 - a_1^2)z}{z^4(z-1)^4} dz^6. \tag{2.22}$$

$\lambda$  is the Seiberg-Witten differential, concretely in terms of coordinates  $(x, z)$  on  $T^*C$ ,  $\lambda = x dz$ . Two sheets of  $\Sigma$  are trivial coverings of  $C$ , the other six sheets form a branched covering of  $C$  with a branch point at  $z_p := \frac{a_1^2}{a_1^2 - a_2^2}$ . Denote this

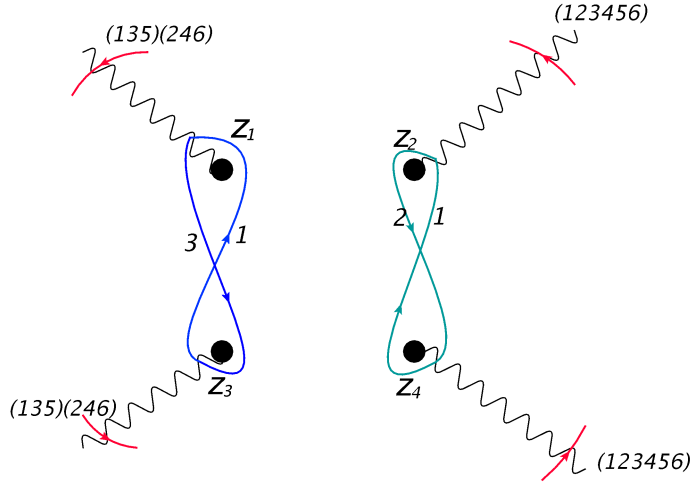


Figure 2.8: Choice of branch cuts for  $\bar{\Sigma}'$  and cycles in homology classes  $\gamma_1$  (blue) and  $\gamma_2$  (green) in  $H_1(\bar{\Sigma}', \mathbb{Z})$ . The four branch points are at  $z_1 = 0$ ,  $z_2 = z_p$ ,  $z_3 = 1$  and  $z_4 = \infty$ . The four branch cuts are represented by wavy lines and they meet at some point on  $\mathbb{CP}^1$ . Each branch cut is labeled with the corresponding sheet permutation and the direction to do the gluing.

branched covering as  $\Sigma'$  and fill in the punctures, we obtain a genus 4 curve  $\bar{\Sigma}'$ .  $\bar{\Sigma}'$  is a branched covering of  $\mathbb{CP}^1$  with four branch points at  $0, 1, \infty, z_p$ . Concretely we could obtain  $\bar{\Sigma}'$  by gluing together six sheets along branch cuts as shown in Figure 2.8, where the six sheets are labeled by the six possible choices of 6-th root of  $\phi^{(6)}$ .

If the Coulomb branch of  $\mathcal{T}_{D_4}$  has the desired factorization, then for any homology class  $\gamma \in H_1(\bar{\Sigma}', \mathbb{Z})$ , the corresponding period integral would take the following form:

$$\oint_{\gamma} \lambda = Au_1^{1/3} + Bu_2^{1/3}, \quad (2.23)$$

where  $A, B \in \mathbb{C}$  and  $u_{1,2}$  are some functions of  $a_{1,2}$ . We would like to confirm

this property and identify  $u_{1,2}$ . First let us look at the cycle in homology class  $\gamma_1$  as depicted in Figure [2.8](#), we have

$$\oint_{\gamma_1} \lambda = (e^{2\pi i/3} - 1) \int_0^1 \frac{(a_2^2 - a_1^2)^{1/6} (z - z_p)^{1/6}}{z^{2/3} (1 - z)^{2/3}} dz \sim (\sqrt{a_1^2} + \sqrt{a_2^2})^{1/3}. \quad (2.24)$$

Similarly for a cycle in homology class  $\gamma_2$  as depicted in Figure [2.8](#),

$$\oint_{\gamma_2} \lambda = (e^{2\pi i/6} - 1) \int_{z_p}^{\infty} \frac{(a_2^2 - a_1^2)^{1/6} (z - z_p)^{1/6}}{z^{2/3} (1 - z)^{2/3}} dz \sim (\sqrt{a_1^2} - \sqrt{a_2^2})^{1/3}. \quad (2.25)$$

Moreover one could argue that for any homology class  $\gamma$  the period integral takes the form of [\(2.23\)](#), with

$$u_1 = \sqrt{a_1^2} + \sqrt{a_2^2}, \quad u_2 = \sqrt{a_1^2} - \sqrt{a_2^2}. \quad (2.26)$$

Concretely, due to the pole/zero order of  $\phi^{(6)}$  at the branch point, to prove [\(2.23\)](#) it is sufficient to check that the integrals between the branch points take the desired form, which is indeed the case. For example,

$$\begin{aligned} \int_1^{\infty} \frac{(a_2^2 - a_1^2)^{1/6} (z - z_p)^{1/6}}{z^{2/3} (1 - z)^{2/3}} dz &\sim (a_2^2 - a_1^2)^{1/6} \cos\left(\frac{1}{3} \arcsin\left[\frac{a_1}{\sqrt{a_1^2 - a_2^2}}\right]\right) \\ &\sim A(\sqrt{a_1^2} + \sqrt{a_2^2})^{1/3} + B(\sqrt{a_1^2} - \sqrt{a_2^2})^{1/3}, \end{aligned} \quad (2.27)$$

where  $A, B \in \mathbb{C}$ <sup>7</sup>.

Although [\(2.23\)](#) offers a strong evidence, it is not enough to prove that the Coulomb branch of  $\mathcal{T}_{D_4}$  is factorized into two copies of the Coulomb branch of the rank-1 Minahan-Nemeschansky  $E_6$  theory. The proof would involve a

---

<sup>7</sup>Here we have used  $\cos(3\alpha) = 4\cos^3\alpha - 3\cos\alpha$ .

detailed study of the electromagnetic charge lattice of the infrared theory, which is still under investigation.

We have seen that even for the simplest example of product SCFTs the study of its supersymmetric vacuum moduli space is already quite complicated. In future work we would like to have a better picture of how the moduli space factorizes, preferably also for more complicated product SCFTs. Another interesting direction that we are pursuing is to understand exactly why and how these product SCFTs appear in class- $\mathcal{S}$  construction.

# Chapter 3

## Line defect Schur indices, Verlinde algebras and $U(1)_r$ fixed points<sup>1</sup>

### 3.1 Introduction

In this chapter we describe a puzzling new feature of the *line defect Schur index* in  $\mathcal{N} = 2$  theories, introduced in [50] and recently reconsidered in [51]. In short, there is an unexpectedly close relation between:

- the Schur index in the presence of a supersymmetric (half) line defect  $L$ ,
- the vevs  $\langle L \rangle$  in  $U(1)_r$ -invariant vacua of the theory compactified on  $S^1$ .

The precise statements and some discussion appear in §3.1.7-§3.1.9 below; the intervening sections provide the necessary notation and background.

#### 3.1.1 Schur indices and chiral algebras

In [52] a novel correspondence between 4d  $\mathcal{N} = 2$  SCFT and 2d chiral algebras was discovered: given an  $\mathcal{N} = 2$  SCFT, there is a corresponding

---

<sup>1</sup>Previously published as A. Neitzke and F. Yan, “Line defect Schur indices, Verlinde algebras and  $U(1)_r$  fixed points”, JHEP 11 (2017) 035 [4]. In collaboration with Andrew Neitzke, I contributed to formulating the commutative diagram relation, testing the relation in various examples, and writing up the paper.

chiral algebra  $\mathcal{A}$ . The operators in the vacuum module of the chiral algebra  $\mathcal{A}$  correspond to local operators in the original  $\mathcal{N} = 2$  theory which contribute to the Schur index  $\mathcal{I}(q)$  (and Macdonald index<sup>2</sup>).

The algebras  $\mathcal{A}$  corresponding to Argyres-Douglas theories have been intensively studied in e.g. [52, 54–60]. In particular, the chiral algebra for the  $(A_1, A_{2N})$  Argyres-Douglas theory<sup>3</sup> was conjectured to be the Virasoro minimal model with  $(p, q) = (2, 2N+3)$ , and the chiral algebra for  $(A_1, D_{2N+1})$  Argyres-Douglas theories was conjectured to be  $\widehat{\mathfrak{sl}(2)}_k$  at level  $k = -4N/(2N+1)$ . The Schur indices for certain Argyres-Douglas theories have been computed and indeed match the vacuum characters of the corresponding 2d chiral algebra [51, 55, 56, 60].

### 3.1.2 Schur indices with half line defects and Verlinde algebra

In [51] this story was extended to include the *non-vacuum* characters of the chiral algebra  $\mathcal{A}$ , by considering a new Schur index  $\mathcal{I}_L(q)$ , which counts operators of the  $\mathcal{N} = 2$  SCFT which sit at the endpoint of a supersymmetric “half line defect”  $L$ . In various examples, [51] found that  $\mathcal{I}_L(q)$  can be expressed as a linear combination of characters associated to modules for the algebra  $\mathcal{A}$ :

$$\mathcal{I}_L(q) = \sum_{\beta} v_{L,\beta}(q) \chi_{\beta}(q) \tag{3.1}$$

---

<sup>2</sup>Macdonald index and its relation to chiral algebra was studied in [53].

<sup>3</sup>Here and below we use the taxonomy of Argyres-Douglas theories from [61], in which they are labeled by pairs of ADE type Lie algebras. Argyres-Douglas theories were first discovered in [62, 63].

where  $\chi_\beta(q)$  are the characters, and  $v_{L,\beta}(q)$  are some simple Laurent polynomials in  $q$ , with integer coefficients.

In the expansion (3.1), the index  $\beta$  is running over some finite collection of modules, which moreover are closed under a canonical action of the modular  $S$  matrix. This being so, we can use the Verlinde formula to define a commutative and associative algebra  $\mathcal{V}$ , generated by the “primaries”  $\Phi_\beta$  corresponding to the modules with characters  $\chi_\beta(q)$ , with product laws of the form

$$[\Phi_\beta] \times [\Phi_\alpha] = c_{\beta\alpha}^\gamma [\Phi_\gamma]. \quad (3.2)$$

In  $(A_1, A_{2N})$  Argyres-Douglas theories this commutative product corresponds to the true fusion operation in the  $(2, 2N + 3)$  Virasoro minimal model. More generally though, we do not claim to interpret this product as any kind of fusion operation: we just use the formal rule provided by the Verlinde formula. In the following we will often refer to these product laws as *modular fusion rules*<sup>4</sup> of the Verlinde-like algebra  $\mathcal{V}$ .

Now, let us return to the expansion (3.1) and specialize the coefficients  $v_{L,\beta}(q)$  to  $q = 1$ , defining

$$V_{L,\beta} = v_{L,\beta}(q = 1). \quad (3.3)$$

Then for every line defect  $L$  we get an element  $f(L) \in \mathcal{V}$  by

$$f(L) = \sum_{\beta} V_{L,\beta} [\Phi_\beta]. \quad (3.4)$$

---

<sup>4</sup>We thank Christopher Beem for suggesting us to make a distinction from the true fusion rules.



Remarkably, [51] found evidence that this map is actually a *homomorphism* of commutative algebras,

$$f : \mathcal{L} \rightarrow \mathcal{V} \tag{3.5}$$

where  $\mathcal{L}$  is the commutative OPE algebra of line defects in the original  $\mathcal{N} = 2$  theory.

$f$  always maps the trivial line defect to the vacuum module, since the Schur index without any line defect insertions is the vacuum character of  $\mathcal{A}$ . Thus the fact that the trivial line defect is the identity in the OPE algebra gets mapped to the fact that the vacuum module is the identity in the Verlinde algebra  $\mathcal{V}$ .

Evidence for the homomorphism property of the line defect Schur index was observed in [51] in the  $(A_1, A_2)$  and  $(A_1, A_4)$  theories. In §3.5.4 below we give evidence that the same is true in the  $(A_1, A_6)$  theory. We also extend to the  $(A_1, D_3)$  and  $(A_1, D_5)$  theories, in §3.6.1 and §3.6.2, but this involves a little twist: see §3.1.8 below.

### 3.1.3 A simple example

Just to fix ideas, we quickly review here the case of the Argyres-Douglas theory of type  $(A_1, A_2)$ . The basic data are:

- There are five distinguished nontrivial line defects  $L_1, \dots, L_5$  in the theory, which generate all the rest by operator products. In fact one only needs products involving *consecutive*  $L_i$ : the most general simple line

defect can be written [\[23\]](#)

$$L = L_i^m L_{i+1}^n \tag{3.6}$$

for  $i \in \{1, \dots, 5\}$  and  $m, n \geq 0$  (letting  $L_6 = L_1$ ). We also have the trivial line defect which we write as 1.

- The chiral algebra  $\mathcal{A}$  is the  $(2, 5)$  Virasoro minimal model, with  $c = -22/5$ . The corresponding Verlinde algebra  $\mathcal{V}$  has two generators  $[\Phi_{1,1}]$ ,  $[\Phi_{1,2}]$  corresponding to the two primaries.  $[\Phi_{1,1}]$  is the identity element, so the only nontrivial product is  $[\Phi_{1,2}] \times [\Phi_{1,2}]$ , which is

$$[\Phi_{1,2}] \times [\Phi_{1,2}] = [\Phi_{1,1}] + [\Phi_{1,2}]. \tag{3.7}$$

The line defect Schur indices come out to [\[51\]](#)

$$\mathcal{I}_1(q) = \chi_{1,1}(q), \quad \mathcal{I}_{L_i}(q) = q^{-\frac{1}{2}}(\chi_{1,1}(q) - \chi_{1,2}(q)). \tag{3.8}$$

Thus the homomorphism  $f$  in this case is

$$f(1) = [\Phi_{1,1}], \quad f(L_i) = [\Phi_{1,1}] - [\Phi_{1,2}]. \tag{3.9}$$

In particular,  $f$  forgets the index  $i$ , so it identifies the 5 generators  $L_i$ .<sup>[5](#)</sup> Moreover,  $f$  collapses the infinite-dimensional algebra  $\mathcal{L}$ , spanned by the operators [\(3.6\)](#), down to the two-dimensional algebra  $\mathcal{V}$ .

---

<sup>5</sup>We will give a derivation of this property of  $f$  in [§3.2.4](#)

### 3.1.4 Diagonalizing the Verlinde algebra

To explain the main new results of this paper, we need a brief digression to recall a structural fact about the Verlinde algebra  $\mathcal{V}$ : the modular  $S$  operator gives a canonical diagonalization of  $\mathcal{V}$  [64]. Concretely, if we choose an ordering of the  $n$  primaries, then we can represent the operation of fusion with  $\Phi_i$  by an  $n \times n$  matrix  $N_{\Phi_i}$ , and likewise  $S$  by an  $n \times n$  matrix; then the statement is that the matrices

$$\hat{N}_{\Phi} = SN_{\Phi}S^{-1} \quad (3.10)$$

are all diagonal.

For example, in the  $(2, 5)$  Virasoro minimal model, if we choose the ordering of the primaries  $(\Phi_{1,1}, \Phi_{1,2})$ , then we have [65]

$$N_{\Phi_{1,1}} = \begin{pmatrix} 1 & 0 \\ 0 & 1 \end{pmatrix}, \quad N_{\Phi_{1,2}} = \begin{pmatrix} 0 & 1 \\ 1 & 1 \end{pmatrix}, \quad S = \frac{2}{\sqrt{5}} \begin{pmatrix} -\sin \frac{2\pi}{5} & \sin \frac{4\pi}{5} \\ \sin \frac{4\pi}{5} & \sin \frac{2\pi}{5} \end{pmatrix}, \quad (3.11)$$

from which we can compute

$$\hat{N}_{\Phi_{1,1}} = \begin{pmatrix} 1 & 0 \\ 0 & 1 \end{pmatrix}, \quad \hat{N}_{\Phi_{1,2}} = \begin{pmatrix} \frac{1-\sqrt{5}}{2} & 0 \\ 0 & \frac{1+\sqrt{5}}{2} \end{pmatrix}. \quad (3.12)$$

The representation of  $\mathcal{V}$  by the diagonal matrices  $\hat{N}_{\Phi}$  shows that  $\mathcal{V}$  is naturally isomorphic to a direct sum of copies of  $\mathbb{C}$ . Moreover these copies correspond canonically to the primaries themselves, using the ordering of the primaries we have chosen. Another way of saying this is:  $\mathcal{V}$  is canonically isomorphic to the algebra of functions on the set of primaries of  $\mathcal{A}$ . We will use the statement in this form, in §3.1.5 below.

### 3.1.5 Verlinde algebra and $U(1)_r$ -fixed points in three dimensions

Now we recall another place where the Verlinde algebra of  $\mathcal{A}$  has recently appeared.

We consider the compactification of our superconformal  $\mathcal{N} = 2$  theory to three dimensions on  $S^1$ . As is well known, beginning with [66], the Coulomb branch of the compactified theory is a hyperkähler space  $\mathcal{N}$ . For example, if our theory is a theory of class  $\mathcal{S}$ , say  $\mathcal{S}[\mathfrak{g}, C]$ , then  $\mathcal{N}$  is a moduli space of solutions of Hitchin equations on  $C$  with gauge algebra  $\mathfrak{g}$  [1, 21].

The  $U(1)_r$  symmetry of the theory acts geometrically on  $\mathcal{N}$ . This action is an important tool in the study of this space. For example, it can be used to compute the Betti numbers of the Hitchin moduli spaces, as was noted already in [21]. More recently [67, 68] this  $U(1)_r$  action has been used to define and compute a new “ $U(1)_r$ -equivariant index” for  $\mathcal{N}$ , related to a Coulomb branch index in the  $\mathcal{N} = 2$  theory. In both computations the starring role is played by the *fixed locus*  $F \subset \mathcal{N}$  of the  $U(1)_r$  symmetry. The points of  $F$  are the  $U(1)_r$ -invariant vacua of the compactified theory.

For our purposes the key fact about  $F$  is the following recent observation: *the points of  $F$  are naturally in 1-1 correspondence with the primaries of  $\mathcal{A}$*  [61, 69–71].<sup>6</sup> Combining this correspondence with the picture of  $\mathcal{V}$  reviewed

---

<sup>6</sup>Some early hints of this appeared in [61], and a precise correspondence of this sort in the case of  $(A_m, A_n)$  Argyres-Douglas theories with  $(m+1, n+1) = 1$  is developed in [69], first reported in [70]. This correspondence was used extensively in [71], where the  $U(1)_R$  weights at the fixed points were also worked out; that work also substantially broadened the scope of the correspondence, well beyond the class of  $(A_m, A_n)$  theories. Despite all

in §3.1.4, we conclude that there is a canonical isomorphism

$$h : \mathcal{V} \rightarrow \mathcal{O}(F), \tag{3.13}$$

where  $\mathcal{O}(F)$  means the algebra of functions on  $F$ . Concretely,  $h$  maps  $[\Phi]$  to the vector of diagonal entries of  $\hat{N}_\Phi$ , using the correspondence above to match up the points of  $F$  with the positions along the diagonal.

### 3.1.6 Fixed points and vevs

We consider the vacuum expectation values of  $\frac{1}{2}$ -BPS line defects wrapped around  $S^1$  in  $S^1 \times \mathbb{R}^3$ . These vevs are functions on the vacuum moduli space  $\mathcal{N}$ ; the process of taking vevs gives a homomorphism of commutative algebras

$$\mathcal{L} \rightarrow \mathcal{O}(\mathcal{N}) \tag{3.14}$$

from the OPE algebra of  $\frac{1}{2}$ -BPS line defects to the algebra  $\mathcal{O}(\mathcal{N})$  of holomorphic functions on  $\mathcal{N}$ .<sup>7</sup> Now consider the *restriction* of these vevs to the  $U(1)_r$ -fixed locus  $F \subset \mathcal{N}$ : this gives another homomorphism of commutative algebras,

$$g : \mathcal{L} \rightarrow \mathcal{O}(F). \tag{3.15}$$

In Argyres-Douglas theories, the map  $g$  is very far from being an isomorphism: it forgets most of the details of a line defect, remembering only

---

this, as far as we know, nobody has yet provided a first-principles explanation of *why* the correspondence between points of  $F$  and primaries of  $\mathcal{A}$  exists. In this paper we just take this correspondence as a given.

<sup>7</sup>In fact, in all examples we know, this is an isomorphism  $\mathcal{L} \simeq \mathcal{O}(\mathcal{N})$ , though we do not need this fact in anything that follows.

its vevs at the finitely many  $U(1)_r$ -invariant vacua. This is reminiscent of the fact that the map  $f$ , built from line defect Schur indices  $\mathcal{I}_L$ , likewise forgets most of the details of the line defects  $L$ . In the next section we flesh this out into a precise sense in which  $f$  and  $g$  are “the same.”

Before we state our main result, we would like to point out that the  $\frac{1}{2}$ -BPS line defects that we are talking about in this section are *full line defects*, which are by definition different from the *half line defects* in [3.1.2](#). However, away from the endpoints of the half line defects they are “locally” the same object. In particular the OPE algebra of half line defects is isomorphic to the OPE algebra of full line defects, both of which we denote as  $\mathcal{L}$ .

### 3.1.7 The commutative diagram

So far in this introduction we have described three *a priori* unrelated commutative algebras associated to an  $\mathcal{N} = 2$  SCFT:

- The OPE algebra  $\mathcal{L}$  of  $\frac{1}{2}$ -BPS line defects,
- The Verlinde algebra  $\mathcal{V}$  associated to the chiral algebra  $\mathcal{A}$ ,
- The algebra  $\mathcal{O}(F)$  of functions on the set of  $U(1)_r$ -invariant vacua of the theory compactified on  $S^1$ .

We also described three *a priori* unrelated maps between these algebras:

- The map  $f : \mathcal{L} \rightarrow \mathcal{V}$  obtained by computing Schur indices in the presence of half line defects and expanding them in terms of characters of  $\mathcal{A}$ ,

- The isomorphism  $h : \mathcal{V} \rightarrow \mathcal{O}(F)$ , constructed using the mysterious identification between  $U(1)_r$ -invariant vacua and chiral primaries, and using also the modular  $S$  matrix,
- The map  $g : \mathcal{L} \rightarrow \mathcal{O}(F)$  obtained by compactifying the theory on  $S^1$  and evaluating line defect vevs in  $U(1)_r$ -invariant vacua of the reduced theory.

These ingredients can be naturally assembled into a diagram:

$$\begin{array}{ccc}
 \mathcal{L} & \xrightarrow{f} & \mathcal{V} \\
 & \searrow g & \downarrow h \\
 & & \mathcal{O}(F)
 \end{array}$$

This raises the natural question of whether the diagram *commutes*, i.e. whether

$$h \circ f = g. \tag{3.16}$$

In §3.5 below, we verify by direct computation that (3.16) indeed holds, in the Argyres-Douglas theories of type  $(A_1, A_2)$ ,  $(A_1, A_4)$ , and  $(A_1, A_6)$ . In §3.6 we verify a similar statement in  $(A_1, D_3)$  and  $(A_1, D_5)$  theories: see §3.1.8 below for more on this.

The commutativity (3.16) is the main new result of this paper. In a sense it is not surprising — once you realize that this diagram exists, it is hard to imagine that it would not commute — but on the other hand its physical meaning is not at all transparent, at least to us. It should be interesting to unravel. We comment a bit further on this question in §3.1.9 below.

### 3.1.8 Flavor symmetries

In  $\mathcal{N} = 2$  theories with flavor symmetries the story described above can be enriched. The Schur index, rather than being a function  $\mathcal{I}_L(q)$ , is promoted to  $\mathcal{I}_L(q, z)$  where  $z$  stands for the flavor fugacities. The chiral algebra  $\mathcal{A}$  also contains currents for the flavor symmetry group, and thus its characters are promoted to  $\chi_i(q, z)$ . It is natural to ask whether there are analogues of the homomorphisms  $f, g, h$  in such theories with the extra parameters  $z$  included.<sup>8</sup>

In §3.6 below we consider this question for the  $(A_1, D_3)$  and  $(A_1, D_5)$  Argyres-Douglas theories, which have flavor symmetry  $SU(2)$ . The Cartan subgroup of  $SU(2)$  consists of matrices  $\text{diag}(z, z^{-1})$  for  $|z| = 1$ ; thus the fugacity in this case is just a single number  $z$ . The chiral algebras in these theories are  $\mathcal{A} = \widehat{\mathfrak{sl}(2)}_{-\frac{4}{3}}$  and  $\mathcal{A} = \widehat{\mathfrak{sl}(2)}_{-\frac{8}{5}}$  respectively.

In the compactification of the theory on  $S^1$ , turning on the fugacity  $z$ , with  $|z| = 1$ , corresponds to switching on a “flavor Wilson line” around the  $S^1$ . Such a Wilson line leads to a deformation of  $\mathcal{N}$  which does not break the  $U(1)_r$  symmetry. Thus for any fixed  $z$  we can consider the fixed locus  $F_z \subset \mathcal{N}_z$ , which turns out to be discrete, just as in the  $(A_1, A_{2n})$  theories we considered above. Evaluating line defect vevs at  $F_z$  we get a homomorphism

$$g_z : \mathcal{L} \rightarrow \mathcal{O}(F_z). \tag{3.17}$$

---

<sup>8</sup>In [51] the case of  $(A_1, D_3)$  was considered, after specializing to  $z \rightarrow 1$  to “forget” the flavor symmetry. Though this limit is very special in the sense that characters of the two non-vacuum admissible representations diverge in this limit and only one linear combination of the two characters is well-defined. This linear combination and the vacuum character transform into each other under modular transformations [72].



Now we would like to repeat the story of §3.1.7 here, i.e. to construct maps  $f_z$  and  $h_z$ , and to verify (3.16). A key question arises: what should we use as “Verlinde algebra”? There are no conventional two-dimensional conformal field theories with  $\mathcal{A}$  as symmetry algebras; the usual candidate with symmetry  $\widehat{\mathfrak{sl}(2)}_k$  would be the WZW model, but that only makes sense for positive integer  $k$ . Thus there is no clear physically-defined notion of Verlinde algebra. Still, it was realized in [73] that at *admissible* levels there is a finite set of *admissible* representations of  $\mathcal{A}$  whose characters span a representation of the modular group  $SL(2, \mathbb{Z})$ . A Verlinde-like algebra built from the *admissible* representations  $\mathcal{V}_1$  was constructed in [74] where the fusion rules were given by naive application of the Verlinde formula [73].  $\mathcal{V}_1$  has the odd feature that some of the structure constants are equal to  $-1$ .<sup>9</sup>

Nevertheless, we could try to construct  $f_z$  and  $h_z$ , and verify (3.16), using this algebra  $\mathcal{V}_1$ . What we find experimentally in §3.6 below is that this does not quite work: we need to use a deformed Verlinde-like algebra  $\mathcal{V}_z$ .  $\mathcal{V}_z$  is obtained from  $\mathcal{V}_1$  by replacing each structure constant  $-1$  by  $-z^2$ . Once we make this modification, the whole story goes through as in §3.1.7 above.

---

<sup>9</sup>Fusion rules of  $\widehat{\mathfrak{sl}(2)}_k$  at admissible negative fractional level have been studied intensively over the years and have been completely solved and understood recently in [75,76] (see also references therein). From this point of view, the negative structure constants have to do with the fact that admissible representations are not closed under fusion. In any case, in our context we are simply considering a Verlinde-like algebra  $\mathcal{V}_1$  defined by naive application of the Verlinde formula, and not worrying too much about whether it has a fusion interpretation.

### 3.1.9 Interpretations and comments

- The main new result of our paper is the commutative diagram in §3.1.7. What is the physical interpretation of this commutative diagram? One tempting possibility is that there is a new *localization* computation of the Schur index. Indeed, if we think of the Schur index as a kind of partition function on  $S^3 \times S^1$ , we could imagine computing it by first reducing on  $S^1$  and then making some computation in the resulting effective theory on  $S^3$ . After this reduction the line defects become local operators, which are determined by their vevs on  $\mathcal{N}$ . In a localization computation using  $U(1)_r$ , they could get further reduced to just their vevs in the  $U(1)_r$ -invariant vacua. This would match our observation that the object  $f(L)$  — which contains much<sup>10</sup> of the information of the Schur index  $\mathcal{I}_L$  — is linearly related to  $g(L)$ , i.e. to the vevs of  $L$  in the  $U(1)_r$ -invariant vacua.
- Our verification of the commutativity (3.16) requires us to evaluate explicitly the vacuum expectation values of  $\frac{1}{2}$ -BPS line defects at the fixed points of the  $U(1)_r$  action on  $\mathcal{N}$ . In the language of the Hitchin system, this amounts to solving an instance of the *nonabelian Hodge correspondence*: for some specific Higgs bundles, we determine the corresponding complex flat connections up to equivalence. It would be very interesting to see how far one can push these ideas: can we compute the vevs in

---

<sup>10</sup>Though not quite all, because of the need to take  $q \rightarrow 1$  in the coefficients  $v$

every case where the vacua are isolated? Can we extend beyond the fixed points, say to get some information about their infinitesimal neighborhoods? Can we say anything about non-isolated fixed points?

- It is natural to ask how broadly the commutative diagram of §3.1.7 exists; so far we have checked it only in five theories. We conjecture that it exists more generally whenever it makes sense, i.e. whenever the  $U(1)_r$ -invariant vacua of the theory reduced on  $S^1$  are all isolated. The  $U(1)_r$ -invariant vacua are isolated in all Argyres-Douglas theories where the question has been investigated, e.g. the  $(A_m, A_n)$  theories for  $\gcd(m+1, n+1) = 1$ , but more generally they are usually not isolated.
- One of the simplest examples where the  $U(1)_r$ -invariant vacua are *not* isolated is  $\mathcal{N} = 2$  super Yang-Mills with  $G = SU(2)$  and  $N_f = 4$ , compactified on  $S^1$  with generic flavor Wilson lines. In this theory it appears that there are 4 isolated  $U(1)_r$ -invariant vacua, but also an  $S^2$  of  $U(1)_r$ -invariant vacua, as explained e.g. in [77]. In this theory [71] argued that nevertheless there is a correspondence between *connected components* of the space of  $U(1)_r$ -invariant vacua and chiral primaries. It would be very interesting to understand how the diagram (3.16) can be extended to this case. (An obstacle to the most naive extension is that the line defect vevs are not constant on the  $S^2$  of invariant vacua. Perhaps one needs instead to take the *average* over this  $S^2$ .)
- In this paper one of the main players is the homomorphism  $f : \mathcal{L} \rightarrow \mathcal{V}$ .

The observation that there is some relation between algebras of line defects and Verlinde algebras was made already in [61]. Indeed, that paper described a map  $f' : \mathcal{L} \rightarrow \mathcal{V}$  in the  $(A_1, A_{2N})$  theories, constructed in a different way, by mapping certain distinguished line defects directly to minimal model primaries.<sup>11</sup> To forestall a possible confusion, we emphasize that  $f$  and  $f'$  are *not* the same. For example, in the  $(A_1, A_2)$  theory we have  $f'(L_i) = [\Phi_{1,2}]$ , while (3.9) says  $f(L_i) = [\Phi_{1,1}] - [\Phi_{1,2}]$ .

- Beyond line defects one could also consider surface defects and interfaces between surface defects. The Schur index in the presence of surface defects, and its relation to 2d chiral algebra, were studied quite recently in [78, 79] and also featured in the ongoing work [80]. It might be interesting to incorporate surface defects into the story of this paper.
- In this paper we focused on examples of  $(A_1, A_{2N})$  and  $(A_1, D_{2N+1})$  Argyres-Douglas theories, mainly because their chiral algebras have been relatively well understood and computation of line defect generators is not too complicated. What about other  $(A_1, \mathfrak{g})$  Argyres-Douglas theories? There is one more example which we expect should be relatively straightforward, namely  $(A_1, D_4)$ , for which the chiral algebra is  $\widehat{\mathfrak{sl}(3)}_{-3/2}$  [55, 56, 81, 82]. Beyond this:

– The chiral algebra for  $(A_1, A_{2N-1})$  Argyres-Douglas theories with

---

<sup>11</sup>The distinguished line defects in question actually coincide with the generators  $A_i, B_i, \dots$  which we use in §3.5

$N > 2$  is conjectured to be the  $\mathcal{B}_{N+1}$  algebra, the subregular quantum Hamiltonian reduction of  $\widehat{\mathfrak{sl}(N)}_{-N^2/(N+1)}$  [57, 72]<sup>12</sup>. As pointed out in [71], the relevant modules associated with the  $U(1)_r$  fixed points depend on the parity of  $N$ , and for even  $N$ , the relevant modules are suitable representatives of local modules which are closed under modular transformation [57, 72, 85, 86]. For odd  $N$ ,  $S$ -transformation turns local modules into twisted modules [57, 72, 85, 86], which makes the matching of  $U(1)_r$  fixed points with relevant modules very subtle [71]. These local and twisted modules and their modular properties are studied in [72, 85, 86].

- The situation is similar for  $(A_1, D_{2N})$  Argyres-Douglas theories with  $N > 2$ . Here the chiral algebra has been conjectured to be the  $\mathcal{W}_N$  algebra coming from a non-regular quantum Hamiltonian reduction of  $\widehat{\mathfrak{sl}(N+1)}_{-(N^2-1)/N}$  [57]. For even  $N$ , [71] confirmed that the relevant modules are suitable representatives of local modules listed in [57], while for odd  $N$  the situation becomes subtle again [71] since  $S$ -transformation turns local modules into twisted modules [57].
- Chiral algebras for  $(A_1, E_{6,7,8})$  Argyres-Douglas theories were conjectured in [56, 58], and at least for  $(A_1, E_6)$  and  $(A_1, E_8)$  there is a natural guess for the relevant class of modules. However, in these theories the computation of line defect generators and their framed

---

<sup>12</sup>Chiral algebra for  $(A_1, A_{2N-1})$  and  $(A_1, D_{2N})$  Argyres-Douglas theories were reproduced in [58] along with new results for generalized Argyres-Douglas theories in the sense of [83, 84].

BPS spectra has not been worked out; it would be interesting to develop it.

## 3.2 Schur indices and their IR formulas

In this section we review the definition and IR formula for the ordinary Schur index and the Schur index with half line defects inserted.

### 3.2.1 The Schur index

The superconformal index of a four-dimensional  $\mathcal{N} = 2$  SCFT is defined as [19, 40]

$$\mathcal{I}(p, q, t, a_i) = \text{Tr}(-1)^F p^{j_2 - j_1 - r} q^{j_2 + j_1 - r} t^{R+r} \prod_i a_i^{f_i} e^{-\beta \delta_{2\dot{-}}}, \quad (3.18)$$

where

$$2\delta_{2\dot{-}} = \{\tilde{Q}_{2\dot{-}}, \tilde{Q}_{2\dot{-}}^\dagger\} = E - 2j_2 - 2R + r. \quad (3.19)$$

Here  $p, q, t$  are three superconformal fugacities,  $a_i$  are flavor symmetry fugacities,  $E$  is the scaling dimension,  $j_1$  and  $j_2$  are Cartan generators of  $SU(2)_1 \times SU(2)_2$ ,  $R$  and  $r$  are the Cartan generators of the  $SU(2)_R \times U(1)_r$   $R$ -symmetry group. The trace is taken over the Hilbert space on  $S^3$  in radial quantization.

The Schur index is obtained by taking the  $q = t$  limit [19, 87],

$$\mathcal{I}(q, a_i) = \text{Tr}(-1)^F q^{E-R} \prod_i a_i^{f_i}. \quad (3.20)$$

Here the contributing states are  $\frac{1}{4}$ -BPS, annihilated by four supercharges:  $Q_-^1$ ,

$\tilde{Q}_{2^-}$ ,  $S_1^-$  and  $\tilde{S}^{2^-}$ . Their quantum numbers satisfy

$$E - j_1 - j_2 - 2R = 0, \quad j_1 - j_2 + r = 0. \quad (3.21)$$

### 3.2.2 The IR formula for the Schur index

Recently an IR formula for the Schur index was conjectured in [56]<sup>13</sup> relating the Schur index to the trace of the “quantum monodromy” operator, a  $q$ -series introduced in [61]:

$$\mathcal{I}(q) = (q)_\infty^{2r} \text{Tr}[M(q)], \quad (q)_\infty := \prod_{j=0}^{\infty} (1 - q^{j+1}). \quad (3.22)$$

In this section we review the mechanics of this formula.

To write down the operator  $M(q)$ , we need to perturb to a point of the Coulomb branch of the theory, where the only massless fields are those of abelian  $\mathcal{N} = 2$  gauge theory.  $M(q)$  will be built out of the massive BPS spectrum of the theory.

Recall that massive BPS states in an  $\mathcal{N} = 2$  theory lie in representations of  $SU(2)_J \times SU(2)_R$ , where  $SU(2)_J$  is the little group. The one-particle Hilbert space is graded by the IR charge lattice  $\Gamma$ , consisting of electromagnetic and flavor charges:<sup>14</sup> thus  $\mathcal{H} = \oplus_{\gamma \in \Gamma} \mathcal{H}_\gamma$ . Factoring out the center-of-mass degrees of freedom, we have:

$$\mathcal{H}_\gamma = [(2, 1) \oplus (1, 2)] \otimes h_\gamma. \quad (3.23)$$

<sup>13</sup>We follow the convention of [51, 56] for fermion number,  $(-1)^F = e^{2\pi i R}$ .

<sup>14</sup>The lattice  $\Gamma$  strictly speaking is the fiber of a local system, depending on the point  $u$  of the Coulomb branch, so we should really write it as  $\Gamma_u$ ; we will suppress this in the notation.

To count BPS particles refined by representations of  $SU(2)_J \times SU(2)_R$ , one consider the protected spin character [\[22\]](#)

$$\mathrm{Tr}_{h_\gamma}[y^J(-y)^R] = \sum_{n \in \mathbb{Z}} \Omega_n(\gamma) y^n, \quad (3.24)$$

with integers  $\Omega_n(\gamma) \in \mathbb{Z}$ , and packages the  $\Omega_n(\gamma)$  into the “Kontsevich-Soibelman factor”:

$$K(q; X_\gamma; \Omega_i(\gamma)) := \prod_{n \in \mathbb{Z}} E_q((-1)^n q^{n/2} X_\gamma)^{(-1)^n \Omega_n(\gamma)}. \quad (3.25)$$

$K$  is a  $q$ -series valued in the algebra of formal variables  $X_\gamma$ ; these variables themselves are valued in the “quantum torus” algebra, obeying the relations

$$X_\gamma X_{\gamma'} = q^{\langle \gamma', \gamma \rangle} X_{\gamma'} X_\gamma = q^{\frac{1}{2} \langle \gamma, \gamma' \rangle} X_{\gamma + \gamma'}, \quad (3.26)$$

where  $\langle, \rangle$  is the Dirac pairing on  $\Gamma$ .  $E_q(z)$  is the quantum dilogarithm defined as

$$E_q(z) = \prod_{j=0}^{\infty} (1 + q^{j+\frac{1}{2}} z)^{-1} = \sum_{n=0}^{\infty} \frac{(-q^{\frac{1}{2}} z)^n}{(q)_n}. \quad (3.27)$$

The quantum monodromy operator  $M(q)$  is defined as

$$M(q) = \prod_{\gamma \in \Gamma}^{\curvearrowright} K(q; X_\gamma; \Omega_i(\gamma)). \quad (3.28)$$

The ordering in this product is based on the central charges  $Z_\gamma$ : if  $\arg(Z_{\gamma_1}) > \arg(Z_{\gamma_2})$  then  $K(X_{\gamma_1})$  is to the right of  $K(X_{\gamma_2})$ . The flavor charges — which have zero Dirac pairing with other charges — form a sublattice  $\Gamma_f \subset \Gamma$ . The trace operation is defined by a truncation to this sublattice:

$$\mathrm{Tr}(X_\gamma) = \begin{cases} 0 & \text{if } \gamma \notin \Gamma_f, \\ X_\gamma & \text{otherwise.} \end{cases} \quad (3.29)$$



If we denote a basis for  $\Gamma_f$  by  $(\gamma_{fa})$ , then the trace is a function of the  $X_{\gamma_{fa}}$ , which are related to the flavor fugacities  $a_i$  in the UV definition of the Schur index [51, 56].

$\text{Tr } M(q)$  is invariant when crossing walls of marginal stability in the Coulomb branch [1, 22, 88, 89]. Of course this is a necessity for (3.22) to make sense, since  $\mathcal{I}(q)$  is defined directly in the UV and does not depend on a point of the Coulomb branch.

As pointed out in [51, 56], (3.22) is only a formal definition: in principle, in evaluating it, we could meet infinitely many terms contributing to the same power of  $q$ . In practice we may hope that these infinitely many terms will come with alternating signs so that they leave a well-defined Laurent series in  $q$ , but at least we need to have some definite prescription for how we will order the terms. In [51] the authors propose a prescription to tackle this problem. First they rewrite (3.22) as

$$\mathcal{I}(q) = (q)_\infty^{2r} \text{Tr}[S(q)\bar{S}(q)], \quad (3.30)$$

where  $S(q)$  is the “quantum spectrum generator” (so called because it contains enough information to reconstruct the full BPS spectrum),

$$S(q) = \prod_{\widehat{\arg}(Z_\gamma) \in [0, \pi)} K(q; X_\gamma; \Omega_i(\gamma)), \quad \bar{S}(q) = \prod_{\widehat{\arg}(Z_\gamma) \in [\pi, 2\pi)} K(q; X_\gamma; \Omega_i(\gamma)). \quad (3.31)$$

Next, they conjecture that  $S(q)$  and  $\bar{S}(q)$  can be expanded as Taylor series in  $q$ , with no negative powers of  $q$  appearing. If this is so, then one can try to

compute the coefficient of  $q^k$  in  $\text{Tr } M(q)$  by expanding  $S(q)$  and  $\bar{S}(q)$  up to some large finite order  $q^N$ . The conjecture is that for large enough  $N$  the coefficient of  $q^k$  will stabilize to some limiting value (in the examples investigated in [51] it is sufficient to take  $N$  larger than some theory-dependent linear function of  $k$ .) In the examples we consider in this paper, we find that the necessary stabilization does indeed occur, and thus we can use the prescription of [51].

### 3.2.3 The Schur index with half line defects

Supersymmetric line defects in  $\mathcal{N} = 2$  theories have been studied extensively: a small sampling of references is [23, 51, 90–92].

The line defects which have been studied most extensively are *full* line defects. These are  $\frac{1}{2}$ -BPS objects extended along a straight line in some fixed direction  $n^\mu \in \mathbb{R}^4$ . For example, there are  $\frac{1}{2}$ -BPS line defects that extend along the time direction and sits at a point in  $\mathbb{R}^3$ , preserving four Poincaré supercharges, time translation,  $SU(2)_J$  rotation around the defect in  $\mathbb{R}^3$ , and  $SU(2)_R$   $R$ -symmetry. The choices of half-BPS subalgebra which can be preserved by such a line defect are parameterized by  $\zeta \in \mathbb{C}^\times$ . When  $|\zeta| = 1$ , so that  $\zeta = e^{-i\theta}$ , the line defect can be interpreted as a heavy external BPS source particle, whose central charge has phase  $\theta$ .

In this section, following [51], we will be interested in *half* line defects in superconformal  $\mathcal{N} = 2$  theories. A half line defect extends along a ray in  $\mathbb{R}^4$  and terminates at a point, say the origin. The half line defect looks like a full line defect except near its endpoint; in particular, the indexing set labeling half

line defects is the same as that for full line defects, and it will sometimes be convenient to let the symbol  $L$  stand simultaneously for a half line defect and for its corresponding full line defect. The endpoint, however, only preserves two Poincaré supercharges, and breaks all translation symmetry. Moreover the endpoint supports a variety of local endpoint operators; these are the operators which will be counted by the line defect Schur index.

More generally we can consider a junction of multiple half line defects  $L_i$ . To preserve some common supersymmetry, these half line defects must lie in a common spatial plane  $\mathbb{R}^2 \subset \mathbb{R}^3$ . Each  $L_i$  ends at the origin and has orientation

$$n_i^\mu = (\cos \theta_i, \sin \theta_i, 0, 0), \quad (3.32)$$

where  $\theta_i$  is the phase of the central charge of  $L_i$ . After conformal mapping to  $S^3 \times S^1$ , each half line defect wraps  $S^1$  and sits at a point on a common great circle on  $S^3$ . This configuration preserves one Poincaré supercharge and one conformal supercharge,

$$Q = Q_-^1 + \tilde{Q}_{2\dot{-}}, \quad S = S_1^- + \tilde{S}^{2\dot{-}}. \quad (3.33)$$

Recall from [19] that  $Q_-^1$ ,  $\tilde{Q}_{2\dot{-}}$ ,  $S_1^-$  and  $\tilde{S}^{2\dot{-}}$  are exactly the four supercharges that annihilate Schur operators. Thus the definition of Schur index can be extended to include these half line defect insertions [50, 51]:

$$\mathcal{I}_{L_1(\theta_1)L_2(\theta_2)\dots L_n(\theta_n)}(q) = \text{Tr}_{\mathcal{H}'}[e^{2\pi i R} q^{E-R}]. \quad (3.34)$$

Here the trace is over the Hilbert space  $\mathcal{H}'$  on  $S^3$  with half line defects  $L_i$

inserted along the great circle at angles  $\theta_i$ .  $\mathcal{H}'$  consists of states annihilated by  $Q$  and  $S$  in (3.33).

For Lagrangian gauge theories with 't Hooft-Wilson half line defects, one could use a localization formula to compute the Schur index, as formulated in [50, 51]. In this paper we consider half line defects in Argyres-Douglas theories, for which we do not have a Lagrangian description available. Instead, we will use the IR formula conjectured by [51], which we describe next.

### 3.2.4 The IR formula for the line defect Schur index

Suppose we fix a full line defect  $L$  in  $\mathbb{R}^4$  and go to a point  $u$  in the Coulomb branch. Let  $\mathcal{H}_{L,u}$  denote the Hilbert space of the theory with line defect  $L$  inserted. In this setting there is a new class of BPS states, called *framed BPS states* [23], which saturate the bound

$$M \geq \text{Re}(Z/\zeta), \quad \zeta = e^{i\theta}. \quad (3.35)$$

Framed BPS states form a subspace  $\mathcal{H}_{L,u}^{\text{BPS}} \subset \mathcal{H}_{L,u}$ . As usual  $\mathcal{H}_{L,u}^{\text{BPS}}$  has a decomposition into sectors labeled by electromagnetic and flavor charges,

$$\mathcal{H}_{L,u}^{\text{BPS}} = \bigoplus_{\gamma \in \Gamma} \mathcal{H}_{L,u,\gamma}^{\text{BPS}}. \quad (3.36)$$

The degeneracies of framed BPS states are counted by the “framed protected spin character” defined in [23]:

$$\overline{\Omega}(L, \gamma, u, q) = \text{Tr}_{\mathcal{H}_{L,u}^{\text{BPS}}} [q^J (-q)^R]. \quad (3.37)$$

In the infrared the line defect  $L$  has a description as a sum of IR line defects, which can be thought of as infinitely heavy dyons with charges  $\gamma \in \Gamma$ . These IR line defects are represented by formal quantum torus variables  $X_\gamma$  with OPE given by (3.26). Then, for each  $L$  one can define a generating function counting the framed BPS states:

$$F(L(\theta)) = \sum_{\gamma \in \Gamma} \overline{\Omega}(L, \gamma, u, q) X_\gamma. \quad (3.38)$$

These generating functions are different in different chambers of the Coulomb branch, undergoing framed wall-crossing at the BPS walls [23].

The IR formula of [51] for the Schur index with insertion of a half line defect  $L$  with phase  $\theta$  is:

$$\mathcal{I}_{L(\theta)}(q) = (q)_\infty^{2r} \text{Tr}[F(L(\theta)) S_\theta(q) S_{\theta+\pi}(q)], \quad (3.39)$$

where

$$S_\theta(q) = \prod_{\arg(Z_\gamma) \in [\theta, \theta+\pi)} K(q; X_\gamma; \Omega_i(\gamma)). \quad (3.40)$$

As demonstrated in [51], the right side of (3.39) is invariant under framed wall-crossing, as is needed since the left side manifestly does not depend on a point of the Coulomb branch. When computing half line defect Schur index we often choose  $\theta = 0$ , in which case  $S_\theta(q)$  and  $S_{\theta+\pi}(q)$  reduce to  $S(q)$  and  $\overline{S}(q)$  respectively.

More generally, for multiple half line defects  $L_i$ ,  $i = 1, \dots, k$ , with phase relations  $\theta_1 < \theta_2 < \dots < \theta_k$ , where there are no ordinary BPS particles with

phases in the interval  $[\theta_1, \theta_k]$ , the IR formula of [51] for the Schur index is

$$\mathcal{I}_{L_1(\theta_1)\dots L_k(\theta_k)} = (q)_\infty^{2r} \text{Tr}[F(L_1(\theta_1)) \dots F(L_k(\theta_k)) S_{\theta_k}(q) S_{\theta_k+\pi}(q)]. \quad (3.41)$$

We note that this formula is “compatible with operator products”, in the following sense. The Schur index with two half line defects inserted,  $\mathcal{I}_{L_1(\theta)L_2(\theta+\delta\theta)}$  with  $\delta\theta$  small, only depends on  $\text{sgn}(\delta\theta)$ . In particular, in the limit of  $\delta\theta \rightarrow 0$  this looks like taking the non-commutative OPE of two parallel half line defects with phase  $\theta$ . Therefore computing  $\mathcal{I}_{L_1(\theta)L_2(\theta+\delta\theta)}$  and taking the  $q \rightarrow 1$  limit in the character expansion coefficient does correspond to the commutative OPE of two parallel half line defects in  $\mathcal{L}$ .

Given the IR formula for half line defect Schur index we would like to point out a general property of half line defect index in Argyres-Douglas theories. Line defect generators in Argyres-Douglas theories can be labeled as  $L_{\rho_i}$  where the index  $i$  is related to the underlying discrete symmetry of the theory. In particular, suppose  $L_{\rho_j}$  and  $L_{\rho_i}$  are two half line defect generators that are related by a monodromy action, namely

$$F(L_{\rho_j}) = M(q)F(L_{\rho_i})M^{-1}(q). \quad (3.42)$$

Then according to the IR formula

$$\begin{aligned} \mathcal{I}_{L_{\rho_j}}(q) &= (q)_\infty^{2r} \text{Tr}[F(L_{\rho_j})S(q)\overline{S}(q)] = (q)_\infty^{2r} \text{Tr}[F(L_{\rho_j})M(q)] \\ &= (q)_\infty^{2r} \text{Tr}[M(q)F(L_{\rho_i})M^{-1}(q)M(q)] \\ &= \mathcal{I}_{L_{\rho_i}}(q). \end{aligned}$$

In particular this proves that Schur index with one half line defect generator insertion does not depend on the  $i$ -index, as first observed in some examples in [51].

### 3.3 Fixed points of the $U(1)_r$ action

#### 3.3.1 The $U(1)_r$ action

Because the four-dimensional theories we consider are superconformal, they have a  $U(1)_r$  symmetry in the UV. Note that the  $U(1)_r$  charges need not be integral (indeed they are not integral in Argyres-Douglas theories), though they are rational in all examples we will consider. Thus the action of  $R_t \in U(1)_r$  is not necessarily trivial when  $t = 2\pi$ , but there is some  $k$  for which  $R_{2\pi k}$  is trivial.

The  $U(1)_r$  symmetry of the four-dimensional superconformal theory acts in particular on the  $\frac{1}{2}$ -BPS line defects. Recall from [23] that each  $\frac{1}{2}$ -BPS line defect preserves some subalgebra of the  $\mathcal{N} = 2$  algebra, with the different possible subalgebras parameterized by  $\zeta \in \mathbb{C}^\times$ . Given a line defect  $L$  preserving the subalgebra with parameter  $\zeta \in \mathbb{C}^\times$ , a rotation  $R_t \in U(1)_r$  maps  $L$  to a new operator  $L(t)$  preserving the subalgebra with parameters  $e^{it}\zeta$ .

Now suppose we consider the dimensional reduction to three dimensions on  $S^1$ . The  $U(1)_r$  symmetry acts on the moduli space  $\mathcal{N}$  of vacua of the three-dimensional theory. In what follows we will be particularly interested in the  $U(1)_r$ -invariant vacua.

### 3.3.2 Line defect vevs in $U(1)_r$ -invariant vacua

Let  $\mathcal{F}_L$  denote the vev of the line defect  $L$  wrapped on  $S^1$ .  $\mathcal{F}_L$  is a function on the moduli space  $\mathcal{N}$ . We specialize to a  $U(1)_r$ -invariant vacuum: after this specialization  $\mathcal{F}_L$  is just a number. Moreover, since the vacuum is invariant,  $\mathcal{F}_L$  is invariant under  $U(1)_r$  acting on  $L$ , i.e. for any  $t, t'$

$$\mathcal{F}_{L(t)} = \mathcal{F}_{L(t')}. \quad (3.43)$$

This simple statement has surprisingly strong consequences, which put constraints on the possible  $U(1)_r$ -invariant vacua, as follows. We imagine making a small perturbation away from the invariant vacuum. After this perturbation the UV line defect  $L(t)$  can be decomposed into IR line defects  $L_\gamma^{IR}(t)$ ,

$$L(t) \rightarrow \sum_{\gamma} \bar{\Omega}(L, \gamma, t) L_\gamma^{IR}(t) \quad (3.44)$$

with a corresponding decomposition of the vev  $\mathcal{F}_{L(t)}$  as a sum of monomials  $\mathcal{X}_\gamma(t)$ ,

$$\mathcal{F}_{L(t)} = \sum_{\gamma} \bar{\Omega}(L, \gamma, t) \mathcal{X}_\gamma(t). \quad (3.45)$$

Here both sides may depend nontrivially on  $t$ , since our perturbation is not  $U(1)_r$  invariant. The expansion coefficients  $\bar{\Omega}(L, \gamma, t) \in \mathbb{Z}$  appearing in (3.45) are the framed BPS state counts which we discussed earlier in (3.37), evaluated in the perturbed vacuum, and specialized to  $q = 1$ .

Now let us take the limit where the perturbation  $\rightarrow 0$ , and optimistically assume that the  $\bar{\Omega}(L, \gamma, t)$  and  $\mathcal{X}_\gamma(t)$  remain well defined in this limit. In



that case we get an interesting equation:<sup>15</sup>

$$\sum_{\gamma} \overline{\Omega}(L, \gamma, t) \mathcal{X}_{\gamma}(t) = \sum_{\gamma} \overline{\Omega}(L, \gamma, t') \mathcal{X}_{\gamma}(t'). \quad (3.46)$$

Requiring (3.46) to hold for *all* UV line defects  $L$  gives a relation on the  $\mathcal{X}_{\gamma}(t)$ . For example, if  $t'$  is sufficiently close to  $t$ , so that  $\overline{\Omega}(L, \gamma, t) = \overline{\Omega}(L, \gamma, t')$  for all  $L$  and  $\gamma$ , then (3.46) says simply that  $\mathcal{X}_{\gamma}(t) = \mathcal{X}_{\gamma}(t')$ . More generally, though, the  $\overline{\Omega}(L, \gamma, t)$  will jump as  $t$  is varied. Then we get a more general relation, of the form [22, 23]

$$\mathcal{X}_{\gamma}(t') = (\mathcal{S}_{t,t'} \mathcal{X})_{\gamma}(t). \quad (3.47)$$

Here  $\mathcal{S}_{t,t'}$  denotes a birational map  $(\mathbb{C}^{\times})^n \rightarrow (\mathbb{C}^{\times})^n$  which can be written concretely in the form

$$\mathcal{S}_{t,t'} = \prod_{\arg(Z_{\gamma}) \in (t,t')}^{\circlearrowleft} T_{\gamma}^{\Omega(\gamma)}, \quad (3.48)$$

where  $T_{\gamma} : (\mathbb{C}^{\times})^n \rightarrow (\mathbb{C}^{\times})^n$  is a transformation of the form [22, 88]<sup>16</sup>

$$T_{\gamma} : (\mathcal{X}_{\mu}) \rightarrow (\mathcal{X}_{\mu}(1 - \sigma(\gamma) \mathcal{X}_{\gamma})^{\langle \mu, \gamma \rangle}) \quad (3.49)$$

and  $\sigma : \Gamma \rightarrow \{\pm 1\}$  is a quadratic refinement of the mod 2 intersection pairing.

The equation (3.47) is an interesting relation, but so far not useful in producing a constraint: it just relates the values of  $\mathcal{X}_{\gamma}(t)$  for different  $t$ .

---

<sup>15</sup>We emphasize that (3.46) is supposed to hold *only* in a  $U(1)_r$ -invariant vacuum. Indeed, when considered as functions on the whole moduli space  $\mathcal{N}$ ,  $\mathcal{X}_{\gamma}(t)$  and  $\mathcal{X}_{\gamma}(t')$  are holomorphic in different complex structures, so they could hardly obey such a relation.

<sup>16</sup> $T_{\gamma}$  should be thought of as the  $q \rightarrow 1$  limit of the operation of conjugation by the operator  $K$  appearing in (3.25).

Now let us specialize to  $t' = t + \pi$ . In that case we have the key relation from [1]

$$\mathcal{X}_\gamma(t + \pi) = \overline{\mathcal{X}_{-\gamma}(t)} \quad (3.50)$$

so we conclude that

$$\mathcal{S}_{t,t+\pi} \mathcal{X}_\gamma(t) = \overline{\mathcal{X}_{-\gamma}(t)}. \quad (3.51)$$

This is a closed equation for the numbers  $\mathcal{X}_\gamma(t)$ , with fixed  $t$ . To make it really concrete, of course, we need some way of computing the “classical spectrum generator”  $\mathcal{S}_{t,t+\pi}$ . We could do so by first computing the BPS spectrum (e.g. by the mutation method) and then directly using the definition (3.48), but there are also various methods available for computing it directly. In general theories of class  $\mathcal{S}$  some of these methods have appeared in [1, 93–95]. In the theories we consider, we will explain a simple method below in §3.3.3.

We believe that (3.51) is likely to be a useful equation for the study of  $U(1)_r$ -invariant vacua in general  $\mathcal{N} = 2$  theories, and it would be interesting to explore it further. For the Argyres-Douglas theories which we consider in this paper, though, a simpler equation suffices. Namely, instead of taking  $t' = t + \pi$  we take  $t' = t + 2\pi$ . Then we get the relation

$$\mathcal{X}_\gamma(t + 2\pi) = \mathcal{X}_\gamma(t), \quad (3.52)$$

leading to the fixed-point constraint

$$\mathcal{S}_{t,t+2\pi} \mathcal{X}_\gamma(t) = \mathcal{X}_\gamma(t). \quad (3.53)$$

The constraint (3.53) has the advantage that it is purely algebraic, not involving a complex conjugation. (3.51) implies (3.53), but not the other way

around: (3.53) can have additional “spurious” solutions not associated to actual  $U(1)_r$ -invariant vacua.<sup>17</sup> In the Argyres-Douglas theories we consider in this paper, such spurious solutions do not occur, as we will see directly just by counting the number of solutions. Thus we will use (3.53) as our criterion for a  $U(1)_r$ -invariant vacuum.

There is one more point which will be important below: we will need to keep track of some discrete information attached to the fixed points  $p \in \mathcal{N}$ , namely the weights of the  $U(1)_r$  action on the tangent space  $T_p\mathcal{N}$ . These weights are easily computable if we have a Higgs bundle description of the fixed point as in [69, 71]. On the other hand, suppose that we only know the fixed point as a solution of the constraint (3.53): how then can we compute the  $U(1)_r$  weights? We will use a trick, as follows.  $\mathcal{S}_{t,t+2\pi}$  acts as  $\exp(2\pi iV)$  where  $V$  is a holomorphic vector field on the twistor space of  $\mathcal{N}$  generating the  $U(1)_r$  action. Thus we have  $d\mathcal{S}_{t,t+2\pi} = \exp(2\pi iV)$  acting on  $T_p\mathcal{N}$ . Thus, by computing  $d\mathcal{S}_{t,t+2\pi}$  at the fixed point, we can get the  $U(1)_r$  weights mod 1.

Fortunately, in the  $(A_1, A_{2N})$  cases we treat in §3.5, knowing the  $U(1)_r$  weights mod 1 is sufficient to determine which fixed point we are looking at. For the  $(A_1, D_{2N+1})$  cases it is not sufficient, which will cause us some headaches in §3.6.

---

<sup>17</sup>For an extreme example, we could consider any superconformal theory in which the  $U(1)_r$  charges are all integral, such as the  $SU(2)$  gauge theory with  $N_f = 4$ ; in such a theory  $\mathcal{S}_{t,t+2\pi}$  is the identity operator, so that (3.53) reduces to the triviality  $\mathcal{X}_\gamma(t) = \mathcal{X}_\gamma(t)$ , which of course imposes no constraint at all on the vacuum. In contrast, even in these theories, (3.51) is a nontrivial constraint.

### 3.3.3 Classical monodromy action in Argyres-Douglas theories

To use (3.53) in practice we need a way of computing  $\mathcal{S}_{t,t+2\pi}$ , which we call the *classical monodromy* map. In this section we describe a convenient way of doing so in  $(A_1, A_m)$  Argyres-Douglas theories.

The starting point is to use the realization of these theories as class  $\mathcal{S}$  theories. This implies that the space  $\mathcal{N}$  is a moduli space of flat connections — in this case, flat  $SL(2, \mathbb{C})$ -connections defined on  $\mathbb{CP}^1$  with an irregular singularity at  $z = \infty$ . In [1] the functions  $\mathcal{X}_\gamma$  appearing in §3.3.2 were described from this point of view; we now review that description.

Given a point of the Coulomb branch and generic  $\zeta \in \mathbb{C}^\times$ , [1] gives a construction of a triangulation of an  $(m+3)$ -gon, the “WKB triangulation.” The vertices of this  $(m+3)$ -gon are asymptotic angular directions on the “circle at infinity,”

$$\arg(z) = \frac{2\theta + 2\pi j}{m+3}, \quad j = 1, \dots, m+3, \quad (3.54)$$

where  $\theta = \arg \zeta$ . Now, given a vacuum in  $\mathcal{N}$  and the parameter  $\zeta \in \mathbb{C}^\times$ , there is a corresponding flat connection  $\nabla$  on  $\mathbb{CP}^1$ , with irregular singularity at  $z = \infty$ . For each of the  $m+3$  asymptotic directions, there is a unique  $\nabla$ -flat section  $s_i$  whose norm is exponentially small as  $z \rightarrow \infty$ . Thus altogether we get  $m+3$  flat sections

$$(s_1, s_2, \dots, s_{m+3}). \quad (3.55)$$

Moreover, this tuple of flat sections is enough information to completely determine the vacuum; one gets coordinates on  $\mathcal{N}$  by computing  $SL(2, \mathbb{C})$ -invariant

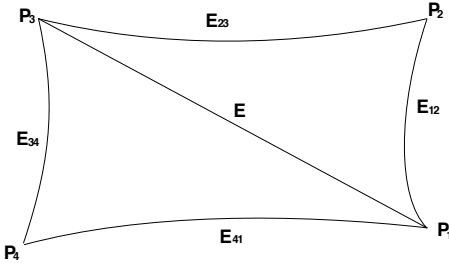


Figure 3.1: The quadrilateral  $Q_E$  associated to edge  $E$ .

cross-ratios from the sections  $s_i$ .

From (3.54) we see that continuously varying  $\theta \rightarrow \theta + 2\pi$  is equivalent to making a shift  $j \rightarrow j + 2$ , i.e. relabeling

$$(s_1, \dots, s_{m+3}) \rightarrow (s_3, s_4, \dots, s_{m+3}, s_1, s_2). \quad (3.56)$$

This is the classical monodromy action on  $\mathcal{N}$ .

Now we would like to understand concretely what this monodromy looks like, relative to the local coordinates  $\mathcal{X}_\gamma$  on  $\mathcal{N}$ . The first step is to explain what the  $\mathcal{X}_\gamma$  are. For each internal edge  $E$  of the triangulation, there is an associated coordinate function  $\mathcal{X}_E$ .  $E$  is bounded by two triangles which make up a quadrilateral  $Q_E$ , as shown in Figure 3.1. Each vertex  $P_i$  is associated with a small flat section  $s_i$ .  $\mathcal{X}_E$  is then defined as:

$$\mathcal{X}_E = -\frac{(s_1 \wedge s_2)(s_3 \wedge s_4)}{(s_2 \wedge s_3)(s_4 \wedge s_1)}, \quad (3.57)$$

where the  $s_i$  are evaluated at a common point in  $Q_E$ . If  $E$  is a boundary edge of the  $(m + 3)$ -gon, by convention, we write  $\mathcal{X}_E = 0$ . Finally to go from the  $\mathcal{X}_E$  to the desired  $\mathcal{X}_\gamma$  one uses a dictionary described in [1] which maps the set of internal edges  $E_i$  to a basis  $(\gamma_{E_i})$  of the charge lattice  $\Gamma$ .

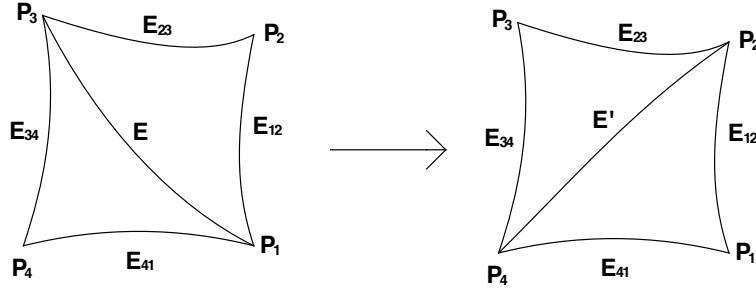


Figure 3.2: Action of a flip on the quadrilateral  $Q_E$ .

In practice, to use this description for computing the classical monodromy, we will need one more fact: we need to know how the coordinates  $\mathcal{X}_E$  change when we change the triangulation. A flip of the edge  $E$  is the transformation from a triangulation  $T$  to another triangulation  $T'$ , where the edge  $E = E_{13}$  in  $T$  is replaced by  $E' = E_{24}$  in  $T'$ , as in Figure [3.2](#). Using the standard relations between cross-ratios one gets the transformation rules:

$$\begin{aligned}
 \mathcal{X}_{E'}^{T'} &= \frac{1}{\mathcal{X}_E^T}, & \mathcal{X}_{E_{12}}^{T'} &= \mathcal{X}_{E_{12}}^T (1 + \mathcal{X}_E^T), \\
 \mathcal{X}_{E_{23}}^{T'} &= \frac{\mathcal{X}_{E_{23}}^T \mathcal{X}_E^T}{1 + \mathcal{X}_E^T}, & \mathcal{X}_{E_{34}}^{T'} &= \mathcal{X}_{E_{34}}^T (1 + \mathcal{X}_E^T), \\
 \mathcal{X}_{E_{41}}^{T'} &= \frac{\mathcal{X}_{E_{41}}^T \mathcal{X}_E^T}{1 + \mathcal{X}_E^T}.
 \end{aligned} \tag{3.58}$$

In examples below, we will compute the classical monodromy as a composition of these flips.

For  $(A_1, D_{2N+1})$  Argyres-Douglas theories the story is very similar: the only difference is that the Hitchin system is defined on  $\mathbb{CP}^1$  with an irregular singularity at  $z = \infty$  plus a regular singularity at  $z = 0$ . The construction of monodromy and coordinates  $\mathcal{X}_\gamma$  is parallel to what we wrote above, except

that the WKB triangulations have one more “internal” vertex, at the location of the regular singularity.

### 3.4 Line defects and their framed BPS states in class $S[A_1]$

We use two different methods for describing the algebra of line defects in Argyres-Douglas theories of type  $(A_1, \mathfrak{g})$  and computing their framed BPS spectra:

- In [92] it was proposed that generators of the ring of line defects and their framed BPS spectra can be computed by methods of quiver quantum mechanics. The calculation of framed BPS spectra is in parallel to the approach previously used for ordinary BPS spectra. In simple cases this leads to an algorithm for determining the spectrum, the “mutation method” as introduced in [23, 61, 96, 97]. This method is easy to implement on a computer. We use it in §3.5 below to compute line defect generators and their generating functions in  $(A_1, A_{2N})$  Argyres-Douglas theories. However, for the  $(A_1, D_{2N+1})$  Argyres-Douglas theories which we consider in §3.5, the framed BPS spectrum in general contains higher spin states, which defeat the mutation method.<sup>18</sup>

---

<sup>18</sup>In these cases the framed BPS spectra could in principle be obtained by studying the Hodge diamond of the moduli space of stable framed quiver representations [92]. However, this is not as automated as the “mutation method,” which prompts us to use an alternative method introduced below.

- Alternatively, we can use the class  $\mathcal{S}[A_1]$  realization of the  $(A_1, A_{2N})$  or  $(A_1, D_{2N+1})$  theories. In this realization, line defect generators are in 1-to-1 correspondence with isotopy classes of simple laminations on the disc or punctured disc [23]. This leads to an algorithm for computing the framed BPS indices, as described in [23]. For our purposes in this paper, this algorithm is not quite sufficient: we also want to know the spin content of the framed BPS spectra. In [98, 99] a method for computing such BPS spectra in class  $\mathcal{S}$  theories has been proposed, extending [23].<sup>19</sup> What we use in this paper is a slight extension of the method in [99] to treat the case of an irregular singularity.

In §3.4.1-§3.4.2 we review the approach via mutations; in §3.4.3-§3.4.5 we review the geometric methods of [23, 25, 98-100]. These two methods will be used for the examples in §3.5-§3.6 below.

### 3.4.1 Line defect generators in $\mathcal{N} = 2$ theories of quiver type

4d  $\mathcal{N} = 2$  theories of quiver type are  $\mathcal{N} = 2$  theories whose BPS spectra can be computed via a four-supercharge multi-particle quantum mechanics system encoded in a quiver [96, 101-103]. In particular, Argyres-Douglas theories are examples of theories of quiver type, as discussed e.g. in [61]. For 4d  $\mathcal{N} = 2$  theories of quiver type, there is a nice way of constructing distinguished

---

<sup>19</sup>The paper [98] treated the spin content for framed BPS spectra associated to certain *interfaces* between surface defects; [99] gave the first complete prescription applicable directly to ordinary line defects.



line defect generators via quiver mutation, developed in [92], which we review in this section.

Fix a point of the Coulomb branch, and fix a half-plane inside the plane of central charges:

$$\mathfrak{h}_\theta = \{Z \in \mathbb{C} \mid \theta < \arg(Z) < \theta + \pi\}, \quad \theta \in [0, 2\pi). \quad (3.59)$$

Then the BPS one-particle representations in the theory can be divided into “particles” and “antiparticles”: particles are those whose central charges lie in  $\mathfrak{h}_\theta$ , antiparticles are the rest. For theories of quiver type there is a canonical positive integral basis  $\{\gamma_i\}$  for  $\Gamma$ , such that the cone

$$\mathcal{C} = \left\{ \sum_{i=1}^{\text{rank}(\Gamma)} a_i \gamma_i \mid a_i \in \mathbb{R}_{\geq 0} \right\} \quad (3.60)$$

contains the charges of all BPS particles. We call such a basis a *seed*. The corresponding quiver has one node for each basis charge  $\gamma_i$ , with the number of arrows from  $\gamma_i$  to  $\gamma_j$  given by  $\langle \gamma_i, \gamma_j \rangle$ .

Correspondingly, in the half-plane  $\mathfrak{h}_\theta$  there is a cone  $Z(\mathcal{C})$  given by the central charge function  $Z$ . The cone of particles is piecewise constant as one varies the parameter  $\theta$  or the point of the Coulomb branch, but jumps when one boundary ray  $Z_{\gamma_i}$  of  $Z(\mathcal{C})$  hits the boundary of  $\mathfrak{h}_\theta$ , i.e. when the central charge of a BPS particle with charge  $\gamma_i$  exits the particle half-plane. At this point the quiver description also jumps discontinuously, by a process of “mutation.” Depending on whether  $Z_{\gamma_i}$  exits  $\mathfrak{h}_\theta$  on the right or on the left, the mutation is denoted as right mutation  $\mu_{Ri}$  or left mutation  $\mu_{Li}$ . The explicit

transformation of the basis charges is [92,96]

$$\mu_{Ri}(\gamma_j) = -\delta_{ij}\gamma_j + (1 - \delta_{ij})(\gamma_j - \text{Min}[\langle\gamma_i, \gamma_j\rangle, 0]\gamma_i), \quad (3.61)$$

$$\mu_{Li}(\gamma_j) = -\delta_{ij}\gamma_j + (1 - \delta_{ij})(\gamma_j + \text{Max}[\langle\gamma_i, \gamma_j\rangle, 0]\gamma_i). \quad (3.62)$$

Now let us see how the quiver technology is related to the spectrum of line defects in the theory. Recall that at low energy a UV line defect  $L$  decomposes into a sum of IR line defects, as in (3.44). Among these IR line defects, the one with the smallest  $\text{Re}(Z_\gamma/\zeta)$  corresponds to the ground state of the UV line defect. The charge of this line defect is called the core charge of the UV line defect. One could define a RG map which maps the UV line defect to its core charge  $\gamma_c$ . As discussed in [23,92] the RG map is a bijection in  $\mathcal{N} = 2$  theories of quiver type. This nice property allows one to identify the set of UV line defects with the IR charge lattice  $\Gamma$ .

The RG map is piecewise constant and jumps at the locus where  $\text{Re}(Z_\gamma/\zeta) = 0$  for some  $\gamma$ , which is the same locus where quiver mutation happens. In particular when  $\gamma$  itself is the charge of some BPS state the jump of  $\gamma_c$  is given by ([92]):

$$\mu_{Ri}(\gamma_c) = \gamma_c - \text{Min}[\langle\gamma_i, \gamma_c\rangle, 0]\gamma_i, \quad \mu_{Li}(\gamma_c) = \gamma_c + \text{Max}[\langle\gamma_i, \gamma_c\rangle, 0]\gamma_i. \quad (3.63)$$

For a given seed  $\{\gamma_i\}$  and its associated particle cone  $\mathcal{C}$ , there exists a dual cone  $\check{\mathcal{C}}$  defined as:

$$\check{\mathcal{C}} = \left\{ \check{\gamma} \in \Gamma_u \otimes_{\mathbb{Z}} \mathbb{R} \mid \langle \check{\gamma}, \gamma \rangle \geq 0 \quad \forall \gamma \in \mathcal{C} \right\}. \quad (3.64)$$

Using the inverse of the RG map we see that the integral points of  $\check{\mathcal{C}}$  correspond to a distinguished set of UV line defects by the inverse of the RG map. Within this set, the OPE relations turn out to be extremely simple. Indeed, if  $\gamma_i$  the core charge of a UV line defect  $L_i$ , and all  $\gamma_i \in \check{\mathcal{C}}$ , then we have simply [92]

$$L_1 L_2 = q^{\frac{\langle \gamma_1, \gamma_2 \rangle}{2}} L_3, \quad (3.65)$$

where  $\gamma_3 = \gamma_1 + \gamma_2$ .

Now pick a point of the Coulomb branch and a particle half-plane  $\mathfrak{h}_\theta$ . This fixes an initial seed  $\mathfrak{s}$ . In addition to the dual cone  $\check{\mathcal{C}}_{\mathfrak{s}}$ , there are other dual cones  $\check{\mathcal{C}}_{\mu(\mathfrak{s})}$ , corresponding to the seeds  $\mu(\mathfrak{s})$  mutated from  $\mathfrak{s}$ . In these other dual cones the line defect OPE also has the nice form (3.65). To put everything in the same footing one can trivialize  $\Gamma$  using the initial seed  $\mathfrak{s}$ , then mutate  $\check{\mathcal{C}}_{\mu(\mathfrak{s})}$  back to  $\mathfrak{s}$  using (3.63). After so doing, one has a collection of dual cones meeting along codimension-one faces in  $\mathbb{Z}^{\text{rank}(\Gamma)} \otimes_{\mathbb{Z}} \mathbb{R}$ . In a general  $\mathcal{N} = 2$  theory, the dual cones obtained in this way cover only some subset of the charge lattice. For Argyres-Douglas theories, however, there are only finitely many dual cones, and they fill up the full charge lattice [92]. Thus the full set of UV line defects is generated by the line defects whose core charges lie at the boundaries of the dual cones.

Concretely, in the  $(A_1, A_{2N})$  Argyres-Douglas theories, although the boundaries of dual cones are in general codimension-1 hyperplanes, these hyperplanes intersect at half-lines, such that line defects with core charges along those half-lines generate the whole space of UV line defects. In these theories

we thus obtain a unique and canonical choice of line defect generators, which is very convenient for computational purposes. (In the  $(A_1, A_2)$  theory we have already mentioned these generators in §3.1.3.)

In contrast, in the  $(A_1, D_{2N+1})$  Argyres-Douglas theories, due to the flavor symmetry, the dual cone picture does not quite give a unique choice of UV line defect generators. In these theories we will use the class  $\mathcal{S}$  picture instead.

### 3.4.2 Framed BPS states from framed quivers

In  $\mathcal{N} = 2$  theories of quiver type, framed BPS spectra associated to line defects can be computed using framed quivers [92].<sup>20</sup> One extends the charge lattice  $\Gamma$  by an extra direction spanned by a new “infinitely heavy” flavor charge  $\gamma_F$ , which has zero pairing with all charges. The line defect with core charge  $\gamma_c$  is then regarded as a particle carrying the charge  $\gamma_c + \gamma_F$ , and framed BPS states supported by the defect are similarly regarded as particles with charges of the form

$$\gamma_c + \gamma_F + \gamma_h, \quad \text{where } \gamma_h = \sum_{i=1}^{\text{rank}(\Gamma)} a_i \gamma_i, \quad a_i \in \mathbb{Z}_{\geq 0}. \quad (3.66)$$

One then defines a new “framed quiver,” obtained by adding to the original quiver a new framing node representing the bare line defect and corresponding arrows. The framed BPS states are given by the unframed BPS states of the framed quiver whose charges are of the form (3.66).

---

<sup>20</sup>As emphasized in [92], this method does not *in general* produce the correct framed BPS spectrum, but it does work for a large class of theories including Argyres-Douglas theories.

BPS states in quiver quantum mechanics can be conveniently computed by the “mutation method” as introduced in [23,61,96,97]. Concretely, we first fix a point in the Coulomb branch and a choice of half-plane  $\mathfrak{h}_\theta$ , then rotate  $\mathfrak{h}_\theta$  counterclockwise<sup>21</sup> until  $\theta$  has increased by  $\pi$ . In this process the original seed undergoes a series of right mutations  $\mu_{Ri}$ , and for each mutation the node  $\gamma_i$  that exits to the right of  $\mathfrak{h}_\theta$  corresponds to a BPS particle. Conversely each BPS particle will be rightmost at some stage of the rotation, so the  $\gamma_i$  obtained in this way exhaust all BPS particles in this chamber. In [96] this method was applied to the ordinary BPS quiver to compute the ordinary (vanilla, unframed) BPS spectrum; here instead we apply it to the framed quiver constructed above, to get the framed BPS spectrum.

### 3.4.3 Line defects in class $\mathcal{S}[A_1]$ theories

In class  $\mathcal{S}[A_1]$  theories there is a natural geometric picture of the  $\frac{1}{2}$ -BPS line defects: they correspond to paths (up to homotopy) on the internal Riemann surface  $C$  [23,90,91,104]. For class  $\mathcal{S}[A_1]$  theories with irregular punctures, one has to consider not only closed paths but also certain combinations of open paths, called *laminations* in [23] (following [105] where the same combinations of open paths were considered.)

The laminations we consider are drawn on a disc, which we think of as the complex plane compactified by adding the “circle at infinity.” The boundary circle is divided into arcs by marked points corresponding to the

---

<sup>21</sup>The choice of counterclockwise vs. clockwise is just a convention.

Stokes directions (see [23] for more on this.) Then a lamination is a collection of paths on the disc, carrying integer weights, subject to some conditions [23,105]: the sum of weights meeting each boundary arc must be zero, and all paths with negative weights must be deformable into a small neighborhood of the boundary.

#### 3.4.4 Framed BPS indices in class $\mathcal{S}[A_1]$ theories, without spin

In [23], a scheme is presented for computing the framed BPS indices associated to a given line defect in a theory of class  $\mathcal{S}[A_1]$ , without spin information. In this scheme one needs two pieces of data:

- the lamination representing the line defect,
- the WKB triangulation determined by the chosen point of the Coulomb branch and phase of the line defect.

It is easiest to illustrate this rule by an example. So, consider the triangulation of the once-punctured triangle and the lamination shown in Figure 3.3. (This example arises in the  $(A_1, D_3)$  theory considered in §3.6.1 below: it corresponds to the line defect called  $B_2$  there.)

We fix an orientation of each component of the lamination. Then we divide each component of the lamination into arcs crossing triangles. To each

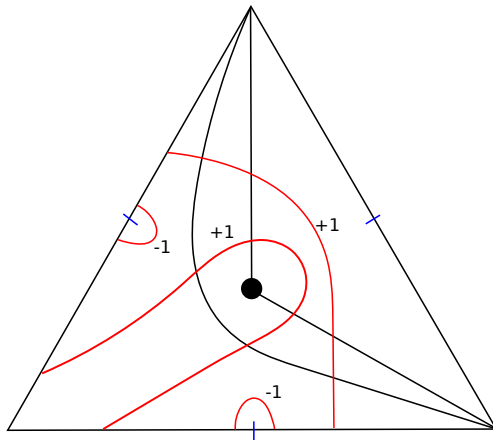


Figure 3.3: An example of a WKB triangulation of the once-punctured triangle and a lamination, corresponding to the line defect  $B_2$  in the  $(A_1, D_3)$  Argyres-Douglas theory.

arc we assign the matrix  $L$  ( $R$ ) if the arc turns left (right).<sup>22</sup>

$$L = \begin{pmatrix} 1 & 0 \\ 1 & 1 \end{pmatrix}, \quad R = \begin{pmatrix} 1 & 1 \\ 0 & 1 \end{pmatrix}. \quad (3.67)$$

When the lamination crosses an internal edge  $E_i$  we assign the matrix

$$M_E = \begin{pmatrix} \sqrt{\mathcal{X}_E} & 0 \\ 0 & 1/\sqrt{\mathcal{X}_E} \end{pmatrix}. \quad (3.68)$$

To the initial and final points of each component we assign the vectors

$$E^R = (0 \ 1), \quad E^L = (1 \ 0), \quad B^R = \begin{pmatrix} 1 \\ 0 \end{pmatrix}, \quad B^L = \begin{pmatrix} 0 \\ 1 \end{pmatrix}, \quad (3.69)$$

choosing  $L$  or  $R$  according to whether the endpoint is on the left or the right of the marked point of the boundary edge. Then we multiply these matrices in

---

<sup>22</sup>The matrices we present here are the *transpose* of the matrices in [23], and correspondingly we take the products in the reverse of the order taken in [23]; this corresponds to the usual order of composition of parallel transports, and makes the construction directly compatible with [25], which will be useful below.

order, with the beginning of the path corresponding to the rightmost matrix, to get a number for each component. If the component has weight  $k$  we raise this number to the  $k$ -th power. Finally we multiply the contributions from all components to get the vev.

In the example of Figure [3.3](#) above, the contribution from the left long component with weight  $+1$  is

$$\begin{aligned}
E^R L M_{E_2} L M_{E_3} R M_{E_1} L M_{E_2} L B^R = \\
\frac{1}{\sqrt{\mathcal{X}_1 \mathcal{X}_3}} + \frac{1}{\sqrt{\mathcal{X}_1 \mathcal{X}_3 \mathcal{X}_2}} + 2 \frac{\sqrt{\mathcal{X}_3}}{\sqrt{\mathcal{X}_1}} + \sqrt{\mathcal{X}_1 \mathcal{X}_3} + \frac{\sqrt{\mathcal{X}_3}}{\sqrt{\mathcal{X}_1 \mathcal{X}_2}} + \frac{\mathcal{X}_2 \sqrt{\mathcal{X}_3}}{\sqrt{\mathcal{X}_1}} + \mathcal{X}_2 \sqrt{\mathcal{X}_1 \mathcal{X}_3}.
\end{aligned}
\tag{3.70}$$

Similarly, the contribution from the right long component with weight  $+1$  is  $\sqrt{\mathcal{X}_3/\mathcal{X}_1}$ . The short components with weight  $-1$  contribute 1. The total contribution from this lamination is

$$\frac{1}{\mathcal{X}_1} + \frac{1}{\mathcal{X}_1 \mathcal{X}_2} + \mathcal{X}_3 + 2 \frac{\mathcal{X}_3}{\mathcal{X}_1} + \frac{\mathcal{X}_3}{\mathcal{X}_1 \mathcal{X}_2} + \mathcal{X}_2 \mathcal{X}_3 + \frac{\mathcal{X}_2 \mathcal{X}_3}{\mathcal{X}_1}.
\tag{3.71}$$

Thus [\(3.71\)](#) gives the generating function of framed BPS states associated to this line defect, without spin information.

### 3.4.5 Framed BPS indices in class $\mathcal{S}[A_1]$ theories, with spin

We continue with our example from [§3.4.4](#). Incorporating the spin information requires us to take each term in [\(3.71\)](#) and assign it the correct power of  $q$ . The work of [\[98, 99\]](#) provides a rule for determining these powers. The first step is to associate the terms in [\(3.71\)](#) to arcs on a branched double



cover  $\Sigma$  of the disc<sup>23</sup> following the “path lifting” rules of [25], as follows.

The double cover  $\Sigma$  is presented concretely: in each triangle we fix one branch point and three branch cuts, as in the left side of Figure 3.4; the double cover has sheets labeled 1 and 2, and at each cut sheet 1 is glued to sheet 2 and vice versa. Next, note that each term in (3.71) comes from products of two specific chains of matrix elements: e.g. the term  $\frac{1}{\lambda_1}$  comes from product of two contributions. As an example, the first contribution comes from taking the  $(2, 2)$  entries of the matrices from the beginning to the second-to-last  $L$ , then taking the  $(2, 1)$  entry of that  $L$ , then the  $(1, 1)$  entries of all the rest. Each of these matrix elements corresponds to an arc on the double cover, which we regard as a “lift” of the corresponding arc of the lamination. In Figure 3.4 we show three arcs corresponding to the three nonzero matrix elements of each of  $L$  and  $R$ ; the arc for the  $(i, j)$  matrix element begins on sheet  $j$  and ends on sheet  $i$ .

Concatenating these arcs gives a long path  $P$  on  $\Sigma$ , associated to the term in (3.71) which we are studying. If  $P$  has no self-intersections then we assign this term the factor  $q^0$ . If there are self-intersections then each contributes a factor  $q^{\frac{1}{2}}$  or  $q^{-\frac{1}{2}}$ , according to Figure 3.6, where the arc which appears later in the path is drawn higher.

---

<sup>23</sup>The double cover  $\Sigma$  is the Seiberg-Witten curve of the  $\mathcal{N} = 2$  theory at a point of its Coulomb branch, or the corresponding spectral curve of the Hitchin system.

To illustrate how this works, we consider the term

$$2 \frac{\mathcal{X}_3}{\mathcal{X}_1} \tag{3.72}$$

in (3.71). The factor 2 here means (3.72) is a sum of two contributions, associated to two different lifted paths: we show one of them in Figure 3.5. There is one crossing in Figure 3.5, where both strands are lifted to sheet 1.<sup>24</sup> Comparing this crossing to Figure 3.6, we see that this term should be weighted by  $q^{\frac{1}{2}}$ . Drawing a similar picture for the other contribution to (3.72) we see that it gets weighted by  $q^{-\frac{1}{2}}$ . Thus altogether (3.72) is replaced by

$$(q^{\frac{1}{2}} + q^{-\frac{1}{2}}) \frac{\mathcal{X}_3}{\mathcal{X}_1}, \tag{3.73}$$

which tells us that the 2 framed BPS states with charge  $\gamma_3 - \gamma_1$  come in a 2-dimensional multiplet of the rotation group  $SO(3)$ . Carrying out similar computations for the other terms one finds (as expected) that all of them come with the factor  $q^0$ , i.e. they are in the trivial representation of  $SO(3)$ . Thus altogether the  $q$ -deformed version of the generating function (3.71) turns out to be

$$\frac{1}{\mathcal{X}_1} + \frac{1}{\mathcal{X}_1 \mathcal{X}_2} + \mathcal{X}_3 + (q^{\frac{1}{2}} + q^{-\frac{1}{2}}) \frac{\mathcal{X}_3}{\mathcal{X}_1} + \frac{\mathcal{X}_3}{\mathcal{X}_1 \mathcal{X}_2} + \mathcal{X}_2 \mathcal{X}_3 + \frac{\mathcal{X}_2 \mathcal{X}_3}{\mathcal{X}_1}. \tag{3.74}$$

This is exactly the generating function for the line defect generator  $B_2$  in §3.6.1 below.

---

<sup>24</sup>The projection of the path to the base has two crossings, but at one of these crossings the two strands are lifted to different sheets, so it is not a crossing for the lifted path.

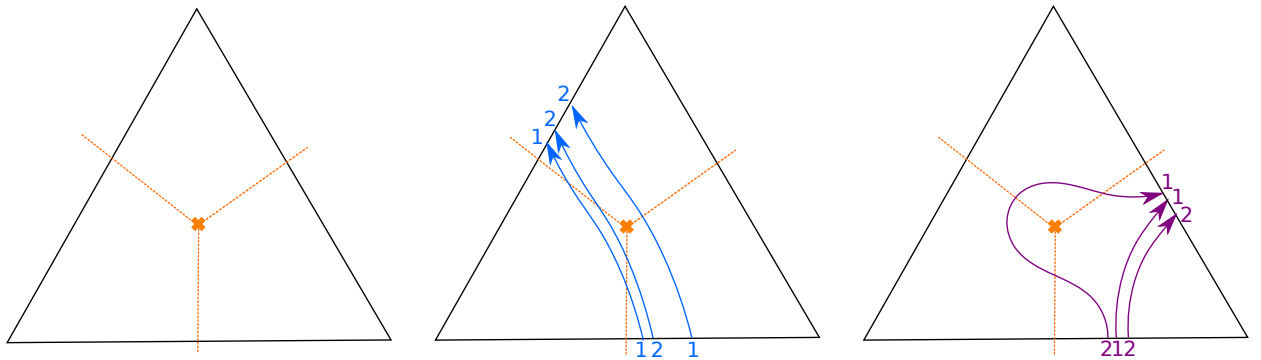


Figure 3.4: Left: a triangle with branch point and branch cuts marked. Middle: lifted left-turn paths. Right: lifted right-turn paths.

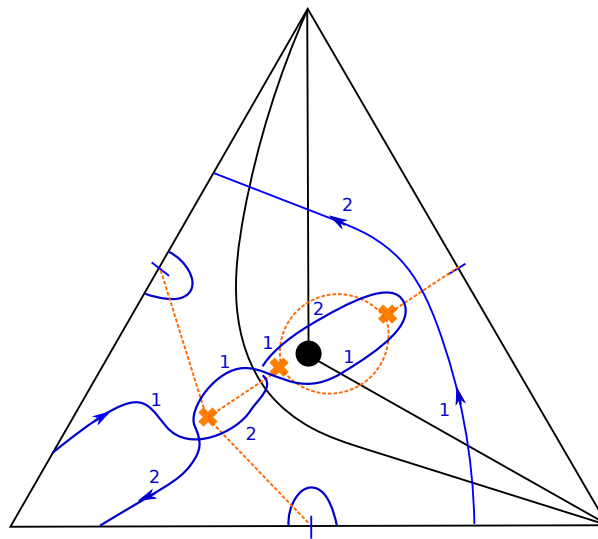


Figure 3.5: One of the lifted paths contributing to the term  $(3.72)$ .

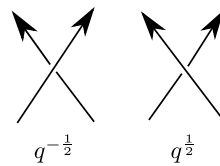


Figure 3.6: Rules for assigning powers of  $q$  to self-crossings of the lifted path.

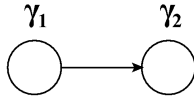


Figure 3.7: A BPS quiver for  $(A_1, A_2)$  Argyres-Douglas theory.

### 3.5 $(A_1, A_{2N})$ Argyres-Douglas theories

In this section we present the results of explicit computations verifying the commutativity (3.16) in the Argyres-Douglas theories of type  $(A_1, A_2)$ ,  $(A_1, A_4)$  and  $(A_1, A_6)$ .

#### 3.5.1 $(A_1, A_2)$ Argyres-Douglas theory

We consider  $(A_1, A_2)$  Argyres-Douglas theory and choose the chamber<sup>25</sup> represented by the BPS quiver in Figure 3.7 containing two BPS particles: (in increasing central charge phase order)

$$\gamma_1, \gamma_2. \tag{3.75}$$

There are five non-identity line defect generators. Assuming the line defect phase is smaller than the phases of all BPS particles, the generating functions

---

<sup>25</sup>In all the examples considered in this paper, to simplify computation, we always work in a chamber for which the number of number of BPS particles is the minimum possible — with one exception in the case of  $(A_1, A_6)$  as noted below.

are [23, 92]:

$$\begin{aligned}
F(L_1) &= X_{\gamma_1}, \\
F(L_2) &= X_{\gamma_2} + X_{\gamma_1+\gamma_2}, \\
F(L_3) &= X_{-\gamma_1} + X_{-\gamma_1+\gamma_2} + X_{\gamma_2}, \\
F(L_4) &= X_{-\gamma_1-\gamma_2} + X_{-\gamma_1}, \\
F(L_5) &= X_{-\gamma_2}.
\end{aligned} \tag{3.76}$$

In the geometric picture these generators  $L_i$  correspond to five laminations which are rotated into each other under the monodromy action. As a result their generating functions are related to each other by the action of powers of the monodromy operator.

The Schur index with  $L_i$  inserted is computed via [51]:

$$\mathcal{I}_{L_i}(q) = (q)_\infty^2 \text{Tr}[F(L_i)S(q)\bar{S}(q)], \quad S(q) = E_q(X_{\gamma_1})E_q(X_{\gamma_2}). \tag{3.77}$$

The corresponding  $2d$  chiral algebra is the  $(2, 5)$  minimal model [52, 54, 56], which has two primaries: the vacuum  $\Phi_{1,1}$  and  $\Phi_{1,2}$  with weight  $-1/5$ . In general, characters of  $\Phi_{s,r}$  in the  $(p, p')$  minimal model ( $1 \leq s \leq p-1$ ,  $1 \leq r \leq p'-1$ ) are given by [65]:

$$\begin{aligned}
\chi_{s,r}(q) &= q^{-\frac{(rp-sp')^2 - (p-p')^2}{4pp'} + \frac{1}{24}(1 - \frac{6(p-p')^2}{pp'})} \left( K_{s,r}^{p,p'}(q) - K_{-s,r}^{p,p'}(q) \right), \\
K_{s,r}^{p,p'}(q) &= \frac{1}{q^{\frac{1}{24}}(q)_\infty} \sum_{n \in \mathbb{Z}} q^{\frac{(2pp'n + pr - p's)^2}{4pp'}}.
\end{aligned} \tag{3.78}$$

The line defect Schur index  $\mathcal{I}_{L_i}(q)$  does not depend on the index  $i$  and admits the following character expansion [51]:

$$\mathcal{I}_L(q) = q^{-\frac{1}{2}} (\chi_{1,1}(q) - \chi_{1,2}(q)). \tag{3.79}$$

Similarly, the Schur index with two  $L_i$  inserted is given by [51]:

$$\mathcal{I}_{L_i L_j}(q) = (q)_\infty^2 \text{Tr}[F(L_i)F(L_j)S(q)\overline{S}(q)]. \quad (3.80)$$

Unlike  $\mathcal{I}_{L_i}(q)$ ,  $\mathcal{I}_{L_i L_j}(q)$  does depend on  $i$  and  $j$ , though this dependence disappears in the limit  $q \rightarrow 1$ . Expansions of  $\mathcal{I}_{L_i L_j}(q)$  in terms of characters are given as follows:

$$\begin{aligned} \mathcal{I}_{L_i L_i}(q) &= \mathcal{I}_{L_i L_{i-1}}(q) = (q^{-1} + q^{-2})\chi_{1,1}(q) - q^{-2}\chi_{1,2}(q), \\ \mathcal{I}_{L_i L_{i+1}}(q) &= \mathcal{I}_{L_i L_{i-2}}(q) = (1 + q^{-1})\chi_{1,1}(q) - q^{-1}\chi_{1,2}(q), \\ \mathcal{I}_{L_i L_{i+2}}(q) &= 2\chi_{1,1}(q) - \chi_{1,2}(q). \end{aligned} \quad (3.81)$$

The map  $f$  is given by

$$I \xrightarrow{f} [\Phi_{1,1}], \quad L_i \xrightarrow{f} [L] := [\Phi_{1,1}] - [\Phi_{1,2}]. \quad (3.82)$$

Moreover,

$$L_i L_j \xrightarrow{f} [LL] := 2[\Phi_{1,1}] - [\Phi_{1,2}]. \quad (3.83)$$

Recall that the non-trivial fusion rule in  $(2, 5)$  minimal model is given by

$$[\Phi_{1,2}] \times [\Phi_{1,2}] = [\Phi_{1,1}] + [\Phi_{1,2}]. \quad (3.84)$$

Combining with (3.82) and (3.83) we have

$$[LL] = [L] \times [L], \quad (3.85)$$

as first observed in [51].

Next we consider the fixed points of  $U(1)_r$ . For this purpose we found it convenient to use the geometric picture as described in §3.3.3. The classical monodromy action  $M$  is directly given by a single flip: see Figure 3.8.

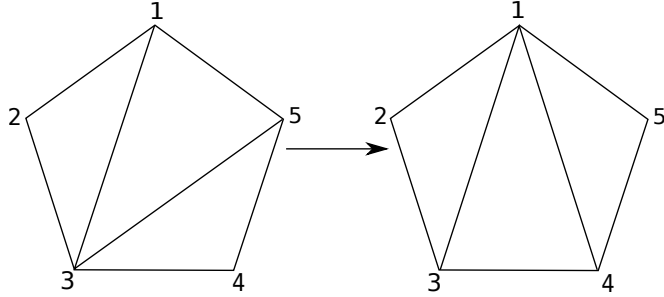


Figure 3.8: The classical monodromy action in the  $(A_1, A_2)$  theory, which rotates the triangulation of the pentagon clockwise by 2 units, is equivalent to a single flip which replaces the 35 edge by a 14 edge.

According to (3.58) the concrete transformation is given by

$$\mathcal{X}_{\gamma_1} \rightarrow \frac{1}{\mathcal{X}_{\gamma_2}}, \quad \mathcal{X}_{\gamma_2} \rightarrow \frac{\mathcal{X}_{\gamma_1} \mathcal{X}_{\gamma_2}}{1 + \mathcal{X}_{\gamma_2}}. \quad (3.86)$$

Thus the fixed locus is

$$\mathcal{X}_{\gamma_1}^2 - \mathcal{X}_{\gamma_1} - 1 = 0, \quad \mathcal{X}_{\gamma_2} = \frac{1}{\mathcal{X}_{\gamma_1}}. \quad (3.87)$$

This locus consists of two points, which we label I, II. At these points the  $X_\gamma$  evaluate to:

$$\text{I} : (\mathcal{X}_{\gamma_1}, \mathcal{X}_{\gamma_2}) = \left( \frac{1 - \sqrt{5}}{2}, -\frac{1 + \sqrt{5}}{2} \right), \quad \text{II} : (\mathcal{X}_{\gamma_1}, \mathcal{X}_{\gamma_2}) = \left( \frac{1 + \sqrt{5}}{2}, -\frac{1 - \sqrt{5}}{2} \right). \quad (3.88)$$

To construct the map  $g : \mathcal{L} \rightarrow \mathcal{O}(F)$ , for any line defect generator  $L_i$  we evaluate  $F(L_i)$  at these two fixed points, using (3.76). As expected, the dependence on  $L_i$  disappears in the process:

$$L_i \xrightarrow{g} (F_{L_i}^{\text{I}}, F_{L_i}^{\text{II}}) = \left( \frac{1 - \sqrt{5}}{2}, \frac{1 + \sqrt{5}}{2} \right). \quad (3.89)$$

Of course we also have the trivial line defect, whose vev is 1 at every fixed point:

$$1 \xrightarrow{g} (1, 1). \quad (3.90)$$

Finally, we follow the recipe described in §3.1.4, §3.1.5 to construct the isomorphism  $h : \mathcal{V} \rightarrow \mathcal{O}(F)$ . We need the fusion matrices, which are given by<sup>26</sup>

$$N_{\Phi_{1,1}} = \begin{pmatrix} 1 & 0 \\ 0 & 1 \end{pmatrix}, \quad N_{\Phi_{1,2}} = \begin{pmatrix} 0 & 1 \\ 1 & 1 \end{pmatrix}. \quad (3.91)$$

The modular  $S$ -matrix is [65]:

$$S = \frac{2}{\sqrt{5}} \begin{pmatrix} -\sin \frac{2\pi}{5} & \sin \frac{4\pi}{5} \\ \sin \frac{4\pi}{5} & \sin \frac{2\pi}{5} \end{pmatrix}. \quad (3.92)$$

Thus the fusion matrices are diagonalized by the  $S$  matrix,

$$\hat{N}_{\Phi_{1,1}} = SN_{\Phi_{1,1}}S^{-1} = \begin{pmatrix} 1 & 0 \\ 0 & 1 \end{pmatrix}, \quad \hat{N}_{\Phi_{1,2}} = SN_{\Phi_{1,2}}S^{-1} = \begin{pmatrix} \frac{1-\sqrt{5}}{2} & 0 \\ 0 & \frac{1+\sqrt{5}}{2} \end{pmatrix}. \quad (3.93)$$

As we explained in §3.1.4-§3.1.5, the map  $h$  takes each of  $\Phi_{1,1}$  and  $\Phi_{1,2}$  to its eigenvalues. So, it takes  $h(\Phi_{1,1}) = (1, 1)$  and *either*  $h(\Phi_{1,2}) = (\frac{1-\sqrt{5}}{2}, \frac{1+\sqrt{5}}{2})$  *or*  $h(\Phi_{1,2}) = (\frac{1+\sqrt{5}}{2}, \frac{1-\sqrt{5}}{2})$ . To decide which is the right ordering, we need to know the dictionary between  $U(1)_r$  fixed points and eigenspaces of the fusion operators. These eigenspaces themselves correspond to primary fields, so equivalently, we need the dictionary between the fixed points I, II and the primary fields  $\Phi_{1,1}$ ,  $\Phi_{1,2}$ . This dictionary is determined by the table below:

---

<sup>26</sup>Our convention is to order the primaries as  $(\Phi_{1,1}, \Phi_{1,2})$ .



fixed point	weights of $M$	weights of $U(1)_r$	primary field
I	$e^{2\pi i(3/5)}, e^{2\pi i(2/5)}$	$\frac{3}{5}, \frac{2}{5}$	$\Phi_{1,2}$
II	$e^{2\pi i(6/5)}, e^{-2\pi i(1/5)}$	$\frac{6}{5}, -\frac{1}{5}$	$\Phi_{1,1}$

In this table, to determine the weights of  $M$  at each fixed point, we computed directly the linearization of the classical monodromy (3.86). On the other side, the dictionary between primary fields and  $U(1)$  weights is taken from [71]. At any rate, we can now read off that  $\Phi_{1,1}$  corresponds to fixed point II and  $\Phi_{1,2}$  corresponds to fixed point I. Combining this with (3.93),  $h$  is given by:

$$[\Phi_{1,1}] \xrightarrow{h} (1, 1), \quad [\Phi_{1,2}] \xrightarrow{h} \left( \frac{1+\sqrt{5}}{2}, \frac{1-\sqrt{5}}{2} \right). \quad (3.94)$$

Composing this with  $f$  from (3.82) we have

$$L_i \xrightarrow{h \circ f} \left( \frac{1-\sqrt{5}}{2}, \frac{1+\sqrt{5}}{2} \right). \quad (3.95)$$

Comparing this with (3.89) we see that the diagram indeed commutes.

### 3.5.2 An intermission on the homomorphism property

To make sure  $f$  is a homomorphism, (3.85) needs to hold not only for the generators  $L_i$  but also for arbitrary line defects. This would involve checking e.g.

$$[LLL] \stackrel{?}{=} [L] \times [L] \times [L] \quad (3.96)$$

and similar relations for higher number of line defect generators<sup>27</sup>. As an example let us consider the case of three line defect generators. The line

---

<sup>27</sup>We would like to comment that the product of  $F(L)$  is associative (due to associativity of the quantum torus algebra of  $X_\gamma$ ) and so is the fusion product.

defect Schur index is given by

$$\mathcal{I}_{L_i L_j L_k}(q) = (q)_\infty^2 \text{Tr}[F(L_i)F(L_j)F(L_k)S(q)\overline{S}(q)]. \quad (3.97)$$

There are many relations between  $\mathcal{I}_{L_i L_j L_k}$ ,

$$\begin{aligned} \mathcal{I}_{L_{i-1} L_i L_{i+2}} &= \mathcal{I}_{L_{i-1} L_i L_{i+1}} = \mathcal{I}_{L_{i-2} L_i L_{i+1}}, \\ \mathcal{I}_{L_i L_i L_{i+2}} &= \mathcal{I}_{L_{i-2} L_i L_{i+2}} = \mathcal{I}_{L_{i-2} L_i L_i}, \\ \mathcal{I}_{L_{i+2} L_i L_{i+1}} &= \mathcal{I}_{L_i L_i L_{i+1}} = \mathcal{I}_{L_{i+2} L_i L_i} = \mathcal{I}_{L_{i-1} L_i L_i} = \mathcal{I}_{L_i L_i L_{i-2}} = \mathcal{I}_{L_{i-1} L_i L_{i-2}}, \\ \mathcal{I}_{L_{i+1} L_i L_i} &= \mathcal{I}_{L_i L_i L_i} = \mathcal{I}_{L_i L_i L_{i-1}} = q^{-2} \mathcal{I}_{L_{i-1} L_i L_{i-2}}, \\ \mathcal{I}_{L_{i+1} L_i L_{i+1}} &= \mathcal{I}_{L_{i-1} L_i L_{i-1}} = \mathcal{I}_{L_{i+1} L_i L_{i-1}} = q^{-1} \mathcal{I}_{L_{i-1} L_i L_{i-2}}, \\ \mathcal{I}_{L_{i+2} L_i L_{i+2}} &= \mathcal{I}_{L_{i+1} L_i L_{i+2}} = \mathcal{I}_{L_{i+2} L_i L_{i-1}} = \mathcal{I}_{L_{i-2} L_i L_{i-1}} = \mathcal{I}_{L_{i+1} L_i L_{i-2}} = \mathcal{I}_{L_{i-2} L_i L_{i-2}}. \end{aligned}$$

The independent indices admit the following character expansions,

$$\begin{aligned} \mathcal{I}_{L_{i-2} L_i L_{i+1}} &= q^{-\frac{1}{2}} \left( (1+2q)\chi_{1,1}(q) - (1+q)\chi_{1,2}(q) \right), \\ \mathcal{I}_{L_{i-2} L_i L_i} &= q^{-\frac{1}{2}} \left( (2+q)\chi_{1,1}(q) - 2\chi_{1,2}(q) \right), \\ \mathcal{I}_{L_{i-1} L_i L_{i-2}} &= q^{-\frac{1}{2}} \left( (1+q^{-1}+q^{-2})\chi_{1,1}(q) - (1+q^{-2})\chi_{1,2}(q) \right), \\ \mathcal{I}_{L_{i+2} L_i L_{i-2}} &= q^{-\frac{1}{2}} \left( 3\chi_{1,1}(q) - 2\chi_{1,2}(q) \right), \\ \mathcal{I}_{L_{i-2} L_i L_{i-2}} &= q^{-\frac{1}{2}} \left( (2+q^{-1})\chi_{1,1}(q) - (1+q^{-1})\chi_{1,2}(q) \right). \end{aligned}$$

We immediately see that

$$L_i L_j L_k \xrightarrow{f} [LLL] := 3[\Phi_{1,1}] - 2[\Phi_{1,2}] = [L] \times [L] \times [L]. \quad (3.98)$$

In principal, to prove that  $f$  is a homomorphism we need to repeat the above calculation for arbitrary number of line defect generator insertions. We

are not able to prove it in this paper. Instead we offer some arguments about why we believe  $f$  is indeed a homomorphism. We have seen explicitly that the images of  $L_i L_j$  and  $L_i L_j L_k$  under  $f$  does not depend on the index  $i$ . In other examples that we consider in this paper we also checked the image of  $L_{\rho i} L_{\mu j}$ <sup>28</sup> does not depend on  $i$ . Although we don't have a proof for now, we conjecture this phenomenon is general, i.e. the image of  $L_{\rho_1 i_1} L_{\rho_2 i_2} \dots L_{\rho_n i_n}$  under  $f$  does not depend on  $i_1, \dots, i_n$ . Combining this conjecture with relations between line defect generating functions one could see that  $f$  is indeed a homomorphism.

We revisit the situation of three line defect generators. To compute the image of  $L_i L_j L_k$  under  $f$  we could pick any three line defect generators. Let's recall the following relation between  $F(L_i)$  [23,92]:

$$F(L_i)F(L_{i+2}) = 1 + q^{\frac{1}{2}}F(L_{i+1}), \quad (3.99)$$

from which follows  $[L] \times [L] = [\Phi_{1,1}] + [L]$ <sup>29</sup> Schur index with insertion of  $L_i, L_{i+2}, L_k$  is then given by

$$\mathcal{I}_{L_i L_{i+2} L_k}(q) = \mathcal{I}_{L_k}(q) + q^{\frac{1}{2}}\mathcal{I}_{L_{i+1} L_k}(q), \quad (3.100)$$

from which it follows that

$$[LLL] = [L] + [LL] = [L] \times [L] \times [L]. \quad (3.101)$$

Similarly one could consider insertion of more line defect generators. By the conjecture, to compute the image of  $L_{i_1} \dots L_{i_n}$  under  $f$ , it doesn't matter what

---

<sup>28</sup>Here  $\rho, \mu$  label different types of line defect generators, see [3.5.3], [3.5.4], [3.6.1], [3.6.2]

<sup>29</sup>As discussed in [3.1.9] in  $(A_1, A_{2N})$  theories the line defect generators themselves correspond to a basis which also realizes fusion rules.

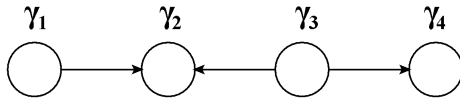


Figure 3.9: A BPS quiver for  $(A_1, A_4)$  Argyres-Douglas theory.

$i_1, \dots, i_n$  are. Then we could again use (3.99) to reduce the number of line defect generators. Moreover this process is consistent with the fusion rules such that

$$[L \dots L] = [L] \times \dots \times [L]. \quad (3.102)$$

For other Argyres-Douglas theories that we are considering in this paper, there are always enough relations between  $F(L_{\alpha i})$  such that the same argument goes through provided our conjecture would hold.

### 3.5.3 $(A_1, A_4)$ Argyres-Douglas theory

We consider the  $(A_1, A_4)$  Argyres-Douglas theory. We choose a chamber represented by the BPS quiver shown in Figure 3.9. Moreover our choice is made such that there are four BPS particles in this chamber. Their charges are (in increasing central charge phase order):

$$\gamma_1, \gamma_3, \gamma_2, \gamma_4 \quad (3.103)$$

Line defect generators in  $(A_1, A_4)$  Argyres-Douglas theory and their generating functions were computed in [51]. For completeness we reproduce their results here. Starting from the initial seed, we apply all possible left mutations to generate other seeds. There are in total 42 seeds. Correspondingly

there are 42 dual cones. Each dual cone is bounded by four half-hyperplanes. Moreover, every three out of the four half-hyperplanes intersect at a half line. In total there are four such half-lines for each dual cone and they form edges of the dual cone. Each edge corresponds to the core charge of one line defect generator. For example, the dual cone for the initial seed is given by:

$$\check{\mathcal{C}}_{\{\gamma_1, \gamma_2, \gamma_3, \gamma_4\}} = \left\{ \sum_{i=1}^4 a_i \gamma_i \mid a_2 \leq 0, a_1 + a_3 \geq 0, a_2 + a_4 \leq 0, a_3 \geq 0 \right\}. \quad (3.104)$$

Then we get four line defect generators whose core charges are given by

$$\gamma_1, -\gamma_1 + \gamma_3, -\gamma_2 + \gamma_4, -\gamma_4. \quad (3.105)$$

Repeating this procedure for all 42 dual cones we get 14 edges. Thus the line defects in  $(A_1, A_4)$  Argyres-Douglas theory are generated by the identity operator and 14 nontrivial generators. Recall that the  $(2, 7)$  minimal model has two non-vacuum modules; therefore we have an expected multiplicity of 7. In the class  $\mathcal{S}$  realization of the theory this would correspond to the  $\mathbb{Z}_7$  symmetry of the 7-gon.

We assume that the line defect phase is smaller than the phases of all vanilla BPS particles, and calculate the generating function using consecutive right mutations on the framed quiver. For example, the line defect generator with core charge  $\gamma_c = \gamma_1 - \gamma_3$  goes through the following mutation sequence:

$$\begin{aligned} \{\gamma_1, \gamma_2, \gamma_3, \gamma_4, \gamma_c\} &\xrightarrow{\mu_{\gamma_c}^R} \{\gamma_1, \gamma_2, \gamma_3, \gamma_4 + \gamma_c, -\gamma_c\} \xrightarrow{\mu_{\gamma_4 + \gamma_c}^R} \\ &\{\gamma_1, \gamma_2, \gamma_3 + \gamma_4 + \gamma_c, -\gamma_4 - \gamma_c, \gamma_4\} \xrightarrow{\mu_{\gamma_3 + \gamma_4 + \gamma_c}^R} \{\gamma_1, \gamma_2, -\gamma_3 - \gamma_4 - \gamma_c, \gamma_3, \gamma_4\}, \end{aligned} \quad (3.106)$$

which implies that its generating function is

$$F(L) = X_{\gamma_1 - \gamma_3} + X_{\gamma_1 - \gamma_3 + \gamma_4} + X_{\gamma_1 + \gamma_4}.$$

The generating functions for all 14 line defect generators are (as given also in [\[51\]](#)):

$$F(A_1) = X_{-\gamma_2 + \gamma_4},$$

$$F(A_2) = X_{-\gamma_1 + \gamma_3},$$

$$F(A_3) = X_{\gamma_2 - \gamma_4} + X_{\gamma_1 + \gamma_2 - \gamma_4},$$

$$F(A_4) = X_{\gamma_1 - \gamma_3 - \gamma_4} + X_{\gamma_1 - \gamma_3},$$

$$F(A_5) = X_{-\gamma_1 - \gamma_4} + X_{-\gamma_1 + \gamma_2 - \gamma_4} + X_{\gamma_2 - \gamma_4},$$

$$F(A_6) = X_{-\gamma_1 - \gamma_2 + \gamma_4} + X_{-\gamma_1 + \gamma_4} + X_{-\gamma_1 + \gamma_3 + \gamma_4},$$

$$F(A_7) = X_{\gamma_1 - \gamma_3} + X_{\gamma_1 - \gamma_3 + \gamma_4} + X_{\gamma_1 + \gamma_4},$$

$$F(B_1) = X_{\gamma_1},$$

$$F(B_2) = X_{-\gamma_4},$$

$$F(B_3) = X_{-\gamma_1 - \gamma_2} + X_{-\gamma_1},$$

$$F(B_4) = X_{\gamma_4} + X_{\gamma_3 + \gamma_4},$$

$$F(B_5) = X_{-\gamma_1} + X_{-\gamma_1 + \gamma_2} + X_{\gamma_2} + X_{-\gamma_1 + \gamma_2 + \gamma_3} + X_{\gamma_2 + \gamma_3},$$

$$F(B_6) = X_{-\gamma_2 - \gamma_3} + X_{-\gamma_3} + X_{-\gamma_2 - \gamma_3 + \gamma_4} + X_{-\gamma_3 + \gamma_4} + X_{\gamma_4},$$

$$F(B_7) = X_{-\gamma_3 - \gamma_4} + X_{\gamma_2 - \gamma_3 - \gamma_4} + X_{\gamma_1 + \gamma_2 - \gamma_3 - \gamma_4} + X_{-\gamma_3} + X_{\gamma_2 - \gamma_3} + X_{\gamma_1 + \gamma_2 - \gamma_3} \\ + X_{\gamma_2} + X_{\gamma_1 + \gamma_2}.$$

The generating functions for  $A_i$  ( $B_i$ ) are related to each other by the action of powers of the monodromy operator. The Schur index with line defect  $A_i$  ( $B_i$ )

inserted is computed using [51]

$$\mathcal{I}_{A_i}(q) = (q)_\infty^4 \text{Tr}[F(A_i)S(q)\overline{S}(q)], \quad \mathcal{I}_{B_i}(q) = (q)_\infty^4 \text{Tr}[F(B_i)S(q)\overline{S}(q)] \quad (3.107)$$

where in this particular chamber  $S(q)$  is given by

$$S(q) = E_q(X_{\gamma_1})E_q(X_{\gamma_3})E_q(X_{\gamma_2})E_q(X_{\gamma_4}). \quad (3.108)$$

As described in [51], the Schur index with one line defect inserted does not depend on  $i \in \{1, \dots, 7\}$ :

$$\begin{aligned} \mathcal{I}_A(q) &= q + q^4 + q^5 + q^6 + 2q^7 + 2q^8 + 3q^9 + 3q^{10} + \dots, \\ \mathcal{I}_B(q) &= -q^{\frac{1}{2}} - q^{\frac{5}{2}} - q^{\frac{7}{2}} - q^{\frac{9}{2}} - 2q^{\frac{11}{2}} - 3q^{\frac{13}{2}} - 3q^{\frac{15}{2}} - 4q^{\frac{17}{2}} - 5q^{\frac{19}{2}} + \dots. \end{aligned} \quad (3.109)$$

The chiral algebra in this case is the  $(2, 7)$  Virasoro minimal model [52, 54, 56]. There are three primary fields: the vacuum  $\Phi_{1,1}$ ,  $\Phi_{1,2}$  with weight  $-2/7$  and  $\Phi_{1,3}$  with weight  $-3/7$ . Line defect Schur indices admit the following expansions in terms of characters:

$$\begin{aligned} \mathcal{I}_A(q) &= q^{-1}(\chi_{1,3}(q) - \chi_{1,2}(q)), \\ \mathcal{I}_B(q) &= q^{-\frac{1}{2}}(\chi_{1,1}(q) - \chi_{1,2}(q)). \end{aligned} \quad (3.110)$$

The map  $f$  between the line defect algebra  $\mathcal{L}$  and the Verlinde algebra  $\mathcal{V}$  is then given by:

$$\begin{aligned} I &\xrightarrow{f} [\Phi_{1,1}], \\ A_i &\xrightarrow{f} [A] = [\Phi_{1,3}] - [\Phi_{1,2}], \\ B_i &\xrightarrow{f} [B] = [\Phi_{1,1}] - [\Phi_{1,2}]. \end{aligned} \quad (3.111)$$

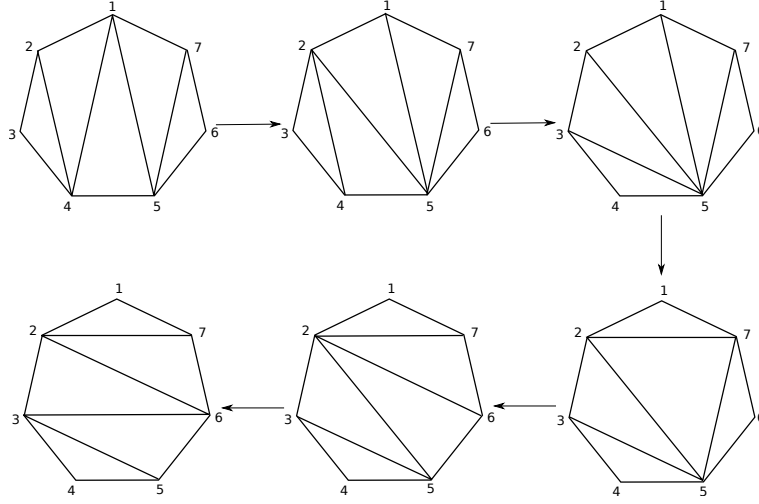


Figure 3.10: The classical monodromy action in the  $(A_1, A_4)$  theory is realized by a sequence of flips of triangulations of the 7-gon. The initial triangulation differs from the final one by a clockwise rotation by 2 units.

The non-trivial fusion rules in the  $(2, 7)$  Virasoro minimal model are:

$$\begin{aligned}
 [\Phi_{1,2}] \times [\Phi_{1,2}] &= [\Phi_{1,1}] + [\Phi_{1,3}], \\
 [\Phi_{1,3}] \times [\Phi_{1,3}] &= [\Phi_{1,1}] + [\Phi_{1,2}] + [\Phi_{1,3}], \\
 [\Phi_{1,2}] \times [\Phi_{1,3}] &= [\Phi_{1,2}] + [\Phi_{1,3}].
 \end{aligned} \tag{3.112}$$

As first checked in [51],

$$\begin{aligned}
 [AA] &= [A] \times [A], \\
 [BB] &= [B] \times [B], \\
 [AB] &= [A] \times [B],
 \end{aligned} \tag{3.113}$$

which gives evidence  $f$  is indeed a homomorphism  $\mathcal{L} \rightarrow \mathcal{V}$ .

Now we turn to study the fixed points under the classical monodromy action  $M$ . By doing a series of flips (see Figure 3.10, the initial zigzag triangulation corresponds to the BPS quiver in Figure 3.9 using the dictionary in [1].



The monodromy action is given as follows:

$$\begin{aligned}
\mathcal{X}_{\gamma_1} &\rightarrow \frac{1 + \mathcal{X}_{\gamma_2} + \mathcal{X}_{\gamma_4} + \mathcal{X}_{\gamma_2}\mathcal{X}_{\gamma_4} + \mathcal{X}_{\gamma_2}\mathcal{X}_{\gamma_3}\mathcal{X}_{\gamma_4}}{\mathcal{X}_{\gamma_2}\mathcal{X}_{\gamma_3}}, \\
\mathcal{X}_{\gamma_2} &\rightarrow \frac{\mathcal{X}_{\gamma_1}\mathcal{X}_{\gamma_2}\mathcal{X}_{\gamma_3}}{(1 + \mathcal{X}_{\gamma_2} + \mathcal{X}_{\gamma_2}\mathcal{X}_{\gamma_3})[1 + \mathcal{X}_{\gamma_4} + \mathcal{X}_{\gamma_2}(1 + \mathcal{X}_{\gamma_1})(1 + \mathcal{X}_{\gamma_4} + \mathcal{X}_{\gamma_3}\mathcal{X}_{\gamma_4})]}, \\
\mathcal{X}_{\gamma_3} &\rightarrow \frac{(1 + \mathcal{X}_{\gamma_2} + \mathcal{X}_{\gamma_1}\mathcal{X}_{\gamma_2})[1 + \mathcal{X}_{\gamma_4} + \mathcal{X}_{\gamma_2}(1 + \mathcal{X}_{\gamma_4} + \mathcal{X}_{\gamma_3}\mathcal{X}_{\gamma_4})]}{\mathcal{X}_{\gamma_1}\mathcal{X}_{\gamma_2}\mathcal{X}_{\gamma_3}\mathcal{X}_{\gamma_4}}, \\
\mathcal{X}_{\gamma_4} &\rightarrow \frac{\mathcal{X}_{\gamma_3}\mathcal{X}_{\gamma_4}}{1 + \mathcal{X}_{\gamma_4} + \mathcal{X}_{\gamma_2}(1 + \mathcal{X}_{\gamma_1})(1 + \mathcal{X}_{\gamma_4} + \mathcal{X}_{\gamma_3}\mathcal{X}_{\gamma_4})}.
\end{aligned} \tag{3.114}$$

There are exactly three fixed points, which we label I, II, III. On the fixed points  $\mathcal{X}_\gamma$  evaluate to

$$\begin{aligned}
\mathcal{X}_{\gamma_4} &: (\alpha_1, \alpha_2, \alpha_3), \\
\mathcal{X}_{\gamma_3} &: (4 + \alpha_1 - 2\alpha_1^2, 4 + \alpha_2 - 2\alpha_2^2, 4 + \alpha_3 - 2\alpha_3^2), \\
\mathcal{X}_{\gamma_2} &: (\alpha_1 - \alpha_1^2, \alpha_2 - \alpha_2^2, \alpha_3 - \alpha_3^2), \\
\mathcal{X}_{\gamma_1} &: (2 + \alpha_1 - \alpha_1^2, 2 + \alpha_2 - \alpha_2^2, 2 + \alpha_3 - \alpha_3^2),
\end{aligned} \tag{3.115}$$

where  $\alpha_i$  are the three roots of the cubic equation

$$\alpha^3 - \alpha^2 - 2\alpha + 1 = 0. \tag{3.116}$$

Concretely,

$$\begin{aligned}
\alpha_1 &= \frac{1}{3}\left(1 - \frac{7}{a}(-1)^{1/3} + a(-1)^{2/3}\right), \quad \alpha_2 = \frac{1}{3}\left(1 + \frac{7}{a}(-1)^{2/3} - a(-1)^{1/3}\right), \\
\alpha_3 &= \frac{1}{3}\left(1 + \frac{7}{a} + a\right), \quad \text{with } a = \left(\frac{7}{2}\right)^{\frac{1}{3}}(-1 + i\sqrt{3})^{\frac{1}{3}}.
\end{aligned}$$

Evaluating the  $F(A_i)$  at the fixed points we find that the values are independent of  $i = 1, \dots, 7$ , and similarly for  $F(B_i)$ , as expected. Concretely, we

get

$$\begin{aligned} A_i &\xrightarrow{g} \left( \frac{1}{1-\alpha_1}, \frac{1}{1-\alpha_2}, \frac{1}{1-\alpha_3} \right), \\ B_i &\xrightarrow{g} \left( \frac{1}{\alpha_1}, \frac{1}{\alpha_2}, \frac{1}{\alpha_3} \right). \end{aligned} \quad (3.117)$$

Finally we want to construct  $h$ . We have the following Verlinde matrices for  $[\Phi_{1,2}]$  and  $[\Phi_{1,3}]$ :

$$N_{\Phi_{1,2}} = \begin{pmatrix} 0 & 1 & 0 \\ 1 & 0 & 1 \\ 0 & 1 & 1 \end{pmatrix}, \quad N_{\Phi_{1,3}} = \begin{pmatrix} 0 & 0 & 1 \\ 0 & 1 & 1 \\ 1 & 1 & 1 \end{pmatrix}. \quad (3.118)$$

As before, we obtain  $h$  by simultaneously diagonalizing  $N_{\Phi_{1,2}}$  and  $N_{\Phi_{1,3}}$  using  $S$ -matrix and then comparing with the correspondence between  $U(1)$  fixed points and primaries of (2, 7) Virasoro minimal model. The  $S$ -matrix for the (2,7) minimal models is [65]:

$$S = \frac{2}{\sqrt{7}} \begin{pmatrix} \cos\frac{3\pi}{14} & -\cos\frac{\pi}{14} & \sin\frac{\pi}{7} \\ -\cos\frac{\pi}{14} & -\sin\frac{\pi}{7} & \cos\frac{3\pi}{14} \\ \sin\frac{\pi}{7} & \cos\frac{3\pi}{14} & \cos\frac{\pi}{14} \end{pmatrix}. \quad (3.119)$$

$N_{\Phi_{1,2}}$  and  $N_{\Phi_{1,3}}$  are simultaneously diagonalized by  $S$ :

$$SN_{\Phi_{1,2}}S^{-1} = \begin{pmatrix} \alpha_1 & 0 & 0 \\ 0 & \alpha_2 & 0 \\ 0 & 0 & \alpha_3 \end{pmatrix}, \quad SN_{\Phi_{1,3}}S^{-1} = \begin{pmatrix} \beta_1 & 0 & 0 \\ 0 & \beta_2 & 0 \\ 0 & 0 & \beta_3 \end{pmatrix}, \quad (3.120)$$

where

$$\begin{aligned} \beta_1 &= \frac{1}{3} \left( 2 + \frac{7}{b} (-1)^{2/3} - b (-1)^{1/3} \right), \quad \beta_2 = \frac{1}{3} \left( 2 - \frac{7}{b} (-1)^{1/3} + b (-1)^{2/3} \right) \\ \beta_3 &= \frac{1}{3} \left( 2 + \frac{7}{b} + b \right), \quad \text{with } b = \left( \frac{7}{2} \right)^{\frac{1}{3}} (1 + i\sqrt{3})^{\frac{1}{3}}. \end{aligned}$$

According to [69,71], the corresponding wild Hitchin moduli space has exactly three  $U(1)_r$ -fixed points, each of which corresponds to a primary field in the  $(2, 7)$  minimal model:

fixed point	weights of $M$	$U(1)_r$ weights	primary field
I	$e^{2\pi i(3/7)}, e^{2\pi i(4/7)}, e^{2\pi i(5/7)}, e^{2\pi i(2/7)}$	$\frac{3}{7}, \frac{4}{7}, \frac{5}{7}, \frac{2}{7}$	$\Phi_{1,3}$
II	$e^{2\pi i(8/7)}, e^{-2\pi i(1/7)}, e^{2\pi i(10/7)}, e^{-2\pi i(3/7)}$	$\frac{8}{7}, -\frac{1}{7}, \frac{10}{7}, -\frac{3}{7}$	$\Phi_{1,1}$
III	$e^{2\pi i(8/7)}, e^{-2\pi i(1/7)}, e^{2\pi i(5/7)}, e^{2\pi i(2/7)}$	$\frac{8}{7}, -\frac{1}{7}, \frac{5}{7}, \frac{2}{7}$	$\Phi_{1,2}$

Using this table and (3.120), the isomorphism  $h$  between  $\mathcal{V}$  and  $\mathcal{O}(F)$  is:

$$\begin{aligned}
[\Phi_{1,1}] &\xrightarrow{h} (1, 1, 1), \\
[\Phi_{1,2}] &\xrightarrow{h} (\alpha_3, \alpha_1, \alpha_2), \\
[\Phi_{1,3}] &\xrightarrow{h} (\beta_3, \beta_1, \beta_2).
\end{aligned} \tag{3.121}$$

The image of  $A_i$  and  $B_i$  under  $h \circ f$  is then:

$$\begin{aligned}
A_i &\xrightarrow{h \circ f} (\beta_3 - \alpha_3, \beta_1 - \alpha_1, \beta_2 - \alpha_2), \\
B_i &\xrightarrow{h \circ f} (1 - \alpha_3, 1 - \alpha_1, 1 - \alpha_2).
\end{aligned} \tag{3.122}$$

Although it is not obvious, one can check that this indeed agrees with (3.117), so the diagram commutes, as desired.

### 3.5.4 $(A_1, A_6)$ Argyres-Douglas theory

Here we consider the  $(A_1, A_6)$  Argyres-Douglas theory. This theory has a new feature: at one of the fixed points (fixed point I below), some of the cluster coordinates  $\mathcal{X}_\gamma$  associated to the canonical chamber blow up. This being so, computing the fixed points of the classical monodromy in that

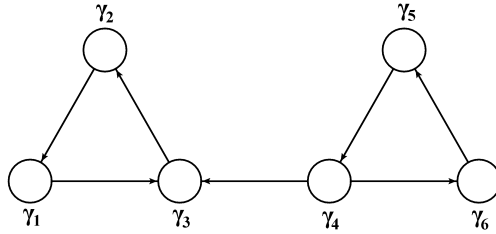


Figure 3.11: A BPS quiver for  $(A_1, A_6)$  Argyres-Douglas theory.

chamber actually misses one fixed point. Thus, with the benefit of hindsight, we choose a different chamber, whose BPS quiver is shown in Figure [3.11](#)

There are eight BPS particles in this chamber, with the following charges (in increasing central charge phase order):

$$\gamma_4, \gamma_6, \gamma_4 + \gamma_5, \gamma_5, \gamma_3, \gamma_1 + \gamma_3, \gamma_2, \gamma_1. \quad (3.123)$$

Quiver mutation starting from this chamber generates in total 429 seeds. After mutating back to the original seed the 429 dual cones span the whole charge lattice. Each dual cone is bounded by six half-hyperplanes. Every five of the six half-hyperplanes intersect at a half line which forms an edge of the dual cone and there are six edges for each dual cone. For example, the six edges of the dual cone for the initial seed  $\check{C}_{\{\gamma_1, \gamma_2, \gamma_3, \gamma_4, \gamma_5, \gamma_6\}}$  are spanned by:

$$\begin{aligned} &\gamma_2 + \gamma_4 + \gamma_5 + \gamma_6, -\gamma_1 + \gamma_4 + \gamma_5 + \gamma_6, \gamma_4 + \gamma_5 + \gamma_6, \\ &-\gamma_1 - \gamma_2 - \gamma_3, -\gamma_1 - \gamma_2 - \gamma_3 + \gamma_6, -\gamma_1 - \gamma_2 - \gamma_3 - \gamma_5. \end{aligned} \quad (3.124)$$

Repeating this for all 429 dual cones we get in total 27 edges. Correspondingly there are 27 nontrivial line defect generators in the  $(A_1, A_6)$  theory. The  $(2, 9)$  minimal model has three non-vacuum modules, so there is a multiplicity of 9,

corresponding to the  $\mathbb{Z}_9$  symmetry of the 9-gon. Assuming that the line defect phase is smaller than central charge phases of all vanilla BPS particles, their generating functions are:

$$F(A_1) = X_{\gamma_1+\gamma_2+\gamma_3-\gamma_6} + X_{\gamma_1+\gamma_2+\gamma_3+\gamma_5-\gamma_6} + X_{\gamma_1+\gamma_2+\gamma_3+\gamma_5},$$

$$F(A_2) = X_{-\gamma_2-\gamma_4-\gamma_5-\gamma_6} + X_{\gamma_1-\gamma_2-\gamma_4-\gamma_5-\gamma_6} + X_{\gamma_1-\gamma_4-\gamma_5-\gamma_6},$$

$$F(A_3) = X_{-\gamma_1-\gamma_2-\gamma_3-\gamma_5},$$

$$F(A_4) = X_{\gamma_2+\gamma_4+\gamma_5+\gamma_6},$$

$$F(A_5) = X_{-\gamma_1-\gamma_2-\gamma_3+\gamma_6},$$

$$F(A_6) = X_{\gamma_1+\gamma_2+\gamma_3+\gamma_5} + X_{\gamma_1+\gamma_2+\gamma_3+\gamma_5+\gamma_6} + X_{\gamma_1+\gamma_2+\gamma_3+\gamma_4+\gamma_5+\gamma_6},$$

$$F(A_7) = X_{\gamma_1-\gamma_4-\gamma_5-\gamma_6} + X_{\gamma_1+\gamma_2-\gamma_4-\gamma_5-\gamma_6} + X_{\gamma_1+\gamma_2+\gamma_3-\gamma_4-\gamma_5-\gamma_6} + X_{\gamma_1+\gamma_2+\gamma_3-\gamma_5-\gamma_6} \\ + X_{\gamma_1+\gamma_2+\gamma_3-\gamma_6},$$

$$F(A_8) = X_{-\gamma_1-\gamma_2-\gamma_3-\gamma_4-\gamma_5-\gamma_6} + X_{-\gamma_1-\gamma_2-\gamma_4-\gamma_5-\gamma_6} + X_{-\gamma_2-\gamma_4-\gamma_5-\gamma_6},$$

$$F(A_9) = X_{-\gamma_1+\gamma_4+\gamma_5+\gamma_6},$$

$$F(B_1) = X_{-\gamma_5-\gamma_6} + X_{-\gamma_6},$$

$$F(B_2) = X_{\gamma_1} + X_{\gamma_1+\gamma_2},$$

$$F(B_3) = X_{\gamma_5} + X_{\gamma_5+\gamma_6},$$

$$F(B_4) = X_{-\gamma_1-\gamma_2} + X_{-\gamma_2},$$

$$F(B_5) = X_{\gamma_6} + X_{\gamma_4+\gamma_6},$$

$$F(B_6) = X_{-\gamma_1-\gamma_3} + X_{-\gamma_1},$$

$$F(B_7) = X_{-\gamma_2-\gamma_3-\gamma_4-\gamma_5} + X_{-\gamma_3-\gamma_4-\gamma_5} + X_{-\gamma_4-\gamma_5} + X_{-\gamma_5},$$

$$F(B_8) = X_{-\gamma_4-\gamma_6} + X_{-\gamma_4} + X_{\gamma_3-\gamma_4-\gamma_6} + X_{\gamma_3-\gamma_4} + X_{\gamma_3} + X_{\gamma_1+\gamma_3-\gamma_4-\gamma_6} + X_{\gamma_1+\gamma_3-\gamma_4} + X_{\gamma_1+\gamma_3},$$

$$F(B_9) = X_{\gamma_2} + X_{\gamma_2+\gamma_3} + X_{\gamma_2+\gamma_3+\gamma_4} + X_{\gamma_2+\gamma_3+\gamma_4+\gamma_5},$$

$$F(C_1) = X_{-\gamma_1-\gamma_2-\gamma_3},$$

$$F(C_2) = X_{\gamma_4+\gamma_5+\gamma_6},$$

$$F(C_3) = X_{\gamma_1+\gamma_2+\gamma_3} + X_{\gamma_1+\gamma_2+\gamma_3+\gamma_4} + X_{\gamma_1+\gamma_2+\gamma_3+\gamma_4+\gamma_5},$$

$$F(C_4) = X_{-\gamma_2-\gamma_3-\gamma_4-\gamma_5-\gamma_6} + X_{-\gamma_3-\gamma_4-\gamma_5-\gamma_6} + X_{-\gamma_4-\gamma_5-\gamma_6},$$

$$F(C_5) = X_{\gamma_1-\gamma_4-\gamma_6} + X_{\gamma_1-\gamma_4} + X_{\gamma_1+\gamma_2-\gamma_4-\gamma_6} + X_{\gamma_1+\gamma_2-\gamma_4} + X_{\gamma_1+\gamma_2+\gamma_3-\gamma_4-\gamma_6} \\ + X_{\gamma_1+\gamma_2+\gamma_3-\gamma_4} + X_{\gamma_1+\gamma_2+\gamma_3},$$

$$F(C_6) = X_{-\gamma_4-\gamma_5-\gamma_6} + X_{\gamma_3-\gamma_4-\gamma_5-\gamma_6} + X_{\gamma_3-\gamma_5-\gamma_6} + X_{\gamma_3-\gamma_6} + X_{\gamma_1+\gamma_3-\gamma_4-\gamma_5-\gamma_6} \\ + X_{\gamma_1+\gamma_3-\gamma_5-\gamma_6} + X_{\gamma_1+\gamma_3-\gamma_6},$$

$$F(C_7) = X_{-\gamma_1-\gamma_2-\gamma_3-\gamma_4-\gamma_5} + X_{-\gamma_1-\gamma_2-\gamma_4-\gamma_5} + X_{-\gamma_1-\gamma_2-\gamma_5} + X_{-\gamma_2-\gamma_4-\gamma_5} + X_{-\gamma_2-\gamma_5},$$

$$F(C_8) = X_{\gamma_2+\gamma_5} + X_{\gamma_2+\gamma_5+\gamma_6} + X_{\gamma_2+\gamma_3+\gamma_5} + X_{\gamma_2+\gamma_3+\gamma_5+\gamma_6} + X_{\gamma_2+\gamma_3+\gamma_4+\gamma_5+\gamma_6},$$

$$F(C_9) = X_{-\gamma_1-\gamma_3+\gamma_6} + X_{-\gamma_1+\gamma_6} + X_{-\gamma_1+\gamma_4+\gamma_6}.$$

In this chosen chamber the spectrum generator  $S(q)$  is given by

$$S(q) = E_q(X_{\gamma_4})E_q(X_{\gamma_6})E_q(X_{\gamma_4+\gamma_5})E_q(X_{\gamma_5})E_q(X_{\gamma_3})E_q(X_{\gamma_1+\gamma_3})E_q(X_{\gamma_2})E_q(X_{\gamma_1}) \\ = \sum_{l_1, \dots, l_8=0}^{\infty} \frac{(-1)^{\sum_{i=1}^8 l_i} q^{\frac{A}{2}}}{(q)_{l_1} \dots (q)_{l_8}} X_{(l_1+l_7)\gamma_1+l_2\gamma_2+(l_3+l_7)\gamma_3+(l_4+l_8)\gamma_4+(l_5+l_8)\gamma_5+l_6\gamma_6},$$

where

$$A = \sum_{i=1}^8 l_i - l_1(l_7 - l_2 + l_3) + l_3(l_2 + l_4 + l_8 - l_7) - l_4(l_8 + l_5 - l_6 - l_7) + l_8(l_7 - l_5) + l_5 l_6. \quad (3.125)$$

For sufficiently large enough  $N$  the truncated  $S_N(q)$  stabilizes to

$$S_N(q) = 1 - \sum_{i=1}^6 X_{\gamma_i} q^{\frac{1}{2}} + (X_{2\gamma_1} + X_{2\gamma_2} + X_{2\gamma_3} + X_{\gamma_1+\gamma_2+\gamma_3} + X_{2\gamma_4} + X_{\gamma_1+\gamma_4}$$

$$\begin{aligned}
& + X_{\gamma_2+\gamma_4} + X_{2\gamma_5} + X_{\gamma_1+\gamma_5} + X_{\gamma_2+\gamma_5} + X_{\gamma_3+\gamma_5} + X_{2\gamma_6} + X_{\gamma_1+\gamma_6} + X_{\gamma_2+\gamma_6} \\
& + X_{\gamma_3+\gamma_6} + X_{\gamma_4+\gamma_5+\gamma_6})q + \dots
\end{aligned}$$

The Schur index with line defect  $L$  ( $L = A_i, B_i, C_i$ ) inserted is given by

$$\mathcal{I}_L(q) = (q)_\infty^6 \text{Tr}[F(L)S(q)\overline{S}(q)]. \quad (3.126)$$

In particular the line defect Schur index forgets the  $i$  index as expected:

$$\begin{aligned}
\mathcal{I}_A(q) &= -q^{\frac{3}{2}}(1 + q^3 + q^4 + q^5 + 2q^6 + 2q^7 + 3q^8 + \dots), \\
\mathcal{I}_B(q) &= -q^{\frac{1}{2}}(1 + q^2 + q^3 + 2q^4 + 2q^5 + 3q^6 + 4q^7 + 6q^8 + \dots), \\
\mathcal{I}_C(q) &= q(1 + q^2 + q^3 + q^4 + 2q^5 + 3q^6 + 3q^7 + 5q^8 + \dots).
\end{aligned} \quad (3.127)$$

The chiral algebra in this case is conjectured to be the  $(2, 9)$  Virasoro minimal model [52, 54, 56]. There are four primary fields:  $\Phi_{1,1}$  which is the vacuum,  $\Phi_{1,2}$  with weight  $-1/3$ ,  $\Phi_{1,3}$  with weight  $-5/9$ , and  $\Phi_{1,4}$  with weight  $-2/3$ . The line defect Schur indices have the following expansions in terms of the characters:

$$\begin{aligned}
\mathcal{I}_A(q) &= q^{-\frac{3}{2}}(\chi_{1,3}(q) - \chi_{1,4}(q)), \\
\mathcal{I}_B(q) &= q^{-\frac{1}{2}}(\chi_{1,1}(q) - \chi_{1,2}(q)), \\
\mathcal{I}_C(q) &= q^{-1}(-\chi_{1,2}(q) + \chi_{1,3}(q)).
\end{aligned} \quad (3.128)$$

Thus the map  $f$  between the line defect OPE algebra  $\mathcal{L}$  and the Verlinde algebra  $\mathcal{V}$  of the  $(2, 9)$  minimal model is:

$$\begin{aligned}
I &\xrightarrow{f} [\Phi_{1,1}], \\
A_i &\xrightarrow{f} [A] = [\Phi_{1,3}] - [\Phi_{1,4}], \\
B_i &\xrightarrow{f} [B] = [\Phi_{1,1}] - [\Phi_{1,2}], \\
C_i &\xrightarrow{f} [C] = -[\Phi_{1,2}] + [\Phi_{1,3}].
\end{aligned} \quad (3.129)$$

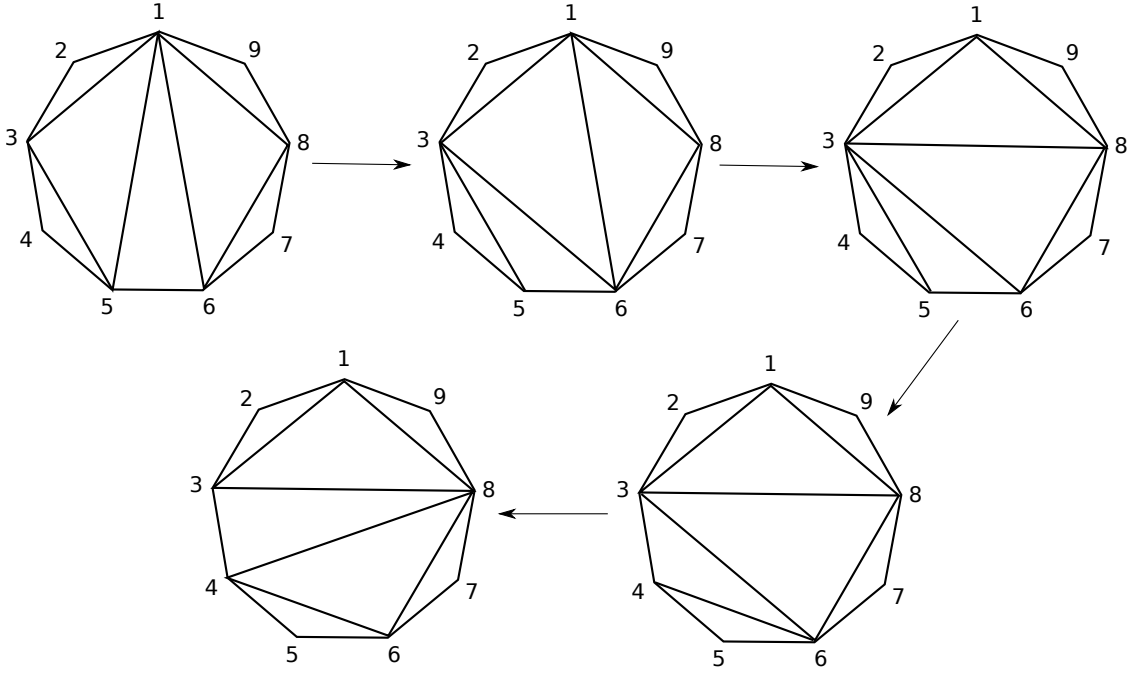


Figure 3.12: Monodromy action via a sequence of flips of triangulations of the 9-gon.

Non-trivial fusion rules in the  $(2, 9)$  minimal model are given by:

$$\begin{aligned}
 [\Phi_{1,2}] \times [\Phi_{1,2}] &= [\Phi_{1,1}] + [\Phi_{1,3}], \\
 [\Phi_{1,2}] \times [\Phi_{1,3}] &= [\Phi_{1,2}] + [\Phi_{1,4}], \\
 [\Phi_{1,2}] \times [\Phi_{1,4}] &= [\Phi_{1,3}] + [\Phi_{1,4}], \\
 [\Phi_{1,3}] \times [\Phi_{1,3}] &= [\Phi_{1,1}] + [\Phi_{1,3}] + [\Phi_{1,4}], \\
 [\Phi_{1,3}] \times [\Phi_{1,4}] &= [\Phi_{1,2}] + [\Phi_{1,3}] + [\Phi_{1,4}], \\
 [\Phi_{1,4}] \times [\Phi_{1,4}] &= [\Phi_{1,1}] + [\Phi_{1,2}] + [\Phi_{1,3}] + [\Phi_{1,4}].
 \end{aligned} \tag{3.130}$$

Using these fusion rules one can check that  $[AA] = [A] \times [A]$ ,  $[AB] = [A] \times [B]$ , and  $[BB] = [B] \times [B]$ .



Now we study the fixed points under the classical monodromy action. By considering the sequence of flips shown in Figure [3.12](#) we compute that the classical monodromy is:

$$\begin{aligned}
\mathcal{X}_{\gamma_1} &\rightarrow \mathcal{X}_{\gamma_2}(1 + \mathcal{X}_{\gamma_3} + \mathcal{X}_{\gamma_3}\mathcal{X}_{\gamma_4}), & \mathcal{X}_{\gamma_2} &\rightarrow \frac{\mathcal{X}_{\gamma_3}\mathcal{X}_{\gamma_4}\mathcal{X}_{\gamma_5}}{1 + \mathcal{X}_{\gamma_3} + \mathcal{X}_{\gamma_3}\mathcal{X}_{\gamma_4}}, \\
\mathcal{X}_{\gamma_3} &\rightarrow \frac{\mathcal{X}_{\gamma_1}}{1 + \mathcal{X}_{\gamma_3}(1 + \mathcal{X}_{\gamma_4})(1 + \mathcal{X}_{\gamma_1})}, \\
\mathcal{X}_{\gamma_4} &\rightarrow \frac{(1 + \mathcal{X}_{\gamma_3} + \mathcal{X}_{\gamma_3}\mathcal{X}_{\gamma_4})(1 + \mathcal{X}_{\gamma_3} + \mathcal{X}_{\gamma_3}\mathcal{X}_{\gamma_1})}{\mathcal{X}_{\gamma_3}\mathcal{X}_{\gamma_4}\mathcal{X}_{\gamma_1}}, \\
\mathcal{X}_{\gamma_5} &\rightarrow \frac{\mathcal{X}_{\gamma_6}[1 + \mathcal{X}_{\gamma_3}(1 + \mathcal{X}_{\gamma_4})(1 + \mathcal{X}_{\gamma_1})]}{1 + \mathcal{X}_{\gamma_3} + \mathcal{X}_{\gamma_3}\mathcal{X}_{\gamma_1}}, & \mathcal{X}_{\gamma_6} &\rightarrow \frac{\mathcal{X}_{\gamma_4}}{1 + \mathcal{X}_{\gamma_3}(1 + \mathcal{X}_{\gamma_4})(1 + \mathcal{X}_{\gamma_1})}.
\end{aligned} \tag{3.131}$$

There are exactly four fixed points which we label I, II, III, IV. At the fixed points  $X_\gamma$  evaluate to:

$$\begin{aligned}
\mathcal{X}_{\gamma_1} &: (-1, \alpha_1, \alpha_2, \alpha_3), & \mathcal{X}_{\gamma_2} &: (-1, 1 - \alpha_2, 1 - \alpha_3, 1 - \alpha_1), \\
\mathcal{X}_{\gamma_3} &: (-1, \alpha_2, \alpha_3, \alpha_1), & \mathcal{X}_{\gamma_4} &: (-1, 1 - \alpha_3, 1 - \alpha_1, 1 - \alpha_2), \\
\mathcal{X}_{\gamma_5} &: (-1, \alpha_1, \alpha_2, \alpha_3), & \mathcal{X}_{\gamma_6} &: (-1, 1 - \alpha_2, 1 - \alpha_3, 1 - \alpha_1),
\end{aligned}$$

where

$$\alpha_1 = (-1)^{\frac{4}{9}} - (-1)^{\frac{5}{9}}, \quad \alpha_2 = (-1)^{\frac{8}{9}} - (-1)^{\frac{1}{9}}, \quad \alpha_3 = (-1)^{\frac{2}{9}} - (-1)^{\frac{7}{9}}.$$

The line defect vevs evaluated at the fixed points satisfy:

$$F(A_i) = F(A_j), \quad F(B_i) = F(B_j), \quad F(C_i) = F(C_j). \tag{3.132}$$

Explicitly, the evaluation map is:

$$\begin{aligned}
A_i &\xrightarrow{g} (1, -\alpha_3, -\alpha_1, -\alpha_2), \\
B_i &\xrightarrow{g} (0, 1 + \alpha_1, 1 + \alpha_2, 1 + \alpha_3), \\
C_i &\xrightarrow{g} (-1, 1 - \alpha_3, 1 - \alpha_1, 1 - \alpha_2).
\end{aligned} \tag{3.133}$$

The fusion matrices for  $[\Phi_{1,2}]$ ,  $[\Phi_{1,3}]$  and  $[\Phi_{1,4}]$  are:

$$N_{\Phi_{1,2}} = \begin{pmatrix} 0 & 1 & 0 & 0 \\ 1 & 0 & 1 & 0 \\ 0 & 1 & 0 & 1 \\ 0 & 0 & 1 & 1 \end{pmatrix}, \quad N_{\Phi_{1,3}} = \begin{pmatrix} 0 & 0 & 1 & 0 \\ 0 & 1 & 0 & 1 \\ 1 & 0 & 1 & 1 \\ 0 & 1 & 1 & 1 \end{pmatrix}, \quad N_{\Phi_{1,4}} = \begin{pmatrix} 0 & 0 & 0 & 1 \\ 0 & 0 & 1 & 1 \\ 0 & 1 & 1 & 1 \\ 1 & 1 & 1 & 1 \end{pmatrix}. \quad (3.134)$$

The  $S$ -matrix for (2,9) minimal model is given by [65]:

$$S = \frac{2}{3} \begin{pmatrix} -\sin\frac{2\pi}{9} & \cos\frac{\pi}{18} & -\sin\frac{\pi}{3} & \sin\frac{\pi}{9} \\ \cos\frac{\pi}{18} & -\sin\frac{\pi}{9} & -\sin\frac{\pi}{3} & \sin\frac{2\pi}{9} \\ -\sin\frac{\pi}{3} & -\sin\frac{\pi}{3} & 0 & \sin\frac{\pi}{3} \\ \sin\frac{\pi}{9} & \sin\frac{2\pi}{9} & \sin\frac{\pi}{3} & \cos\frac{\pi}{18} \end{pmatrix}. \quad (3.135)$$

The fusion matrices are simultaneously diagonalized by  $S$ :

$$SN_{\Phi_{1,2}}S^{-1} = \begin{pmatrix} -\alpha_3 & 0 & 0 & 0 \\ 0 & -\alpha_1 & 0 & 0 \\ 0 & 0 & 1 & 0 \\ 0 & 0 & 0 & -\alpha_2 \end{pmatrix}, \quad SN_{\Phi_{1,3}}S^{-1} = \begin{pmatrix} 1 + \alpha_1 & 0 & 0 & 0 \\ 0 & 1 + \alpha_2 & 0 & 0 \\ 0 & 0 & 0 & 0 \\ 0 & 0 & 0 & 1 + \alpha_3 \end{pmatrix}, \quad (3.136)$$

$$SN_{\Phi_{1,4}}S^{-1} = \begin{pmatrix} 1 - \alpha_3 & 0 & 0 & 0 \\ 0 & 1 - \alpha_1 & 0 & 0 \\ 0 & 0 & -1 & 0 \\ 0 & 0 & 0 & 1 - \alpha_2 \end{pmatrix}.$$

According to [69,71], the correspondence between  $U(1)_r$ -fixed points in  $\mathcal{N}$  and the primaries of the (2, 9) Virasoro minimal model is:

fixed point	$U(1)$ weights	primary field
I	$\frac{4}{9}, \frac{5}{9}, \frac{7}{9}, \frac{2}{9}, \frac{10}{9}, -\frac{1}{9}$	$\Phi_{1,3}$
II	$\frac{7}{9}, \frac{2}{9}, \frac{10}{9}, -\frac{1}{9}, \frac{4}{3}, -\frac{1}{3}$	$\Phi_{1,2}$
III	$\frac{1}{3}, \frac{2}{3}, \frac{4}{9}, \frac{5}{9}, \frac{7}{9}, \frac{2}{9}$	$\Phi_{1,4}$
IV	$\frac{4}{3}, -\frac{1}{3}, \frac{10}{9}, -\frac{1}{9}, \frac{14}{9}, -\frac{5}{9}$	$\Phi_{1,1}$

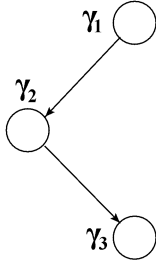


Figure 3.13: A BPS quiver for the  $(A_1, D_3)$  Argyres-Douglas theory.

Based on this table and (3.136), the isomorphism  $h : \mathcal{V} \rightarrow \mathcal{O}(F)$  is:

$$\begin{aligned}
 [\Phi_{1,1}] &\xrightarrow{h} (1, 1, 1, 1), \\
 [\Phi_{1,2}] &\xrightarrow{h} (1, -\alpha_1, -\alpha_2, -\alpha_3), \\
 [\Phi_{1,3}] &\xrightarrow{h} (0, 1 + \alpha_2, 1 + \alpha_3, 1 + \alpha_1), \\
 [\Phi_{1,4}] &\xrightarrow{h} (-1, 1 - \alpha_1, 1 - \alpha_2, 1 - \alpha_3).
 \end{aligned} \tag{3.137}$$

Combining (3.129), (3.133) and (3.137) confirms that  $h \circ f = g$  in the  $(A_1, A_6)$  Argyres-Douglas theory.

### 3.6 $(A_1, D_{2N+1})$ Argyres-Douglas theories

In this section we present the results of explicit computations verifying the commutativity (3.16) in the Argyres-Douglas theories of type  $(A_1, D_3)$  and  $(A_1, D_5)$ , with the appropriate modifications to take care of the flavor symmetry in these theories.

#### 3.6.1 $(A_1, D_3)$ Argyres-Douglas theory

We consider  $(A_1, D_3)$  Argyres-Douglas theory. This is equivalently the  $(A_1, A_3)$  Argyres-Douglas theory. Line defect generators and their generating

functions in this description were studied in [23, 51]. Line defect Schur indices and the relation to the Verlinde algebra were studied in [51]. Here we use the  $(A_1, D_3)$  description instead.

We choose a chamber where the BPS quiver is as in Figure 3.13, containing BPS particles with charges (in increasing phase order):

$$\gamma_1, \gamma_2, \gamma_3.$$

Note that  $\gamma_1 + \gamma_3$  has zero Dirac pairing with any charge, and thus is a pure flavor charge.

The corresponding Hitchin system is defined on  $\mathbb{CP}^1$ , with one irregular singularity at  $z = \infty$  and one regular singularity at  $z = 0$ . There are three Stokes rays emerging from the irregular singularity. Correspondingly there are three marked points on the  $S^1$  bounding the cut-out disc around  $z = \infty$ , as in Figure 3.14a. The WKB triangulation for the chosen chamber is shown in Figure 3.14b. Here  $\mathcal{X}_{\gamma_1}$  corresponds to edge 14,  $\mathcal{X}_{\gamma_2}$  corresponds to edge 13, and  $\mathcal{X}_{\gamma_3}$  corresponds to edge 34.

Now we use the method reviewed in §3.4.3 to describe a generating set of line defects. There are seven generators, including a pure flavor line defect  $C$  whose corresponding lamination is a loop around the regular singularity. The other six generators come in two types,  $A$  and  $B$ , corresponding to two different kinds of laminations: see Figure 3.15. We denote the six generators as  $A_i, B_i$  ( $i = 1, 2, 3$ ), where  $A_1$  and  $B_1$  correspond to the laminations shown in Figure 3.15. The lamination for  $A_{i+1}$  ( $B_{i+1}$ ) is given by rotating the lamination

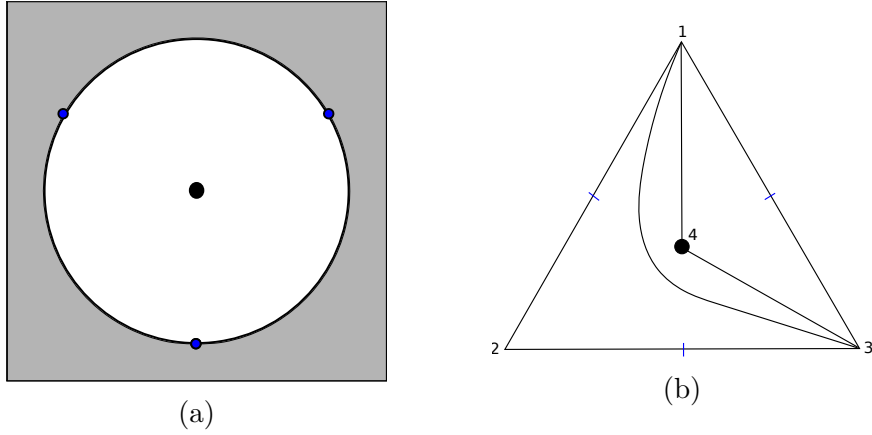


Figure 3.14: (a):  $\mathbb{CP}^1 \setminus D_\infty$  where  $D_\infty$  is a disk around  $z = \infty$  bounded by  $S^1$  with three marked points colored in blue. The regular singularity at  $z = 0$  is colored in black. (b): A triangulation in the  $(A_1, D_3)$  Argyres-Douglas theory. There are three boundary edges. The blue marks correspond to the positions of three Stokes rays.

for  $A_i$  ( $B_i$ ) counterclockwise by  $2\pi/3$ . The flavor charge is normalized to be  $(\gamma_1 + \gamma_3)/2$ , and the corresponding  $X_\gamma$  is equal to the  $SU(2)$  flavor fugacity  $z$ :

$$z = X_{\frac{\gamma_1 + \gamma_3}{2}}. \quad (3.138)$$

Moreover we define

$$X_{\gamma'} := X_{\frac{\gamma_1 - \gamma_3}{2}}. \quad (3.139)$$

We computed generating functions of line defect generators using the method reviewed in §3.4.3. They are listed below (these differ slightly from the analogous formulas in [51] because we are computing in a different chamber):

$$F(A_1) = z^{-1}X_{-\gamma_2} + X_{-\gamma'} + X_{-\gamma' - \gamma_2},$$

$$F(A_2) = X_{-\gamma'} + X_{-\gamma' + \gamma_2} + zX_{\gamma_2},$$

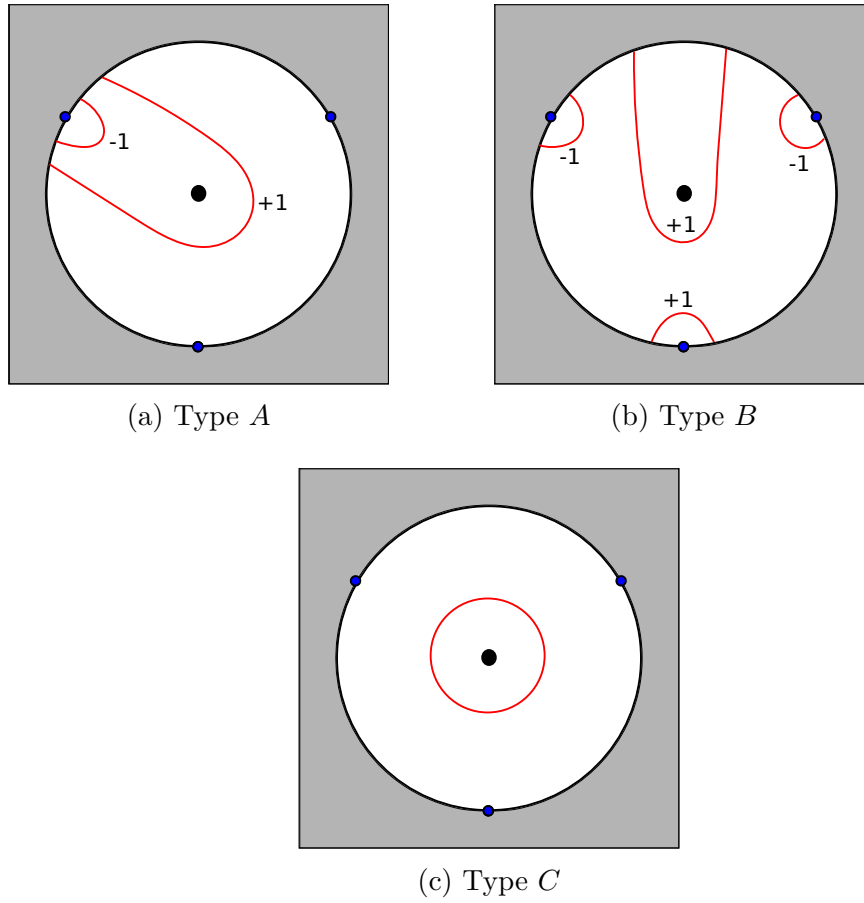


Figure 3.15: Three types of laminations in  $(A_1, D_3)$  Argyres-Douglas theory.

$$F(A_3) = X_{\gamma'},$$

$$F(B_1) = X_{-\gamma_2} + z^{-1}X_{-\gamma_2+\gamma'},$$

$$F(B_2) = X_{-2\gamma'+\gamma_2} + X_{-2\gamma'-\gamma_2} + zX_{-\gamma'+\gamma_2} + (q^{\frac{1}{2}} + q^{-\frac{1}{2}})X_{-2\gamma'} + (z + z^{-1})X_{-\gamma'} + z^{-1}X_{-\gamma'-\gamma_2},$$

$$F(B_3) = X_{\gamma_2} + zX_{\gamma_2+\gamma'},$$

$$F(C) = z + z^{-1}.$$

The pure flavor line defect  $C$  is a Wilson line in the fundamental representation of the  $SU(2)$  flavor symmetry.

The Schur index with one line defect  $L$  inserted is computed as

$$\mathcal{I}_L(q, z) = (q)_\infty^2 \text{Tr}[F(L)S(q)\bar{S}(q)], \quad \text{with} \quad S(q) = E_q(X_{\gamma_1})E_q(X_{\gamma_2})E_q(X_{\gamma_3}). \quad (3.140)$$

As usual the Schur indices with defects  $A_i$  and  $B_i$  inserted do not depend on the index  $i$ ; concretely (these do match [51], as they should since they are chamber-independent):

$$\begin{aligned} \mathcal{I}_A(q, z) &= -q^{\frac{1}{2}}(\chi_{\mathbf{2}} + \chi_{\mathbf{4}q} + \chi_{\mathbf{2} \oplus \mathbf{4} \oplus \mathbf{6}q^2} + \chi_{\mathbf{2} \oplus \mathbf{2} \oplus \mathbf{4} \oplus \mathbf{2} \oplus \mathbf{6} \oplus \mathbf{8}q^3} + \chi_{\mathbf{2} \oplus \mathbf{3} \oplus \mathbf{4} \oplus \mathbf{3} \oplus \mathbf{6} \oplus \mathbf{3} \oplus \mathbf{8} \oplus \mathbf{10}q^4} \\ &\quad + \chi_{\mathbf{2} \oplus \mathbf{4} \oplus \mathbf{4} \oplus \mathbf{6} \oplus \mathbf{6} \oplus \mathbf{4} \oplus \mathbf{8} \oplus \mathbf{3} \oplus \mathbf{10} \oplus \mathbf{12}q^5} + \dots), \\ \mathcal{I}_B(q, z) &= -q^{\frac{1}{2}}(1 + \chi_{\mathbf{3}q^2} + \chi_{\mathbf{1} \oplus \mathbf{3}q^3} + \chi_{\mathbf{1} \oplus \mathbf{3} \oplus \mathbf{5}q^4} + \chi_{\mathbf{1} \oplus \mathbf{3} \oplus \mathbf{2} \oplus \mathbf{5}q^5} + \chi_{\mathbf{1} \oplus \mathbf{2} \oplus \mathbf{3} \oplus \mathbf{3} \oplus \mathbf{5} \oplus \mathbf{2} \oplus \mathbf{7}q^6} + \dots), \end{aligned}$$

where framed BPS states organize themselves into representations of  $SU(2)$ <sup>[30]</sup>.

The associated chiral algebra is  $\widehat{\mathfrak{sl}(2)}_{-\frac{4}{3}}$  [52, 54–56, 59]. There are three

---

<sup>30</sup>We label irreducible  $SU(2)$  representations by their dimensions.

admissible representations [65, 73] with highest weights:

$$\Phi_0 = \left[ -\frac{4}{3}, 0 \right], \quad \Phi_1 = \left[ -\frac{2}{3}, -\frac{2}{3} \right], \quad \Phi_2 = \left[ 0, -\frac{4}{3} \right] \quad (3.141)$$

where  $\Phi_0$  is the highest weight for the vacuum module. Their characters were computed using the Kazhdan-Lusztig formula in [51, 65]. In particular the line defect Schur indices could be written as:

$$\begin{aligned} \mathcal{I}_A(q, z) &= q^{-\frac{1}{2}} z^{-1} \left( -\chi_1(q, z) + \chi_2(q, z) \right), \\ \mathcal{I}_B(q, z) &= q^{-\frac{1}{2}} \left( \chi_0(q, z) - \chi_1(q, z) + z^{-2} \chi_2(q, z) \right). \end{aligned} \quad (3.142)$$

The expansions of  $\mathcal{I}_{A_i A_j}$ ,  $\mathcal{I}_{B_i B_j}$  and  $\mathcal{I}_{A_i B_j}$  in terms of characters are:

$$\begin{aligned} \mathcal{I}_{A_i A_i}(q, z) &= \mathcal{I}_{A_i A_{i+1}}(q, z) = (1 + q^{-1}) \chi_0(q, z) - q^{-1} \chi_1(q, z) + q^{-1} z^{-2} \chi_2(q, z), \\ \mathcal{I}_{A_i A_{i-1}}(q, z) &= 2 \chi_0(q, z) - \chi_1(q, z) + z^{-2} \chi_2(q, z), \\ \mathcal{I}_{B_i B_i}(q, z) &= \mathcal{I}_{B_i B_{i+1}}(q, z) = (1 + q^{-1} + q^{-2}) \chi_0(q, z) - [q^{-1}(1 + z^{-2}) + q^{-2}] \chi_1(q, z) \\ &\quad + [q^{-1}(1 + z^{-2}) + q^{-2} z^{-2}] \chi_2(q, z), \\ \mathcal{I}_{B_i B_{i-1}}(q, z) &= (2 + q) \chi_0(q, z) - (2 + z^{-2}) \chi_1(q, z) + (1 + 2z^{-2}) \chi_2(q, z), \\ \mathcal{I}_{A_i B_i}(q, z) &= q^{-1} (z + z^{-1}) \chi_0(q, z) - (q^{-1} + q^{-2}) z^{-1} (\chi_1(q, z) - \chi_2(q, z)), \\ \mathcal{I}_{A_i B_{i+1}}(q, z) &= \mathcal{I}_{A_i B_{i-1}}(q, z) = (z + z^{-1}) \chi_0(q, z) - (1 + q^{-1}) z^{-1} (\chi_1(q, z) - \chi_2(q, z)). \end{aligned}$$

In [51] the authors take the limit  $q \rightarrow 1, z \rightarrow 1$  and relate the line defect algebra to the Verlinde-like algebra of  $\widehat{\mathfrak{sl}(2)}_{-\frac{4}{3}}$ . Here we keep  $z$  general while taking  $q \rightarrow 1$ . In this limit the expansion coefficients do not depend on the  $i$  index anymore, just as in the  $(A_1, A_{2N})$  case. We introduce a  $z$ -deformed



Verlinde-like algebra  $\mathcal{V}_z$  with the  $z$ -deformed modular fusion rules:

$$\begin{aligned} [\Phi_1] \times [\Phi_1] &= [\Phi_2], \\ [\Phi_1] \times [\Phi_2] &= -z^2[\Phi_0], \\ [\Phi_2] \times [\Phi_2] &= -z^2[\Phi_1]. \end{aligned} \tag{3.143}$$

If we take  $z = 1$ , this reduces to the naive modular fusion rules of  $\widehat{\mathfrak{sl}(2)}_{-\frac{4}{3}}$  [51,65]. The homomorphism  $f : \mathcal{L} \rightarrow \mathcal{V}_z$  is given by:

$$\begin{aligned} I &\xrightarrow{f} [\Phi_0], \\ A_i &\xrightarrow{f} [A] = z^{-1}([\Phi_2] - [\Phi_1]), \\ B_i &\xrightarrow{f} [B] = [\Phi_0] - [\Phi_1] + z^{-2}[\Phi_2]. \end{aligned} \tag{3.144}$$

$f$  is believed to be a homomorphism since

$$\begin{aligned} [AA] &= 2[\Phi_0] - [\Phi_1] + z^{-2}[\Phi_2] = [A] \times [A], \\ [BB] &= 3[\Phi_0] - (2 + z^{-2})[\Phi_1] + (1 + 2z^{-2})[\Phi_2] = [B] \times [B], \\ [AB] &= (z + z^{-1})[\Phi_0] - 2z^{-1}([\Phi_1] - [\Phi_2]) = [A] \times [B]. \end{aligned} \tag{3.145}$$

We emphasize that this holds if and only if the  $z$ -deformed modular fusion rules are as given in (3.143).

The fusion matrices for  $[\Phi_1]$  and  $[\Phi_2]$  are:

$$N_{\Phi_1} = \begin{pmatrix} 0 & 1 & 0 \\ 0 & 0 & 1 \\ -z^2 & 0 & 0 \end{pmatrix}, \quad N_{\Phi_2} = \begin{pmatrix} 0 & 0 & 1 \\ -z^2 & 0 & 0 \\ 0 & -z^2 & 0 \end{pmatrix}. \tag{3.146}$$

These two matrices are simultaneously diagonalizable for  $z \neq 0$ , with eigenvalues:

eigenvector	$\lambda_{\Phi_1}$	$\lambda_{\Phi_2}$
$(1, -z^{2/3}, z^{4/3})$	$-z^{2/3}$	$z^{4/3}$
$(1, (-1)^{1/3}z^{2/3}, (-1)^{2/3}z^{4/3})$	$(-1)^{1/3}z^{2/3}$	$(-1)^{2/3}z^{4/3}$
$(1, -(-1)^{2/3}z^{2/3}, -(-1)^{1/3}z^{4/3})$	$-(-1)^{2/3}z^{2/3}$	$-(-1)^{1/3}z^{4/3}$

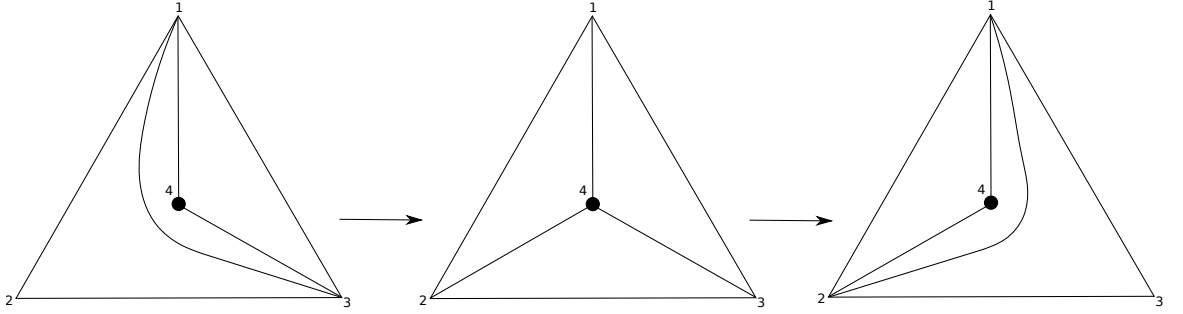


Figure 3.16: Classical monodromy action via two flips in  $(A_1, D_3)$  Argyres-Douglas theory.

Now we turn to study fixed loci of the classical monodromy in this chamber. Through a composition of two flips (see Figure [3.16](#)) the monodromy action is:

$$\begin{aligned}
 \mathcal{X}_{\gamma_1} &\rightarrow \frac{1 + \mathcal{X}_{\gamma_3} + \mathcal{X}_{\gamma_2} \mathcal{X}_{\gamma_3}}{\mathcal{X}_{\gamma_2}}, \\
 \mathcal{X}_{\gamma_2} &\rightarrow \frac{1}{\mathcal{X}_{\gamma_3} + \mathcal{X}_{\gamma_2} \mathcal{X}_{\gamma_3}}, \\
 \mathcal{X}_{\gamma_3} &\rightarrow \frac{\mathcal{X}_{\gamma_1} \mathcal{X}_{\gamma_2} \mathcal{X}_{\gamma_3}}{1 + \mathcal{X}_{\gamma_3} + \mathcal{X}_{\gamma_2} \mathcal{X}_{\gamma_3}}.
 \end{aligned} \tag{3.147}$$

The fixed locus is determined by the equations

$$\mathcal{X}_{\gamma_2} (1 + \mathcal{X}_{\gamma_2}) \mathcal{X}_{\gamma_3} = 1, \quad \mathcal{X}_{\gamma_1} = \mathcal{X}_{\gamma_3} (2 + \mathcal{X}_{\gamma_2} + \mathcal{X}_{\gamma_3} + \mathcal{X}_{\gamma_2} \mathcal{X}_{\gamma_3}). \tag{3.148}$$

To make connection with the flavor fugacity, we rewrite these equations in terms of  $\mathcal{X}_{\gamma_2}$ ,  $z$  and  $x := \mathcal{X}_{\gamma'}$ ; this gives

$$\mathcal{X}_{\gamma_2}^3 z^2 = 1, \quad x = \mathcal{X}_{\gamma_2} (1 + \mathcal{X}_{\gamma_2}) z. \tag{3.149}$$

One can check that this is exactly the same locus where  $F(A_i) = F(A_j)$  and  $F(B_i) = F(B_j)$ . In particular, this implies the evaluation map  $g$  forgets the  $i$  index as expected.

Now recall that the value of  $z$  corresponds to the  $SU(2)$  flavor holonomy that could be turned on when compactifying the 4d theory on  $S^1$ . With this in mind we first fix  $z$  and then look for the  $U(1)_r$ -fixed points. For each value of  $z \neq 0$ , there are three  $U(1)_r$ -fixed points, which matches the number of admissible representations of  $\widehat{\mathfrak{sl}(2)}_{-\frac{4}{3}}$ . The evaluation map  $g$  is concretely given by:

$$\begin{aligned}
1 &\xrightarrow{g} (1, 1, 1), \\
A_i &\xrightarrow{g} (z^{1/3} + z^{-1/3}, -(-1)^{1/3}z^{1/3} + (-1)^{2/3}z^{-1/3}, -(-1)^{1/3}z^{-1/3} + (-1)^{2/3}z^{1/3}), \\
B_i &\xrightarrow{g} (1 + z^{2/3} + z^{-2/3}, 1 + (-1)^{2/3}z^{2/3} - (-1)^{1/3}z^{-2/3}, \\
&\quad 1 + (-1)^{2/3}z^{-2/3} - (-1)^{1/3}z^{2/3}).
\end{aligned} \tag{3.150}$$

Now, in contrast to the cases we studied in §3.5, in this case the weights of the classical monodromy action are not sufficient to distinguish the three  $U(1)_r$ -fixed points, as we see from the following table ( $U(1)_r$  weights and correspondence between fixed points and primary fields taken from results of [69, 71]):

fixed point	weights of $M$	weights of $U(1)_r$	primary field
I	$-\frac{1 \pm i\sqrt{3}}{2}$	$\frac{1}{3}, \frac{2}{3}$	$\Phi_1$
II	$-\frac{1 \pm i\sqrt{3}}{2}$	$-\frac{1}{3}, \frac{4}{3}$	$\Phi_0$
III	$-\frac{1 \pm i\sqrt{3}}{2}$	$-\frac{1}{3}, \frac{4}{3}$	$\Phi_2$

Thus we cannot determine *a priori* which  $U(1)_r$ -fixed point should correspond to which eigenspace of the fusion matrices. This gives an  $S_3$  ambiguity in constructing the map  $h$ . Still, we can just try all of the 6 possible mappings

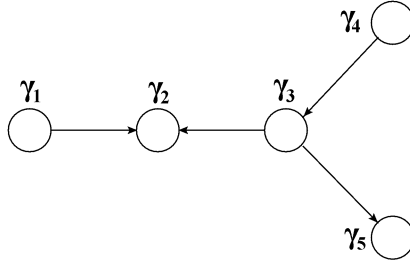


Figure 3.17: A BPS quiver for the  $(A_1, D_5)$  Argyres-Douglas theory.

and see if one of them works. Indeed, suppose we take:

$$\begin{aligned} [\Phi_1] &\xrightarrow{h} (-z^{2/3}, -(-1)^{2/3}z^{2/3}, (-1)^{1/3}z^{2/3}), \\ [\Phi_2] &\xrightarrow{h} (z^{4/3}, -(-1)^{1/3}z^{4/3}, (-1)^{2/3}z^{4/3}). \end{aligned} \tag{3.151}$$

Combining this with [\(3.144\)](#) and [\(3.150\)](#), we find that indeed  $h \circ f = g$  for every  $z \neq 0$ .

### 3.6.2 $(A_1, D_5)$ Argyres-Douglas theory

We choose the canonical chamber represented by the BPS quiver given in Figure [3.17](#), with five BPS particles (in increasing central charge phase order):

$$\gamma_1, \gamma_4, \gamma_3, \gamma_2, \gamma_5.$$

The corresponding Hitchin system is defined on  $\mathbb{CP}^1$  with one regular singularity at  $z = 0$  and one irregular singularity at  $z = \infty$  with five stokes rays emerging from it, i.e. there are five marked points on the  $S^1$  which bounds  $D_\infty$ , the disk around  $z = \infty$  that's cut out from  $\mathbb{CP}^1$ . The situation is depicted in Figure [3.18](#). The corresponding WKB triangulation for this chamber is given in Figure [3.19](#), where  $\mathcal{X}_{\gamma_1}$  corresponds to edge 13,  $\mathcal{X}_{\gamma_2}$  corresponds to edge 35,

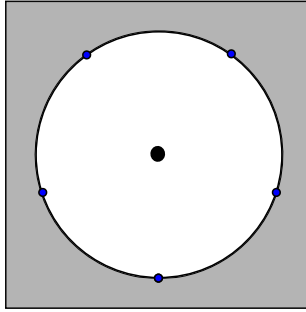


Figure 3.18:  $\mathbb{CP}^1 \setminus D_\infty$  where  $D_\infty$  is a disk around  $z = \infty$  bounded by  $S^1$  with five marked points colored in blue. The regular singularity at  $z = 0$  is colored in black.

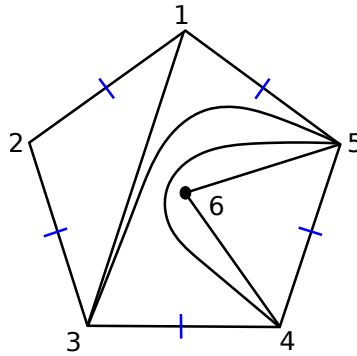


Figure 3.19: A triangulation in the  $(A_1, D_5)$  Argyres-Douglas theory. There are five boundary edges. The blue marks correspond to positions of five Stokes rays.

$\mathcal{X}_{\gamma_3}$  corresponds to edge 45,  $\mathcal{X}_{\gamma_4}$  corresponds to edge 56 and  $\mathcal{X}_{\gamma_5}$  corresponds to edge 46.

The line defect generators correspond to laminations that can not be expressed as sum of other laminations. In this case there are 21 such laminations. The lamination  $(E)$  which is a loop around the regular singularity corresponds to the pure flavor line defect. The other 20 laminations come in four types  $A, B, C$  and  $D$ . We label their corresponding generators as  $A_i, B_i,$

$C_i$  and  $D_i$  ( $i = 1, \dots, 5$ ) and list laminations corresponding to the generators  $A_1, B_1, C_1, D_1$  and  $E$  in Figure [3.20](#). Laminations corresponding to e.g. generators  $A_{i+1}$  are obtained by rotating laminations for  $A_i$  clockwise by  $4\pi/5$ . We define the flavor charge  $\gamma_f$  and  $\gamma'$  as follows:

$$\gamma_f = \frac{\gamma_4 + \gamma_5}{2}, \quad \gamma' = \frac{\gamma_4 - \gamma_5}{2}. \quad (3.152)$$

The  $SU(2)$  flavor fugacity is  $z := \text{Tr}(X_{\gamma_f})$ . The generating functions are computed using the method as reviewed in [§3.4.3](#). In particular, the line defect generator  $D_2$  has framed BPS states with charge  $2\gamma_2$  in a 3-dimensional multiplet of  $SO(3)$ :

$$\begin{aligned} F(A_1) &= X_{-\gamma_1} + X_{-\gamma_1-\gamma_2}, \\ F(A_2) &= X_{-\gamma_1} + X_{\gamma_2} + X_{-\gamma_1+\gamma_2} + X_{\gamma_2+\gamma_3} + X_{-\gamma_1+\gamma_2+\gamma_3} + zX_{\gamma_2+\gamma_3+\gamma'} + zX_{-\gamma_1+\gamma_2+\gamma_3+\gamma'}, \\ F(A_3) &= X_{\gamma_2} + X_{\gamma_1+\gamma_2} + X_{-\gamma_3} + X_{\gamma_2-\gamma_3} + X_{\gamma_1+\gamma_2-\gamma_3} + z^{-1}X_{-\gamma_3+\gamma'} + z^{-1}X_{\gamma_2-\gamma_3+\gamma'} \\ &\quad + z^{-1}X_{\gamma_1+\gamma_2-\gamma_3+\gamma'}, \\ F(A_4) &= X_{\gamma_1}, \\ F(A_5) &= (z + z^{-1})X_{-\gamma'} + z^{-1}X_{-\gamma_3-\gamma'} + z^{-1}X_{-\gamma_2-\gamma_3-\gamma'} + zX_{\gamma_3-\gamma'} + (q^{1/2} + q^{-1/2})X_{-2\gamma'} \\ &\quad + X_{-\gamma_2-2\gamma'} + X_{-\gamma_3-2\gamma'} + X_{-\gamma_2-\gamma_3-2\gamma'} + X_{\gamma_3-2\gamma'}, \\ F(B_1) &= X_{-\gamma_1-\gamma'} + X_{-\gamma_1-\gamma_2-\gamma'} + X_{-\gamma_1+\gamma_3-\gamma'} + zX_{-\gamma_1+\gamma_3}, \\ F(B_2) &= X_{-\gamma_1+\gamma'} + X_{\gamma_2+\gamma'} + X_{-\gamma_1+\gamma_2+\gamma'}, \\ F(B_3) &= X_{\gamma_2+\gamma'} + X_{\gamma_1+\gamma_2+\gamma'}, \\ F(B_4) &= z^{-1}X_{\gamma_1-\gamma_3} + X_{\gamma_1-\gamma'} + X_{\gamma_1-\gamma_3-\gamma'}, \\ F(B_5) &= X_{-\gamma_2-\gamma'}, \end{aligned}$$

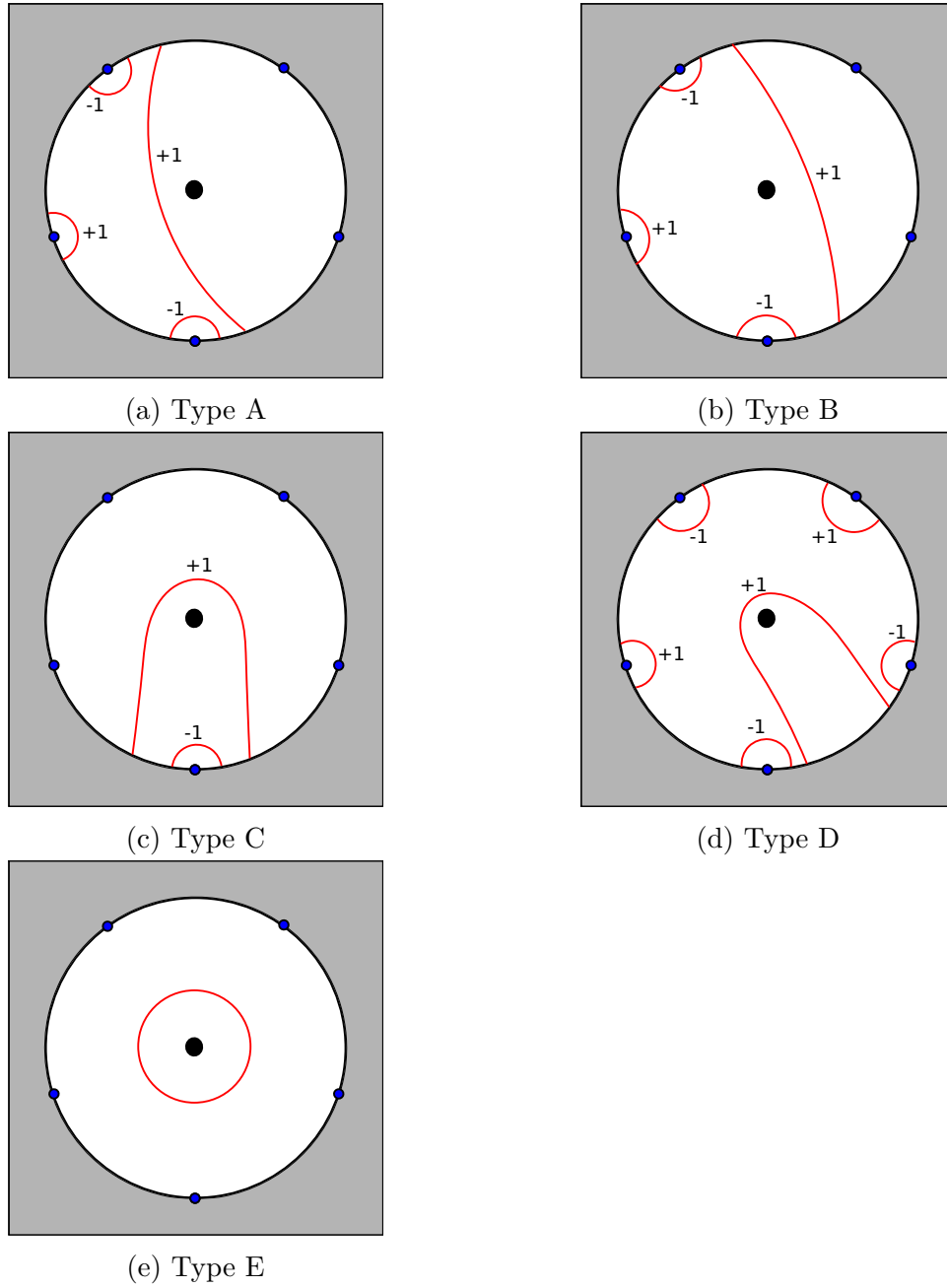


Figure 3.20: Five types of laminations in  $(A_1, D_5)$  Argyres-Douglas theory.

$$F(C_1) = X_{-\gamma'} + X_{\gamma_3-\gamma'} + zX_{\gamma_3},$$

$$\begin{aligned} F(C_2) &= (q^{1/2} + q^{-1/2})(X_{-\gamma_1-\gamma'} + X_{\gamma_2-\gamma'} + X_{-\gamma_1+\gamma_2-\gamma'} + X_{-\gamma_1-\gamma_3-\gamma'} + z^{-1}X_{-\gamma_1-\gamma_3}) \\ &\quad + X_{-\gamma'} + X_{-\gamma_3-\gamma'} + X_{-\gamma_1-\gamma_2-\gamma_3-\gamma'} + X_{\gamma_2-\gamma_3-\gamma'} + X_{-\gamma_1+\gamma_2-\gamma_3-\gamma'} + X_{\gamma_2+\gamma_3-\gamma'} \\ &\quad + X_{-\gamma_1+\gamma_2+\gamma_3-\gamma'} + (z + z^{-1})X_{-\gamma_1} + (z + z^{-1})X_{\gamma_2} + (z + z^{-1})X_{-\gamma_1+\gamma_2} + z^{-1}X_{-\gamma_3} \\ &\quad + z^{-1}X_{-\gamma_1-\gamma_2-\gamma_3} + z^{-1}X_{\gamma_2-\gamma_3} + z^{-1}X_{-\gamma_1+\gamma_2-\gamma_3} + zX_{\gamma_2+\gamma_3} + zX_{-\gamma_1+\gamma_2+\gamma_3}, \end{aligned}$$

$$F(C_3) = X_{\gamma'},$$

$$\begin{aligned} F(C_4) &= (q^{1/2} + q^{-1/2})(X_{\gamma_2-\gamma'} + X_{\gamma_1+\gamma_2-\gamma'}) + X_{-\gamma'} + X_{-\gamma_3-\gamma'} + X_{\gamma_2-\gamma_3-\gamma'} + X_{\gamma_1+\gamma_2-\gamma_3-\gamma'} \\ &\quad + X_{\gamma_2+\gamma_3-\gamma'} + X_{\gamma_1+\gamma_2+\gamma_3-\gamma'} + z^{-1}X_{\gamma_2} + z^{-1}X_{\gamma_1+\gamma_2} + z^{-1}X_{-\gamma_3} + z^{-1}X_{\gamma_2-\gamma_3} \\ &\quad + z^{-1}X_{\gamma_1+\gamma_2-\gamma_3} + zX_{\gamma_2} + zX_{\gamma_1+\gamma_2} + zX_{\gamma_2+\gamma_3} + zX_{\gamma_1+\gamma_2+\gamma_3}, \end{aligned}$$

$$F(C_5) = X_{-\gamma'} + X_{-\gamma_3-\gamma'} + X_{-\gamma_2-\gamma_3-\gamma'} + z^{-1}X_{-\gamma_3} + z^{-1}X_{-\gamma_2-\gamma_3},$$

$$F(D_1) = X_{-\gamma_1+\gamma_3} + zX_{-\gamma_1+\gamma_3+\gamma'},$$

$$\begin{aligned} F(D_2) &= (q^{1/2} + q^{-1/2})X_{\gamma_2} + (q^{1/2} + q^{-1/2})X_{-\gamma_1+\gamma_2} + (1 + 1 + q + q^{-1})X_{2\gamma_2} \\ &\quad + (q^{1/2} + q^{-1/2})X_{-\gamma_1+2\gamma_2} + (q^{1/2} + q^{-1/2})X_{\gamma_1+2\gamma_2} + X_{-\gamma_1-\gamma_3} + (q^{1/2} + q^{-1/2})X_{\gamma_2-\gamma_3} \\ &\quad + (q^{1/2} + q^{-1/2})X_{-\gamma_1+\gamma_2-\gamma_3} + (q^{1/2} + q^{-1/2})X_{2\gamma_2-\gamma_3} + X_{-\gamma_1+2\gamma_2-\gamma_3} + X_{\gamma_1+2\gamma_2-\gamma_3} \\ &\quad + (q^{1/2} + q^{-1/2})X_{2\gamma_2+\gamma_3} + X_{-\gamma_1+2\gamma_2+\gamma_3} + X_{\gamma_1+2\gamma_2+\gamma_3} + (z + z^{-1})X_{\gamma_2+\gamma'} \\ &\quad + (z + z^{-1})X_{-\gamma_1+\gamma_2+\gamma'} + (z + z^{-1})(q^{1/2} + q^{-1/2})X_{2\gamma_2+\gamma'} + (z + z^{-1})X_{-\gamma_1+2\gamma_2+\gamma'} \\ &\quad + (z + z^{-1})X_{\gamma_1+2\gamma_2+\gamma'} + z^{-1}X_{-\gamma_1-\gamma_3+\gamma'} + (q^{1/2} + q^{-1/2})z^{-1}X_{\gamma_2-\gamma_3+\gamma'} \\ &\quad + (q^{1/2} + q^{-1/2})z^{-1}X_{-\gamma_1+\gamma_2-\gamma_3+\gamma'} + (q^{1/2} + q^{-1/2})z^{-1}X_{2\gamma_2-\gamma_3+\gamma'} + z^{-1}X_{-\gamma_1+2\gamma_2-\gamma_3+\gamma'} \\ &\quad + z^{-1}X_{\gamma_1+2\gamma_2-\gamma_3+\gamma'} + (q^{1/2} + q^{-1/2})zX_{2\gamma_2+\gamma_3+\gamma'} + zX_{-\gamma_1+2\gamma_2+\gamma_3+\gamma'} + zX_{\gamma_1+2\gamma_2+\gamma_3+\gamma'}, \end{aligned}$$

$$F(D_3) = X_{\gamma_1-\gamma_3} + z^{-1}X_{\gamma_1-\gamma_3+\gamma'},$$

$$F(D_4) = (q^{1/2} + q^{-1/2})X_{\gamma_1-2\gamma'} + X_{\gamma_1-\gamma_3-2\gamma'} + X_{\gamma_1+\gamma_3-2\gamma'} + z^{-1}X_{\gamma_1-\gamma'} + z^{-1}X_{\gamma_1-\gamma_3-\gamma'}$$



$$\begin{aligned}
& + zX_{\gamma_1-\gamma'} + zX_{\gamma_1+\gamma_3-\gamma'}, \\
F(D_5) &= (q^{1/2} + q^{-1/2})(X_{-\gamma_1-2\gamma'} + X_{-\gamma_1-\gamma_2-2\gamma'} + X_{-\gamma_1-\gamma_2-\gamma_3-2\gamma'} + z^{-1}X_{-\gamma_1-\gamma_2-\gamma_3-\gamma'}) \\
& + X_{-\gamma_1-\gamma_3-2\gamma'} + X_{-\gamma_1-2\gamma_2-\gamma_3-2\gamma'} + X_{-\gamma_1+\gamma_3-2\gamma'} + (z + z^{-1})X_{-\gamma_1-\gamma'} \\
& + (z + z^{-1})X_{-\gamma_1-\gamma_2-\gamma'} + z^{-1}X_{-\gamma_1-\gamma_3-\gamma'} + z^{-1}X_{-\gamma_1-2\gamma_2-\gamma_3-\gamma'} + zX_{-\gamma_1+\gamma_3-\gamma'}, \\
F(E) &= z + z^{-1}.
\end{aligned}$$

The line defect Schur index is

$$\begin{aligned}
\mathcal{I}_L(q, z) &= (q)_\infty^4 \text{Tr}[F(L)S(q)\bar{S}(q)], \quad \text{with} \\
S(q) &= E_q(X_{\gamma_1})E_q(X_{\gamma_4})E_q(X_{\gamma_3})E_q(X_{\gamma_2})E_q(X_{\gamma_5}).
\end{aligned} \tag{3.153}$$

After inserting generating functions the calculation boils down to computing the following:

$$\begin{aligned}
& (q)_\infty^4 \text{Tr}[X_{a\gamma_1+b\gamma_2+c\gamma_3+d\gamma'}S(q)\bar{S}(q)] \\
&= (q)_\infty^4 \sum_{l_i, k_i=0}^{\infty} \frac{(-1)^{a+b+c+d} q^{A/2} z^{l_4+l_5-k_4-k_5}}{(q)_{l_1} \cdots (q)_{l_5} (q)_{k_1} \cdots (q)_{k_5}} \delta_{k_1, l_1+a} \delta_{k_2, l_2+b} \delta_{k_3, l_3+c} \delta_{k_4, l_4-l_5+k_5+d}, \quad \text{with} \\
A &= \frac{1}{2} \left( a + b + ab + c + bc - cd + d(1 + 2c + 2l_3) + 2(l_1 + l_2 + al_2 + cl_2 + l_1l_2 + l_3 \right. \\
& \quad \left. + l_2l_3 + k_5(1 + c + l_3) + l_4 + l_3l_4) \right).
\end{aligned}$$

Within the same class line defect Schur indices are the same. The coefficients in  $q$  are again characters of certain  $SU(2)$  representations:

$$\begin{aligned}
\mathcal{I}_A(q, z) &= -q^{\frac{1}{2}}(1 + \chi_{\mathbf{3}}q + \chi_{\mathbf{1} \oplus \mathbf{3} \oplus \mathbf{5}}q^2 + \chi_{\mathbf{1} \oplus \mathbf{3} \oplus \mathbf{5} \oplus \mathbf{7}}q^3 + \cdots), \\
\mathcal{I}_B(q, z) &= q(\chi_{\mathbf{2}} + \chi_{\mathbf{4}}q + \chi_{\mathbf{2} \oplus \mathbf{4} \oplus \mathbf{6}}q^2 + \chi_{\mathbf{2} \oplus \mathbf{2} \oplus \mathbf{4} \oplus \mathbf{6} \oplus \mathbf{8}}q^3 + \cdots), \\
\mathcal{I}_C(q, z) &= -q^{\frac{1}{2}}(\chi_{\mathbf{2}} + \chi_{\mathbf{4}}q + \chi_{\mathbf{2} \oplus \mathbf{2} \oplus \mathbf{4} \oplus \mathbf{6}}q^2 + \chi_{\mathbf{2} \oplus \mathbf{2} \oplus \mathbf{4} \oplus \mathbf{3} \oplus \mathbf{6} \oplus \mathbf{8}}q^3 + \cdots), \\
\mathcal{I}_D(q, z) &= q(1 + \chi_{\mathbf{3}}q^2 + \chi_{\mathbf{1} \oplus \mathbf{3}}q^3 + \cdots).
\end{aligned} \tag{3.154}$$

The chiral algebra corresponding to the  $(A_1, D_5)$  Argyres-Douglas theory is  $\widehat{\mathfrak{sl}(2)}_{-\frac{8}{5}}$  [52, 54, 56, 59], which has five admissible representations with the following highest weights:

$$\begin{aligned}\Phi_0 &= \left[-\frac{8}{5}, 0\right], & \Phi_1 &= \left[-\frac{6}{5}, -\frac{2}{5}\right], & \Phi_2 &= \left[-\frac{4}{5}, -\frac{4}{5}\right], \\ \Phi_3 &= \left[-\frac{2}{5}, -\frac{6}{5}\right], & \Phi_4 &= \left[0, -\frac{8}{5}\right],\end{aligned}\tag{3.155}$$

where  $\Phi_0$  is the highest weight for the vacuum module. The characters of these representations can be worked out using the Kac-Wakimoto formula [73], which is a special case of the Kazhdan-Lusztig formula [106] (see also [65] for expressions in terms of generalized theta functions):

$$\begin{aligned}\chi_0(q, z) &= \frac{\sum_{m=0}^{\infty} (-1)^m \frac{z^{2m+1} - z^{-(2m+1)}}{z - z^{-1}} q^{\frac{5m(m+1)}{2}}}{\prod_{n=1}^{\infty} (1 - q^n)(1 - z^2 q^n)(1 - z^{-2} q^n)}, \\ \chi_1(q, z) &= \frac{1 + \sum_{m=1}^{\infty} (-1)^m (z^{-2m} q^{\frac{m(5m-3)}{2}} + z^{2m} q^{\frac{m(5m+3)}{2}})}{(1 - z^{-2}) \prod_{n=1}^{\infty} (1 - q^n)(1 - z^2 q^n)(1 - z^{-2} q^n)}, \\ \chi_2(q, z) &= \frac{1 + \sum_{m=1}^{\infty} (-1)^m (z^{-2m} q^{\frac{m(5m-1)}{2}} + z^{2m} q^{\frac{m(5m+1)}{2}})}{(1 - z^{-2}) \prod_{n=1}^{\infty} (1 - q^n)(1 - z^2 q^n)(1 - z^{-2} q^n)}, \\ \chi_3(q, z) &= \frac{1 + \sum_{m=1}^{\infty} (-1)^m (z^{2m} q^{\frac{m(5m-1)}{2}} + z^{-2m} q^{\frac{m(5m+1)}{2}})}{(1 - z^{-2}) \prod_{n=1}^{\infty} (1 - q^n)(1 - z^2 q^n)(1 - z^{-2} q^n)}, \\ \chi_4(q, z) &= \frac{1 + \sum_{m=1}^{\infty} (-1)^m (z^{2m} q^{\frac{m(5m-3)}{2}} + z^{-2m} q^{\frac{m(5m+3)}{2}})}{(1 - z^{-2}) \prod_{n=1}^{\infty} (1 - q^n)(1 - z^2 q^n)(1 - z^{-2} q^n)}.\end{aligned}\tag{3.156}$$

The  $\mathcal{S}$  matrix for these five admissible representations, in the order [3.155], is [65]:

$$\mathcal{S} = \frac{1}{\sqrt{5}} \begin{pmatrix} 1 & -1 & 1 & -1 & 1 \\ -1 & -(-1)^{3/5} & (-1)^{1/5} & (-1)^{4/5} & -(-1)^{2/5} \\ 1 & (-1)^{1/5} & (-1)^{2/5} & (-1)^{3/5} & (-1)^{4/5} \\ -1 & (-1)^{4/5} & (-1)^{3/5} & (-1)^{2/5} & (-1)^{1/5} \\ 1 & -(-1)^{2/5} & (-1)^{4/5} & (-1)^{1/5} & -(-1)^{3/5} \end{pmatrix}.\tag{3.157}$$

Working out the conjugation matrix  $\mathcal{C} = \mathcal{S}^2$  it's clear that  $\Phi_1$  and  $\Phi_4$  are conjugate to each other,  $\Phi_2$  and  $\Phi_3$  are conjugate to each other. Using the Verlinde formula [64] the modular fusion rules for  $\widehat{\mathfrak{sl}(2)}_{-\frac{8}{5}}$  are given by:

$$\begin{aligned}
[\Phi_1] \times [\Phi_1] &= [\Phi_2], & [\Phi_1] \times [\Phi_2] &= [\Phi_3], & [\Phi_1] \times [\Phi_3] &= [\Phi_4], \\
[\Phi_1] \times [\Phi_4] &= -[\Phi_0], & [\Phi_2] \times [\Phi_2] &= [\Phi_4], & [\Phi_2] \times [\Phi_3] &= -[\Phi_0], \\
[\Phi_2] \times [\Phi_4] &= -[\Phi_1], & [\Phi_3] \times [\Phi_3] &= -[\Phi_1], & [\Phi_3] \times [\Phi_4] &= -[\Phi_2], \\
[\Phi_4] \times [\Phi_4] &= -[\Phi_3].
\end{aligned} \tag{3.158}$$

As we will see shortly, multiplications in the deformed Verlinde-like algebra are again given by multiplying the  $-1$  coefficients in the original modular fusion rules by a factor of  $z^2$ .

The line defect Schur indices for defect generators of type  $A$ ,  $B$ ,  $C$  and  $D$  admit the following character expansions:

$$\begin{aligned}
\mathcal{I}_A(q, z) &= q^{-1/2}(\chi_0(q, z) - \chi_1(q, z) + z^{-2}\chi_4(q, z)), \\
\mathcal{I}_B(q, z) &= q^{-1}z^{-1}(\chi_2(q, z) - \chi_3(q, z)), \\
\mathcal{I}_C(q, z) &= q^{-1/2}z^{-1}(-\chi_1(q, z) + \chi_2(q, z) - \chi_3(q, z) + \chi_4(q, z)), \\
\mathcal{I}_D(q, z) &= \chi_0(q, z) - q^{-1}(\chi_1(q, z) - \chi_2(q, z) + z^{-2}\chi_3(q, z) - z^{-2}\chi_4(q, z)).
\end{aligned} \tag{3.159}$$

Now we again take the  $q \rightarrow 1$  limit while keeping  $z$  general, giving the map

$$\begin{aligned}
I &\xrightarrow{f} [\Phi_0], \\
A_i &\xrightarrow{f} [A] = [\Phi_0] - [\Phi_1] + z^{-2}[\Phi_4], \\
B_i &\xrightarrow{f} [B] = z^{-1}([\Phi_2] - [\Phi_3]), \\
C_i &\xrightarrow{f} [C] = z^{-1}(-[\Phi_1] + [\Phi_2] - [\Phi_3] + [\Phi_4]), \\
D_i &\xrightarrow{f} [D] = [\Phi_0] - [\Phi_1] + [\Phi_2] - z^{-2}[\Phi_3] + z^{-2}[\Phi_4].
\end{aligned} \tag{3.160}$$

This map is believed to be a homomorphism  $f : \mathcal{L} \rightarrow \mathcal{V}_z$ , when we define the deformed Verlinde-like algebra  $\mathcal{V}_z$  by the following  $z$ -deformed modular fusion rules:

$$\begin{aligned}
[\Phi_1] \times [\Phi_1] &= [\Phi_2], & [\Phi_1] \times [\Phi_2] &= [\Phi_3], & [\Phi_1] \times [\Phi_3] &= [\Phi_4], \\
[\Phi_1] \times [\Phi_4] &= -z^2[\Phi_0], & [\Phi_2] \times [\Phi_2] &= [\Phi_4], & [\Phi_2] \times [\Phi_3] &= -z^2[\Phi_0], \\
[\Phi_2] \times [\Phi_4] &= -z^2[\Phi_1], & [\Phi_3] \times [\Phi_3] &= -z^2[\Phi_1], & [\Phi_3] \times [\Phi_4] &= -z^2[\Phi_2], \\
[\Phi_4] \times [\Phi_4] &= -z^2[\Phi_3].
\end{aligned} \tag{3.161}$$

To check the homomorphism property we consider Schur indices with insertion of two half line defects, which can also be expanded in terms of characters of admissible representations. After setting  $q \rightarrow 1$  the expansion coefficients do not depend on the  $i$ -index anymore:

$$\begin{aligned}
A_i A_j &\xrightarrow{f} 3[\Phi_0] - 2[\Phi_1] + [\Phi_2] - z^{-2}[\Phi_3] + 2z^{-2}[\Phi_4], \\
A_i B_j &\xrightarrow{f} z^{-1}(-[\Phi_1] + 2[\Phi_2] - 2[\Phi_3] + [\Phi_4]), \\
A_i C_j &\xrightarrow{f} (z + z^{-1})[\Phi_0] - 2z^{-1}([\Phi_1] - [\Phi_4]) + 3z^{-1}([\Phi_2] - [\Phi_3]), \\
A_i D_j &\xrightarrow{f} 3[\Phi_0] - 3[\Phi_1] + (2 + z^{-2})[\Phi_2] - (1 + 2z^{-2})[\Phi_3] + 3z^{-2}[\Phi_4], \\
B_i B_j &\xrightarrow{f} 2[\Phi_0] - [\Phi_1] + z^{-2}[\Phi_4], \\
B_i C_j &\xrightarrow{f} 2[\Phi_0] - 2[\Phi_1] + [\Phi_2] - z^{-2}[\Phi_3] + 2z^{-2}[\Phi_4], \\
B_i D_j &\xrightarrow{f} (z + z^{-1})[\Phi_0] + 2z^{-1}(-[\Phi_1] + [\Phi_2] - [\Phi_3] + [\Phi_4]), \\
C_i C_j &\xrightarrow{f} 4[\Phi_0] - 3[\Phi_1] + (2 + z^{-2})[\Phi_2] - (1 + 2z^{-2})[\Phi_3] + 3z^{-2}[\Phi_4], \\
C_i D_j &\xrightarrow{f} 2(z + z^{-1})[\Phi_0] - (z + 3z^{-1})[\Phi_1] + 4z^{-1}([\Phi_2] - [\Phi_3]) + (3z^{-1} + z^{-3})[\Phi_4], \\
D_i D_j &\xrightarrow{f} 5[\Phi_0] - (4 + z^{-2})[\Phi_1] + (3 + 2z^{-2})[\Phi_2] - (2 + 3z^{-2})[\Phi_3] + (1 + 4z^{-2})[\Phi_4].
\end{aligned}$$

$f$  is a homomorphism if and only if the  $z$ -deformed fusion rules are as defined in (3.161).

The fusion matrices for non-vacuum modules are given as follows:

$$\begin{aligned}
N_{\Phi_1} &= \begin{pmatrix} 0 & 1 & 0 & 0 & 0 \\ 0 & 0 & 1 & 0 & 0 \\ 0 & 0 & 0 & 1 & 0 \\ 0 & 0 & 0 & 0 & 1 \\ -z^2 & 0 & 0 & 0 & 0 \end{pmatrix}, & N_{\Phi_2} &= \begin{pmatrix} 0 & 0 & 1 & 0 & 0 \\ 0 & 0 & 0 & 1 & 0 \\ 0 & 0 & 0 & 0 & 1 \\ -z^2 & 0 & 0 & 0 & 0 \\ 0 & -z^2 & 0 & 0 & 0 \end{pmatrix}, \\
N_{\Phi_3} &= \begin{pmatrix} 0 & 0 & 0 & 1 & 0 \\ 0 & 0 & 0 & 0 & 1 \\ -z^2 & 0 & 0 & 0 & 0 \\ 0 & -z^2 & 0 & 0 & 0 \\ 0 & 0 & -z^2 & 0 & 0 \end{pmatrix}, & N_{\Phi_4} &= \begin{pmatrix} 0 & 0 & 0 & 0 & 1 \\ -z^2 & 0 & 0 & 0 & 0 \\ 0 & -z^2 & 0 & 0 & 0 \\ 0 & 0 & -z^2 & 0 & 0 \\ 0 & 0 & 0 & -z^2 & 0 \end{pmatrix}.
\end{aligned} \tag{3.162}$$

For generic  $z$  these four matrices are simultaneously diagonalizable with the following eigenvalues:

eigenspace	$\lambda_{\Phi_1}$	$\lambda_{\Phi_2}$	$\lambda_{\Phi_3}$	$\lambda_{\Phi_4}$
1	$-z^{2/5}$	$z^{4/5}$	$-z^{6/5}$	$z^{8/5}$
2	$(-1)^{1/5} z^{2/5}$	$(-1)^{2/5} z^{4/5}$	$(-1)^{3/5} z^{6/5}$	$(-1)^{4/5} z^{8/5}$
3	$-(-1)^{2/5} z^{2/5}$	$(-z)^{4/5}$	$(-1)^{1/5} z^{6/5}$	$-(-1)^{3/5} z^{8/5}$
4	$(-1)^{3/5} z^{2/5}$	$-(-1)^{1/5} z^{4/5}$	$-(-1)^{4/5} z^{6/5}$	$(-1)^{2/5} z^{8/5}$
5	$-(-1)^{4/5} z^{2/5}$	$-(-1)^{3/5} z^{4/5}$	$-(-1)^{2/5} z^{6/5}$	$-(-1)^{1/5} z^{8/5}$

The classical monodromy action in this chamber can be worked out as a composition of flips, as in Figure 3.21:

$$\begin{aligned}
\mathcal{X}_{\gamma_1} &\rightarrow \frac{1 + \mathcal{X}_{\gamma_5} + \mathcal{X}_{\gamma_3} \mathcal{X}_{\gamma_5} + C}{\mathcal{X}_{\gamma_2} \mathcal{X}_{\gamma_3} \mathcal{X}_{\gamma_4}}, \\
\mathcal{X}_{\gamma_2} &\rightarrow \frac{\mathcal{X}_{\gamma_1} \mathcal{X}_{\gamma_2} \mathcal{X}_{\gamma_3} \mathcal{X}_{\gamma_4}}{(1 + \mathcal{X}_{\gamma_2} (1 + \mathcal{X}_{\gamma_3} + \mathcal{X}_{\gamma_3} \mathcal{X}_{\gamma_4})) (1 + \mathcal{X}_{\gamma_5} + \mathcal{X}_{\gamma_3} \mathcal{X}_{\gamma_5} + (1 + \mathcal{X}_{\gamma_1}) C)}, \\
\mathcal{X}_{\gamma_3} &\rightarrow \frac{(1 + (1 + \mathcal{X}_{\gamma_1}) \mathcal{X}_{\gamma_2} (1 + \mathcal{X}_{\gamma_3})) (1 + \mathcal{X}_{\gamma_5} + \mathcal{X}_{\gamma_3} \mathcal{X}_{\gamma_5} + C)}{\mathcal{X}_{\gamma_1} \mathcal{X}_{\gamma_2} \mathcal{X}_{\gamma_3} (1 + \mathcal{X}_{\gamma_3}) \mathcal{X}_{\gamma_4} \mathcal{X}_{\gamma_5}},
\end{aligned}$$

$$\begin{aligned}\mathcal{X}_{\gamma_4} &\rightarrow \frac{1 + \mathcal{X}_{\gamma_5} + \mathcal{X}_{\gamma_3}\mathcal{X}_{\gamma_5} + (1 + \mathcal{X}_{\gamma_1})C}{\mathcal{X}_{\gamma_3}}, \\ \mathcal{X}_{\gamma_5} &\rightarrow \frac{\mathcal{X}_{\gamma_3}\mathcal{X}_{\gamma_4}\mathcal{X}_{\gamma_5}}{1 + \mathcal{X}_{\gamma_5} + \mathcal{X}_{\gamma_3}\mathcal{X}_{\gamma_5} + (1 + \mathcal{X}_{\gamma_1})C},\end{aligned}$$

where

$$C = \mathcal{X}_{\gamma_2}(1 + \mathcal{X}_{\gamma_3})(1 + \mathcal{X}_{\gamma_5}(1 + \mathcal{X}_{\gamma_3} + \mathcal{X}_{\gamma_3}\mathcal{X}_{\gamma_4})).$$

For generic fixed  $z \neq 0$ , there are exactly five fixed points, matching the number of admissible representations of  $\widehat{\mathfrak{sl}(2)}_{-\frac{8}{5}}$ . Concretely, at the fixed locus  $\mathcal{X}_{\gamma_3}$  satisfies the following quintic equation:

$$z^6\mathcal{X}_{\gamma_3}^5 - 5z^4\mathcal{X}_{\gamma_3}^3 - 10z^4\mathcal{X}_{\gamma_3}^2 - 5z^4\mathcal{X}_{\gamma_3} - (z^4 + z^2 + 1) = 0, \quad (3.163)$$

and  $\mathcal{X}_{\gamma_1}, \mathcal{X}_{\gamma_2}, \mathcal{X}_{\gamma'}$  are all determined by  $\mathcal{X}_{\gamma_3}$  and  $z$  (by complicated algebraic expressions which we will not present here.) As in previous examples, the values of line defect vevs at the fixed points do not depend on the index  $i$ .

The Galois group of the quintic (3.163) is solvable according to `sage`, so in principle one can give a solution in radicals; we have not carried this out, however. Thus, here we cannot give a closed form for the values of the  $\mathcal{X}_\gamma$  at the fixed points. Moreover, we also have the same problem as in §3.6.1 above: we do not know *a priori* how to match the five fixed points and the five primaries. Nevertheless we numerically sampled various values of  $z$  and confirmed that, for each  $z$ , there does exist a matching between fixed points and primaries, such that the corresponding  $h$  makes the diagram commute.

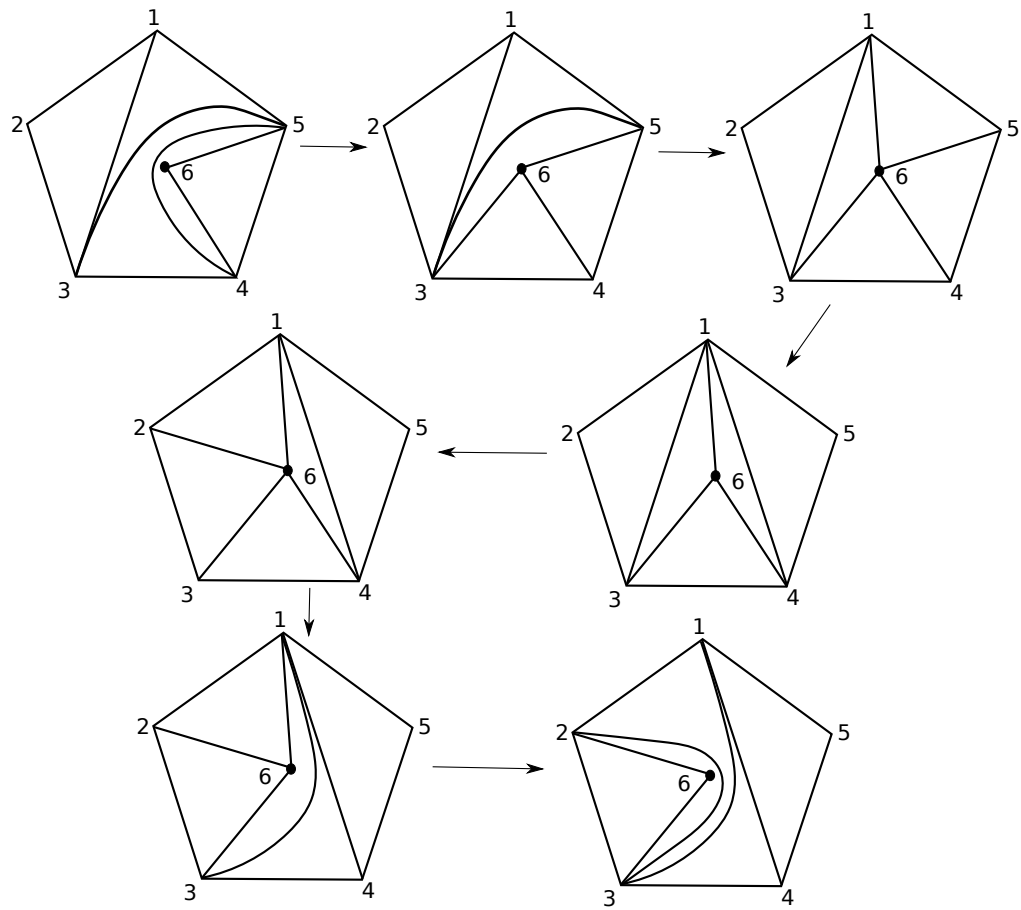


Figure 3.21: Monodromy action as a sequence of flips in the  $(A_1, D_5)$  Argyres-Douglas theory.

### 3.7 Verlinde algebra from Fixed Points Analysis

Given the relations that we have discussed between the three algebras, one might ask whether we could say something about the Verlinde algebra through values of generating functions at the fixed points<sup>31</sup>. The answer is that we can not determine Verlinde algebra from fixed points analysis alone, but we do obtain useful information about Verlinde algebra<sup>32</sup> and expansion of line defect Schur index in terms of characters.

First we would like to stress that, in principal one could obtain the (deformed) Verlinde algebra through computing Schur index with one half line and two half lines inserted and studying their images under the homomorphism  $f$ . In fact this is practically how we found the deformed Verlinde algebra in the  $D_3$  and  $D_5$  cases. However, in practice (at least for us) character expansions of line defect Schur index (especially Schur index with more than one line defect inserted) are not very easy to obtain. It would be nice if there is some way to simplify this procedure.

To begin with, suppose that we already know the image of  $[\Phi_\alpha]$  under the isomorphism  $h$ , then the modular fusion rules among them are very easy to obtain since the corresponding multiplication in  $\mathcal{O}(F)$  is given directly by pointwise multiplication. Concretely, suppose that

$$[\Phi_\alpha] \xrightarrow{h} \phi_\alpha := (\lambda_\alpha^1, \dots, \lambda_\alpha^n),$$

---

<sup>31</sup>We thank Shu-Heng Shao for mentioning this interesting perspective.

<sup>32</sup>More precisely we mean Verlinde-like algebra of the set of highest weight modules that correspond to the  $U(1)_r$  fixed points, from direct application of the Verlinde formula.



then by expanding e.g.

$$\phi_\alpha \phi_\beta = \sum_\gamma c_{\alpha\beta}^\gamma \phi_\gamma,$$

the modular fusion coefficients are given by  $c_{\alpha\beta}^\gamma$ <sup>33</sup>. Now how do we determine  $\phi_\alpha$ ? Since we know the values of  $F_{L_{\alpha i}}$  at the  $U(1)_r$  fixed points, if in addition we also know the image of  $L_{\alpha i}$  under  $f$ , then  $\phi_\alpha$  is given by taking the inverse of the linear relations. So we still need to work out the character expansions for single line defect Schur index. But this already saves the effort of working out the character expansions of two line defect Schur index.

Now suppose that the only data given are generating functions of line defect generators and their values at the  $U(1)_r$  fixed points, what “constraints” could we possibly put on the (deformed) Verlinde algebra? We illustrate this by looking at two simplest examples  $A_2$  and  $D_3$  Argyres-Douglas theories. Of course the Verlinde algebra in these cases were already known for a long time (see [65] and references therein), the hope is that this might shed light on unknown Verlinde algebras of certain 2d chiral algebras.

In  $A_2$  case there are two fixed points, the values of  $F_{L_i}$  don’t depend on  $i$  at the fixed points so we denote them as  $F_L$ . Over the fixed points

$$F_L^2 = I + F_L. \tag{3.164}$$

This equation is understood in the context of values of line defects at fixed points. This could be obtained either by direct computation or through the

---

<sup>33</sup>Here to get the fusion coefficients we don’t need to “order” the fixed points. We don’t need to know the exact correspondence between  $U(1)_r$  fixed points and primaries.

relation

$$L_i L_{i+2} = 1 + q^{\frac{1}{2}} L_{i+1}. \quad (3.165)$$

As discussed in §3.1.9 in  $(A_1, A_{2N})$  theories the vev of line defect generators themselves realize fusion rules over  $U(1)_r$  fixed points. In particular (3.164) is the non-trivial fusion rule of the  $(2, 5)$  minimal model. However this is a special phenomenon only in  $(A_1, A_{2N})$  theories. We would like to rediscover fusion rules in the basis of  $[\Phi_\alpha]$  instead for the purpose of generalization.

We make the following ansatz for the image of  $L_i$  under  $f$ :

$$L_i \xrightarrow{f} [L] := a[\Phi_0] + b[\Phi_1], \quad (3.166)$$

where  $\Phi_0$  is the vacuum. We also make an ansatz for the fusion rule:

$$[\Phi_1] \times [\Phi_1] = c[\Phi_0] + d[\Phi_1].$$

(3.164) would imply

$$[LL] = [L] \times [L] = (a + 1)[\Phi_0] + b[\Phi_1], \quad (3.167)$$

by comparing coefficients we get the following equations for  $a, b, c, d$ :

$$a^2 + b^2 c = a + 1, \quad 2ab + b^2 d = b. \quad (3.168)$$

Now,  $a$  and  $b$  have to be integers. This was the observation made in [51]. We do not have an explanation but it is true in all the examples that we considered in this paper so we use this as an assumption. The fusion coefficients  $c$  and  $d$

have to be 0 or 1<sup>34</sup>. Moreover given each candidate fusion rule one could check whether the solution is consistent with eigenvalues of the Verlinde matrix. These constraints pin down the only possible fusion rule to be the desired one in (2, 5) minimal model namely  $c = 1$  and  $d = 1$ . There are two solutions for  $a$  and  $b$ :

$$(a, b) = (1, -1) \quad \text{or} \quad (a, b) = (0, 1). \quad (3.169)$$

The wrong answer could be easily ruled out by computing the single line defect Schur index. In more complicated cases the finite number of solutions of  $(a, b)$  also offers ansatz for the character expansion of single line defect Schur index.

In the  $D_3$  case we have more constraints due to the  $z$ -deformed Verlinde algebra. We take an assumption that the  $z$ -deformed Verlinde algebra always replaces the  $-1$  coefficient by  $-z^2$ <sup>35</sup>. In that case by taking  $z = i$  all the fusion coefficients are either 0 or 1. So this reduces to a similar case as in  $A_2$ . When  $z = i$ ,

$$[AB] = 2[A], \quad [AA] = [\Phi_0] + [B], \quad [BB] = 2[\Phi_0] + [B]. \quad (3.170)$$

Again this was obtained either by directly looking at values of  $F(L)$  at fixed points or through relations between generating functions. Similarly by making ansatz and comparing coefficients one could obtain the consistent fusion rules.

---

<sup>34</sup>We will discuss how this works for modular fusion rules with apparent  $-1$  coefficients momentarily.

<sup>35</sup>We conjecture this is true at least for  $(A_1, D_{2N+1})$  Argyres-Douglas theories. For other theories one could first work out simple examples to find out patterns of deformed modular fusion rules.

Note that in this case there is one more constraint coming into play, namely the fusion matrices  $N_{\Phi_1}$  and  $N_{\Phi_2}$  have to be simultaneously diagonalizable. The only fusion rules passing these constraints are

$$\begin{aligned} [\Phi_1] \times [\Phi_1] &= [\Phi_2], \\ [\Phi_1] \times [\Phi_2] &= [\Phi_0], \\ [\Phi_2] \times [\Phi_2] &= [\Phi_1]. \end{aligned} \tag{3.171}$$

Note that here we can not physically distinguish  $[\Phi_1]$  and  $[\Phi_2]$ , e.g. we can not compute their conformal weights etc in our setup. They only appear in our ansatz (for  $z = i$ ) for  $[A]$  and  $[B]$ . This is the reason why we can't actually pin down the fusion rules. Now in the deformed fusion rules each  $+1$  coefficient in (3.171) could be either  $+1$  or  $-z^2$ . We again make ansatz for  $[A]$  and  $[B]$ , only now the coefficients are monomials in  $z$  with integer coefficients. Again this is an assumption that we make through observations of known examples. For general  $z$  the following holds:

$$\begin{aligned} [AB] &= (z + z^{-1})[\Phi_0] + 2[A], \\ [AA] &= [\Phi_0] + [B], \\ [BB] &= 2[\Phi_0] + (z + z^{-1})[A] + [B]. \end{aligned} \tag{3.172}$$

Imposing constraints and comparing coefficients gives us two possibilities. One of them, which is also the correct one, is

$$\begin{aligned} [\Phi_1] \times [\Phi_1] &= [\Phi_2], \\ [\Phi_1] \times [\Phi_2] &= -z^2[\Phi_0], \\ [\Phi_2] \times [\Phi_2] &= -z^2[\Phi_1], \end{aligned}$$

with the following images of  $A_i$  and  $B_i$  under  $f$ :

$$[A] = \frac{1}{z}([\Phi_2] - [\Phi_1]),$$
$$[B] = [\Phi_0] - [\Phi_1] + z^{-2}[\Phi_2].$$

The other solution is simply given by swapping  $[\Phi_1]$  with  $[\Phi_2]$ . Note that this is reasonable since we can not physically distinguish  $[\Phi_1]$  and  $[\Phi_2]$ . So this is the best we could do with the available ansatz. In reality given access to characters of admissible representations it would be easy to rule out the wrong answer.

## Bibliography

- [1] D. Gaiotto, G. W. Moore, and A. Neitzke, “Wall-crossing, Hitchin systems, and the WKB approximation,” [arXiv:0907.3987 \[hep-th\]](#).
- [2] D. Gaiotto, “ $\mathcal{N} = 2$  dualities,” [JHEP 08 \(2012\) 034](#), [arXiv:0904.2715 \[hep-th\]](#).
- [3] J. Distler, B. Ergun, and F. Yan, “Product SCFTs in Class-S,” [arXiv:1711.04727 \[hep-th\]](#).
- [4] A. Neitzke and F. Yan, “Line defect Schur indices, Verlinde algebras and  $U(1)_r$  fixed points,” [JHEP 11 \(2017\) 035](#), [arXiv:1708.05323 \[hep-th\]](#).
- [5] S. H. Katz, A. Klemm, and C. Vafa, “Geometric engineering of quantum field theories,” [Nucl. Phys. B497 \(1997\) 173–195](#), [arXiv:hep-th/9609239 \[hep-th\]](#).
- [6] S. Katz, P. Mayr, and C. Vafa, “Mirror symmetry and exact solution of 4-D  $N=2$  gauge theories: 1.,” [Adv. Theor. Math. Phys. 1 \(1998\) 53–114](#), [arXiv:hep-th/9706110 \[hep-th\]](#).
- [7] L. Rastelli and S. S. Razamat, “The Superconformal Index of Theories of Class  $\mathcal{S}$ ,” in *New Dualities of Supersymmetric Gauge Theories*,

- J. Teschner, ed., pp. 261–305. 2016. [arXiv:1412.7131 \[hep-th\]](#).  
<https://inspirehep.net/record/1335343/files/arXiv:1412.7131.pdf>.
- [8] Y. Tachikawa, “Six-dimensional  $D_N$  theory and four-dimensional SO-USp quivers,” [JHEP 07 \(2009\) 067](#), [arXiv:0905.4074 \[hep-th\]](#).
- [9] O. Chacaltana, J. Distler, and Y. Tachikawa, “Nilpotent orbits and codimension-two defects of 6d  $N = (2, 0)$  theories,” [Int. J. Mod. Phys. A28 \(2013\) 1340006](#), [arXiv:1203.2930 \[hep-th\]](#).
- [10] O. Chacaltana, J. Distler, and Y. Tachikawa, “Gaiotto duality for the twisted  $A_{2N-1}$  series,” [JHEP 1505 \(2015\) 075](#), [arXiv:1212.3952 \[hep-th\]](#).
- [11] O. Chacaltana, J. Distler, and A. Trimm, “Tinkertoys for the twisted D-series,” [JHEP 1504 \(2015\) 173](#), [arXiv:1309.2299 \[hep-th\]](#).
- [12] O. Chacaltana, J. Distler, and A. Trimm, “Tinkertoys for the twisted  $E_6$  theory,” [JHEP 04 \(2015\) 173](#), [arXiv:1501.00357 \[hep-th\]](#).
- [13] L. F. Alday, D. Gaiotto, and Y. Tachikawa, “Liouville Correlation Functions from Four-dimensional Gauge Theories,” [Lett. Math. Phys. 91 \(2010\) 167–197](#), [arXiv:0906.3219 \[hep-th\]](#).
- [14] N. Wyllard, “A(N-1) conformal Toda field theory correlation functions from conformal  $N = 2$  SU(N) quiver gauge theories,” [JHEP 11 \(2009\) 002](#), [arXiv:0907.2189 \[hep-th\]](#).

- [15] L. Hollands, C. A. Keller, and J. Song, “From SO/Sp instantons to W-algebra blocks,” *JHEP* **03** (2011) 053, [arXiv:1012.4468 \[hep-th\]](#).
- [16] L. Hollands, C. A. Keller, and J. Song, “Towards a 4d/2d correspondence for Sicilian quivers,” *JHEP* **10** (2011) 100, [arXiv:1107.0973 \[hep-th\]](#).
- [17] C. A. Keller, N. Mekareeya, J. Song, and Y. Tachikawa, “The ABCDEFG of Instantons and W-algebras,” *JHEP* **03** (2012) 045, [arXiv:1111.5624 \[hep-th\]](#).
- [18] A. Gadde, E. Pomoni, L. Rastelli, and S. S. Razamat, “S-duality and 2d Topological QFT,” *JHEP* **03** (2010) 032, [arXiv:0910.2225 \[hep-th\]](#).
- [19] A. Gadde, L. Rastelli, S. S. Razamat, and W. Yan, “Gauge theories and Macdonald polynomials,” *Commun. Math. Phys.* **319** (2013) 147–193, [arXiv:1110.3740 \[hep-th\]](#).
- [20] M. Lemos, W. Peelaers, and L. Rastelli, “The superconformal index of class  $S$  theories of type  $D$ ,” *JHEP* **05** (2014) 120, [arXiv:1212.1271 \[hep-th\]](#).
- [21] N. J. Hitchin, “The self-duality equations on a Riemann surface,” *Proc. London Math. Soc.* (3) **55** no. 1, (1987) 59–126.



- [22] D. Gaiotto, G. W. Moore, and A. Neitzke, “Four-dimensional wall-crossing via three-dimensional field theory,” *Commun. Math. Phys.* **299** (2010) 163–224, [arXiv:0807.4723 \[hep-th\]](#).
- [23] D. Gaiotto, G. W. Moore, and A. Neitzke, “Framed BPS States,” *Adv. Theor. Math. Phys.* **17** no. 2, (2013) 241–397, [arXiv:1006.0146 \[hep-th\]](#).
- [24] D. Gaiotto, G. W. Moore, and A. Neitzke, “Wall-Crossing in Coupled 2d-4d Systems,” *JHEP* **12** (2012) 082, [arXiv:1103.2598 \[hep-th\]](#).
- [25] D. Gaiotto, G. W. Moore, and A. Neitzke, “Spectral networks,” *Annales Henri Poincare* **14** (2013) 1643–1731, [arXiv:1204.4824 \[hep-th\]](#).
- [26] O. Chacaltana and J. Distler, “Tinkertoys for the  $D_N$  series,” *JHEP* **02** (2013) 110, [arXiv:1106.5410 \[hep-th\]](#).
- [27] E. Witten, “Five-branes and M-theory on an orbifold,” *Nucl. Phys.* **B463** (1996) 383–397, [arXiv:hep-th/9512219](#).
- [28] E. Witten, “Some comments on string dynamics,” in *Future Perspectives in String Theory. Proceedings of Strings '95, Los Angeles, USA, March 13-18, 1995*, pp. 501–523. 1995. [arXiv:hep-th/9507121 \[hep-th\]](#).
- [29] O. Chacaltana, J. Distler, and A. Trimm, “Tinkertoys for the  $\mathbb{Z}_3$ -twisted  $D_4$  theory,” [arXiv:1601.02077 \[hep-th\]](#).

- [30] Y. Tachikawa, “ $\mathcal{N} = 2$  S-duality via outer-automorphism twists,” [J. Phys. A44 \(2011\) 182001](#), [arXiv:1009.0339 \[hep-th\]](#).
- [31] O. Chacaltana and J. Distler, “Tinkertoys for Gaiotto duality,” [JHEP 1011 \(2010\) 099](#), [arXiv:1008.5203 \[hep-th\]](#).
- [32] O. Chacaltana, J. Distler, and A. Trimm, “Tinkertoys for the  $E_6$  theory,” [JHEP 09 \(2015\) 007](#), [arXiv:1403.4604 \[hep-th\]](#).
- [33] O. Chacaltana, J. Distler, and A. Trimm, “Seiberg-Witten for  $Spin(n)$  with spinors,” [JHEP 08 \(2015\) 027](#), [arXiv:1404.3736 \[hep-th\]](#).
- [34] O. Chacaltana, J. Distler, and A. Trimm, “A family of  $4D \mathcal{N} = 2$  interacting SCFTs from the twisted  $A_{2N}$  series,” [arXiv:1412.8129 \[hep-th\]](#).
- [35] O. Chacaltana, J. Distler, A. Trimm, and Y. Zhu, “Tinkertoys for the  $E_7$  theory,” [arXiv:1704.07890 \[hep-th\]](#).
- [36] J. A. Minahan and D. Nemeschansky, “An  $N = 2$  superconformal fixed point with  $E_6$  global symmetry,” [Nucl. Phys. B482 \(1996\) 142–152](#), [arXiv:hep-th/9608047 \[hep-th\]](#).
- [37] J. A. Minahan and D. Nemeschansky, “Superconformal fixed points with  $E_N$  global symmetry,” [Nucl. Phys. B489 \(1997\) 24–46](#), [arXiv:hep-th/9610076](#).

- [38] O. Chacaltana, J. Distler, A. Trimm, and Y. Zhu, “Tinkertoys for the  $E_8$  Theory,” [arXiv:1802.09626 \[hep-th\]](#).
- [39] J. Distler and B. Ergun, “Product SCFTs for the  $E_7$  Theory,” [arXiv:1803.02425 \[hep-th\]](#).
- [40] J. Kinney, J. M. Maldacena, S. Minwalla, and S. Raju, “An index for 4 dimensional superconformal theories,” *Commun. Math. Phys.* **275** (2007) 209–254, [arXiv:hep-th/0510251 \[hep-th\]](#).
- [41] F. A. Dolan and H. Osborn, “On short and semi-short representations for four-dimensional superconformal symmetry,” *Annals Phys.* **307** (2003) 41–89, [arXiv:hep-th/0209056 \[hep-th\]](#).
- [42] D. Green, Z. Komargodski, N. Seiberg, Y. Tachikawa, and B. Wecht, “Exactly marginal deformations and global symmetries,” *JHEP* **06** (2010) 106, [arXiv:1005.3546 \[hep-th\]](#).
- [43] P. Argyres, M. Lotito, Y. Lü, and M. Martone, “Geometric constraints on the space of  $\mathcal{N} = 2$  SCFTs I: Physical constraints on relevant deformations,” [arXiv:1505.04814 \[hep-th\]](#).
- [44] P. C. Argyres, M. Lotito, Y. Lü, and M. Martone, “Geometric constraints on the space of  $\mathcal{N} = 2$  SCFTs II: Construction of special Kähler geometries and RG flows,” [arXiv:1601.00011 \[hep-th\]](#).

- [45] P. C. Argyres, M. Lotito, Y. Lü, and M. Martone, “Expanding the landscape of  $\mathcal{N} = 2$  rank 1 SCFTs,” [JHEP 05 \(2016\) 088](#), [arXiv:1602.02764 \[hep-th\]](#).
- [46] P. Argyres, M. Lotito, Y. Lü, and M. Martone, “Geometric constraints on the space of  $\mathcal{N} = 2$  SCFTs III: Enhanced Coulomb branches and central charges,” [arXiv:1609.04404 \[hep-th\]](#).
- [47] P. B. Kronheimer, “Instantons and the geometry of the nilpotent variety,” *J. Differential Geom.* **32** no. 2, (1990) 473–490.
- [48] S. Benvenuti, A. Hanany, and N. Mekareeya, “The Hilbert series of the one instanton moduli space,” [JHEP 1006 \(2010\) 100](#), [arXiv:1005.3026 \[hep-th\]](#).
- [49] L. Hollands and A. Neitzke, “BPS states in the Minahan-Nemeschansky  $E_6$  theory,” [Commun. Math. Phys. 353 no. 1, \(2017\) 317–351](#), [arXiv:1607.01743 \[hep-th\]](#).
- [50] T. Dimofte, D. Gaiotto, and S. Gukov, “3-Manifolds and 3d Indices,” [Adv. Theor. Math. Phys. 17 no. 5, \(2013\) 975–1076](#), [arXiv:1112.5179 \[hep-th\]](#).
- [51] C. Córdova, D. Gaiotto, and S.-H. Shao, “Infrared Computations of Defect Schur Indices,” [JHEP 11 \(2016\) 106](#), [arXiv:1606.08429 \[hep-th\]](#).

- [52] C. Beem, M. Lemos, P. Liendo, W. Peelaers, L. Rastelli, *et al.*,  
“Infinite chiral symmetry in four dimensions,” *Commun. Math. Phys.*  
**336** no. 3, (2015) 1359–1433, [arXiv:1312.5344 \[hep-th\]](#).
- [53] J. Song, “Macdonald Index and Chiral Algebra,” *JHEP* **08** (2017) 044,  
[arXiv:1612.08956 \[hep-th\]](#).
- [54] C. Beem, M. Lemos, P. Liendo, L. Rastelli, and B. C. van Rees, “The  
 $\mathcal{N} = 2$  superconformal bootstrap,” *JHEP* **03** (2016) 183,  
[arXiv:1412.7541 \[hep-th\]](#).
- [55] M. Buican and T. Nishinaka, “On the superconformal index of  
Argyres–Douglas theories,” *J. Phys. A* **49** no. 1, (2016) 015401,  
[arXiv:1505.05884 \[hep-th\]](#).
- [56] C. Córdova and S.-H. Shao, “Schur Indices, BPS Particles, and  
Argyres-Douglas Theories,” *JHEP* **01** (2016) 040, [arXiv:1506.00265](#)  
[\[hep-th\]](#).
- [57] T. Creutzig, “W-algebras for Argyres-Douglas theories,”  
[arXiv:1701.05926 \[hep-th\]](#).
- [58] J. Song, D. Xie, and W. Yan, “Vertex operator algebras of  
Argyres-Douglas theories from M5-branes,” [arXiv:1706.01607](#)  
[\[hep-th\]](#).
- [59] D. Xie, W. Yan, and S.-T. Yau, “Chiral algebra of Argyres-Douglas  
theory from M5 brane,” [arXiv:1604.02155 \[hep-th\]](#).

- [60] M. Buican and T. Nishinaka, “On Irregular Singularity Wave Functions and Superconformal Indices,” [arXiv:1705.07173 \[hep-th\]](#).
- [61] S. Cecotti, A. Neitzke, and C. Vafa, “R-Twisting and 4d/2d Correspondences,” [arXiv:1006.3435 \[hep-th\]](#).
- [62] P. C. Argyres and M. R. Douglas, “New phenomena in SU(3) supersymmetric gauge theory,” *Nucl. Phys.* **B448** (1995) 93–126, [arXiv:hep-th/9505062 \[hep-th\]](#).
- [63] P. C. Argyres, M. R. Plesser, N. Seiberg, and E. Witten, “New N=2 superconformal field theories in four-dimensions,” *Nucl. Phys.* **B461** (1996) 71–84, [arXiv:hep-th/9511154 \[hep-th\]](#).
- [64] E. P. Verlinde, “Fusion Rules and Modular Transformations in 2D Conformal Field Theory,” *Nucl. Phys.* **B300** (1988) 360–376.
- [65] P. Di Francesco, P. Mathieu, and D. Sénéchal, *Conformal field theory*. Springer-Verlag, New York, 1997.
- [66] N. Seiberg and E. Witten, “Gauge dynamics and compactification to three-dimensions,” in *The Mathematical Beauty of Physics: A memorial volume for Claude Itzykson. Proceedings: Saclay, France, June 5-7, 1996*, pp. 333–366. 1996. [arXiv:hep-th/9607163 \[hep-th\]](#).

- [67] S. Gukov and D. Pei, “Equivariant Verlinde formula from fivebranes and vortices,” [Commun. Math. Phys. \*\*355\*\* no. 1, \(2017\) 1–50,](#)  
[arXiv:1501.01310 \[hep-th\].](#)
- [68] S. Gukov, D. Pei, W. Yan, and K. Ye, “Equivariant Verlinde algebra from superconformal index and Argyres-Seiberg duality,”  
[arXiv:1605.06528 \[hep-th\].](#)
- [69] L. Fredrickson and A. Neitzke, “From  $S^1$ -fixed points to  $\mathcal{W}$ -algebra representations,” [arXiv:1709.06142 \[math.DG\].](#)
- [70] L. Fredrickson. Talk at the workshop “New perspectives on Higgs bundles, branes and quantization” at Simons Center for Geometry and Physics, June 2016.
- [71] L. Fredrickson, D. Pei, W. Yan, and K. Ye, “Argyres-Douglas Theories, Chiral Algebras and Wild Hitchin Characters,” [arXiv:1701.08782](#)  
[\[hep-th\].](#)
- [72] C. Beem and L. Rastelli, “Vertex operator algebras, Higgs branches, and modular differential equations,” [arXiv:1707.07679 \[hep-th\].](#)
- [73] V. G. Kac and M. Wakimoto, “Modular invariant representations of infinite-dimensional Lie algebras and superalgebras,” [Proc. Nat. Acad. Sci. U.S.A. \*\*85\*\* no. 14, \(1988\) 4956–4960.](#)  
<http://dx.doi.org/10.1073/pnas.85.14.4956>.

- [74] I. Koh and P. Sorba, “Fusion rules and (sub)modular invariant partition functions in nonunitary theories,” *Phys. Letter. B* **215** (1988) 723–729.
- [75] T. Creutzig and D. Ridout, “Modular Data and Verlinde Formulae for Fractional Level WZW Models I,” *Nucl. Phys.* **B865** (2012) 83–114, [arXiv:1205.6513 \[hep-th\]](#).
- [76] T. Creutzig and D. Ridout, “Modular Data and Verlinde Formulae for Fractional Level WZW Models II,” *Nucl. Phys.* **B875** (2013) 423–458, [arXiv:1306.4388 \[hep-th\]](#).
- [77] T. Hausel, *Geometry of the moduli space of Higgs bundles*. PhD thesis, Oxford University, 1998. [arXiv:math/0107040](#).
- [78] C. Córdova, D. Gaiotto, and S.-H. Shao, “Surface Defect Indices and 2d-4d BPS States,” [arXiv:1703.02525 \[hep-th\]](#).
- [79] C. Córdova, D. Gaiotto, and S.-H. Shao, “Surface Defects and Chiral Algebras,” *JHEP* **05** (2017) 140, [arXiv:1704.01955 \[hep-th\]](#).
- [80] C. Beem, W. Peelaers, and L. Rastelli. Work in progress.
- [81] C. Beem, “Chiral symmetry algebras from superconformal symmetry in four dimensions.”. Seminar at Crete Center for Theoretical Physics, July 2014.



- [82] L. Rastelli, “Infinite chiral symmetry in four and six dimensions.”  
Seminar at Harvard University, November 2014.
- [83] D. Xie, “General Argyres-Douglas Theory,” [JHEP 01 \(2013\) 100](#),  
[arXiv:1204.2270 \[hep-th\]](#).
- [84] Y. Wang and D. Xie, “Classification of Argyres-Douglas theories from  
M5 branes,” [Phys. Rev. D94 no. 6, \(2016\) 065012](#), [arXiv:1509.00847](#)  
[\[hep-th\]](#).
- [85] J. Auger, T. Creutzig, S. Kanade, and M. Rupert. To appear.
- [86] C. Beem and W. Peelaers. Work in progress.
- [87] A. Gadde, L. Rastelli, S. S. Razamat, and W. Yan, “The 4d  
superconformal index from q-deformed 2d Yang-Mills,” [Phys. Rev.](#)  
[Lett. 106 \(2011\) 241602](#), [arXiv:1104.3850 \[hep-th\]](#).
- [88] M. Kontsevich and Y. Soibelman, “Stability structures, motivic  
Donaldson-Thomas invariants and cluster transformations,”  
[arXiv:0811.2435 \[math.AG\]](#).
- [89] T. Dimofte, S. Gukov, and Y. Soibelman, “Quantum Wall Crossing in  
N=2 Gauge Theories,” [Lett. Math. Phys. 95 \(2011\) 1–25](#),  
[arXiv:0912.1346 \[hep-th\]](#).
- [90] N. Drukker, J. Gomis, T. Okuda, and J. Teschner, “Gauge Theory  
Loop Operators and Liouville Theory,” [JHEP 02 \(2010\) 057](#),  
[arXiv:0909.1105 \[hep-th\]](#).

- [91] N. Drukker, D. R. Morrison, and T. Okuda, “Loop operators and S-duality from curves on Riemann surfaces,” [JHEP 09 \(2009\) 031](#), [arXiv:0907.2593 \[hep-th\]](#).
- [92] C. Córdova and A. Neitzke, “Line Defects, Tropicalization, and Multi-Centered Quiver Quantum Mechanics,” [JHEP 09 \(2014\) 099](#), [arXiv:1308.6829 \[hep-th\]](#).
- [93] A. Goncharov and L. Shen, “Donaldson-thomas transformations of moduli spaces of  $G$ -local systems,” [arXiv:1602.06479](#).
- [94] P. Longhi, “Wall-Crossing Invariants from Spectral Networks,” [arXiv:1611.00150 \[hep-th\]](#).
- [95] M. Gabella, P. Longhi, C. Y. Park, and M. Yamazaki, “BPS Graphs: From Spectral Networks to BPS Quivers,” [JHEP 07 \(2017\) 032](#), [arXiv:1704.04204 \[hep-th\]](#).
- [96] M. Alim, S. Cecotti, C. Córdova, S. Espahbodi, A. Rastogi, and C. Vafa, “ $\mathcal{N} = 2$  quantum field theories and their BPS quivers,” [Adv. Theor. Math. Phys. 18 no. 1, \(2014\) 27–127](#), [arXiv:1112.3984 \[hep-th\]](#).
- [97] S. Cecotti and M. Del Zotto, “On Arnold’s 14 ‘exceptional’  $N=2$  superconformal gauge theories,” [JHEP 10 \(2011\) 099](#), [arXiv:1107.5747 \[hep-th\]](#).

- [98] D. Galakhov, P. Longhi, and G. W. Moore, “Spectral Networks with Spin,” *Commun. Math. Phys.* **340** no. 1, (2015) 171–232, [arXiv:1408.0207 \[hep-th\]](#).
- [99] M. Gabella, “Quantum Holonomies from Spectral Networks and Framed BPS States,” *Commun. Math. Phys.* **351** no. 2, (2017) 563–598, [arXiv:1603.05258 \[hep-th\]](#).
- [100] D. Gaiotto, G. W. Moore, and A. Neitzke, “Spectral Networks and Snakes,” *Annales Henri Poincaré* **15** (2014) 61–141, [arXiv:1209.0866 \[hep-th\]](#).
- [101] M. R. Douglas and G. W. Moore, “D-branes, quivers, and ALE instantons,” [arXiv:hep-th/9603167 \[hep-th\]](#).
- [102] M. R. Douglas, B. Fiol, and C. Romelsberger, “Stability and BPS branes,” *JHEP* **09** (2005) 006, [arXiv:hep-th/0002037 \[hep-th\]](#).
- [103] M. R. Douglas, B. Fiol, and C. Romelsberger, “The Spectrum of BPS branes on a noncompact Calabi-Yau,” *JHEP* **09** (2005) 057, [arXiv:hep-th/0003263 \[hep-th\]](#).
- [104] L. F. Alday, D. Gaiotto, S. Gukov, Y. Tachikawa, and H. Verlinde, “Loop and surface operators in  $N=2$  gauge theory and Liouville modular geometry,” *JHEP* **01** (2010) 113, [arXiv:0909.0945 \[hep-th\]](#).

- [105] V. Fock and A. Goncharov, “Moduli spaces of local systems and higher Teichmüller theory,” *Publ. Math. Inst. Hautes Études Sci.* no. 103, (2006) 1–211, [math/0311149](#).
- [106] K. De Vos and P. Van Driel, “The Kazhdan-Lusztig conjecture for W algebras,” *J. Math. Phys.* **37** (1996) 3587, [arXiv:hep-th/9508020](#) [[hep-th](#)].